Pathway Analysis for Biocrystallisation and Biodeposition of Pd(II) and Pt(II) Metals by Sulfate-Reducing Bacteria

by

Khanyisile Bridgete Malunga

Submitted in partial fulfilment of the requirements for the degree

Master of Science (Applied Science) (Water Utilisation)

In the

Department of Chemical Engineering

Faculty of Engineering, Built Environment, and Information Technology

University of Pretoria

2021

ABSTRACT

Pathway Analysis for Biocrystallisation and Biodeposition of Pd(II) and Pt(II) Metals by Sulfate-Reducing Bacteria

Author:	Khanyisile Bridgete Malunga
Supervisor:	Evans Chirwa
Co-Supervisor:	Shepherd Tichapondwa
Department:	Chemical Engineering
University:	University of Pretoria
Degree:	Master of Science (Applied Science) (Water Utilisation)

Despite limited availability of platinum group metals such as palladium and platinum, there is an increasing demand to use them especially as catalysts for fossil fuel free energy sources, such as electric cars and hydrogen fuel cells. Despite this increase in demand, conventional recovery of these metals from wastewater and solid waste streams is still not practiced, and the release of large amounts of metals tends to upset the delicate balance of biodiversity in sensitive ecosystems. Therefore, with the effect of climate change being apparent research focus has shifted to non-carbon energy systems such as biotechnology.

Microbial recovery of platinum group metals is emerging as a clean alternative bioremediation processes as compared to the traditional physical and chemical recovery processes, and Sulfate-Reducing Bacteria have drawn a great deal of attention because they have proven to have excellent metal reaction properties for platinum group metals such as palladium and platinum. However, to effectively reduce palladium and platinum to their elemental form a clear understanding of the following is needed; the particle physics, how the organisms interact with the metals under certain environmental conditions as well as the limitations posed by the metal's occurrence in chelated states on the adsorption and uptake by living organisms.

Therefore, the aim of the study was to investigate the use of Sulfate-Reducing Bacteria and *Desulfovibrio desulfuricans* DSM642 in the bioreduction, biodeposition and biocrystallisation of palladium and platinum. Sulfate-Reducing Bacteria were isolated from sludge from a wastewater treatment plant in the North west, South Africa, and *Desulfovibrio desulfuricans* DSM642 was

purchased from Deutsche Sammlung von Mikroorganismen und Zellkulturen (DSMZ) in Germany. Batch experiments were conducted at different palladium and platinum concentrations from 356.3 mg/L to 1928 mg/L for palladium and 20 mg/L to 140 mg/L for platinum. The experiments were conducted at an optimum pH of 4, a temperature of 30°C under 120 rpm shaking in a dark room under oxygen free nitrogen to achieve anerobic conditions

After cell preparation, cells were harvested and challenged with different concentrations of $Pd(NH_3)_4Cl_2$ and Platinum Standard solution. Removal of the metals by the cells happened at the expanse of formate as an electron donor for 6 and 7 hours for palladium and platinum respectively. After incubation a maximum of 96 % and 99 % of palladium was removed and a maximum of 59% and 56% of platinum was removed by Sulfate-Reducing Bacteria and *Desulfovibrio desulfuricans* respectively. TEM analysis revealed black oblique deposits on the cell wall of both treatments, which revealed the biomineralisation processes happened on the cell membrane.

Palladium deposits were confirmed by X-Ray Diffraction (XRD) to be elemental palladium nanoparticles with a maximum crystal size of 16.9 nm, confirming bioreduction and statistical analysis of the data proved that both treatments have the potential to bioremediate palladium and platinum contaminated environments.

Keywords: Biocrystallisation, Biodeposition, Bioremediation, *Desulfovibrio desulfuricans* Palladium, Platinum, Sulfate-Reducing Bacteria

DECLARATION

I, Khanyisile Bridgete Malunga, hereby declare that all the work provided in this dissertation is to the best of my knowledge original (except where cited) and that neither the whole work nor any part of it has been or is to be submitted for another degree at this or any other University or tertiary education institution or examining body.

SIGNATURE:  DATE: 12 July 2021

DEDICATION

To my parents

For their endless love and support,

My siblings

Who always encouraged me in all my adventures including this one,

My partner

My biggest cheerleader, who always believed in my abilities of attaining this degree

ACKNOWLEDGEMENTS

It is with immense gratitude that I acknowledge the support and help of my project leader Professor Evans Chirwa. I Thank him for his patience, motivation, and invested faith in me to complete this degree.

My sincere thanks also go to Doctor Shepherd. M Tichapondwa, Doctor HG Brink and Doctor F Bezza for their guidance and technical advice.

My heart felt gratitude goes to my colleagues for their support and stimulating discussions that assisted me with innovative ideas for the project, and to Ms. Elmarie Otto and Mrs. Alette Devega for always attending to my needs around the laboratory.

Lastly, I would like to thank the staff at the microscopy laboratory from the University of Pretoria for their assistance with TEM and SEM analysis.

TABLE OF CONTENTS

LIST OF FIGURES

LIST OF TABLES

LIST OF ABBREVIATIONS

Bio-Pd	Biogenic Palladium
Bio-Pt	Biogenic Platinum
Chem-Pd	Chemical Palladium
DSMZ	Deutsche Sammlung von Mikroorganismen und Zellkulturen
EDS	Energy Dispersive Spectroscopy
FTIR	Fourier-transform infrared spectroscopy
HFO	Ferric Oxyhydroxide
PGM	Platinum Group Metals
rRna	Ribosomal Ribonucleic acid
SEM	Scanning Electron Microscopy
SRB	Sulfate-Reducing Bacteria
TEM	Transmission Electron Microscopy

REASERCH OUTPUTS

1. **Malunga K.**, Chirwa E., 2019, Recovery of Palladium(ii) by Biocrystallization and Biodeposition Using a Pure Culture and Mixed Culture, *Chemical Engineering Transactions*, 74, 1519-1524.
2. **Malunga K.B.**, Chirwa E.M.N., 2019, Redox Potential and Proton Demand in an Anaerobic Palladium (II) Reducing Culture of *Desulfovibrio Desulfuricans* Seroval, *Chemical Engineering Transactions*, 76, 1309-1314.
3. **Malunga K.B**,, Chirwa E.M.N. 2019, Recovery of Palladium(ii) by Biocrystallization and Biodeposition Using a Pure Culture and Mixed Culture. *The 14th International congress on Chemical and Process Engineering*. 26 -29 May 2019 Bologna, Italy (Poster).
4. **Malunga K.B**,, Chirwa E.M.N. 2019 Redox Potential and Proton Demand in an Anaerobic Palladium (II) Reducing Culture of Desulfovibrio Desulfuricans Serova. *Process Intergration for Energy Saving and Pollution Reduction*. 20 – 23 October 2019 Angio Nikolaos, Crete, Greece

CHAPTER 1: INTRODUCTION

1.1 Background

1.1.1 Origins of Platinum Group Metals (PGMs) and Precious Metal Elements (PMEs)

Lately, some scientists have proposed that most of the Platinum Group Elements (PGEs) arrived on Earth as a result of earlier asteroid impacts carrying iron-loving elements around 4.5 billion years ago. Models suggesting the intrusion of PGE carrying asteroids were published in the journal Science in 2015 (Bottke et al., 2015). In these models, the authors suggested that large PGE carrying asteroids may have impacted the Earth with their cores transiting the molten Earth resulting in re-accretion on the surface thereby creating discontinuous extrusions represented by the current day precious metal bearing reefs.

One of these precious metals, chromium (atomic number 24, atomic weight 51.996 g/mole), is closely associated with the platinum group element (PGE) bearing rock formations in the so-called Bushveld Igneous Complex (BIC) located in the upper Transvaal Region of South Africa also known as "the great trough" (Figure 1.1).

One of the PGEs, chromium, was discovered by a French chemist Louis Vauquelin in 1797. Vauquelin gave the element the Greek name 'χρωμα' ('*chroma*') which means colour due to the many different colours found in its compounds (Mohan and Pittman, 2006). The gemstones 'emerald' and 'ruby' owe their colours to traces of chromium in the matrix. Chromium is the earth's twenty-first most abundant element detected at a concentration of approximately 122 mg per kg of Earth's crust. Among the transitional metals, it is the sixth most abundant element. Notably, chromium does not occur in nature in pure elemental form but is rather bonded in complex mineral forms.

The geological material in earthly materials are deficient in precious metals and PGM groups. On the other hand, most meteorites and asteroids are rich in these elements. Recently, the theory of elemental admixture from asteroid impacts has been proposed. For example, it is suggested the PGM and gold rich Bushveld trough (Figure 1.1) was formed due an impact by a large PGM rich asteroid in early to mid-bombardment period when the Earth's surface had not completely

solidified but was viscous enough to prevent complete admixture of the asteroid material into the surrounding basaltic and silicate bearing crust (Elvis, 2013).

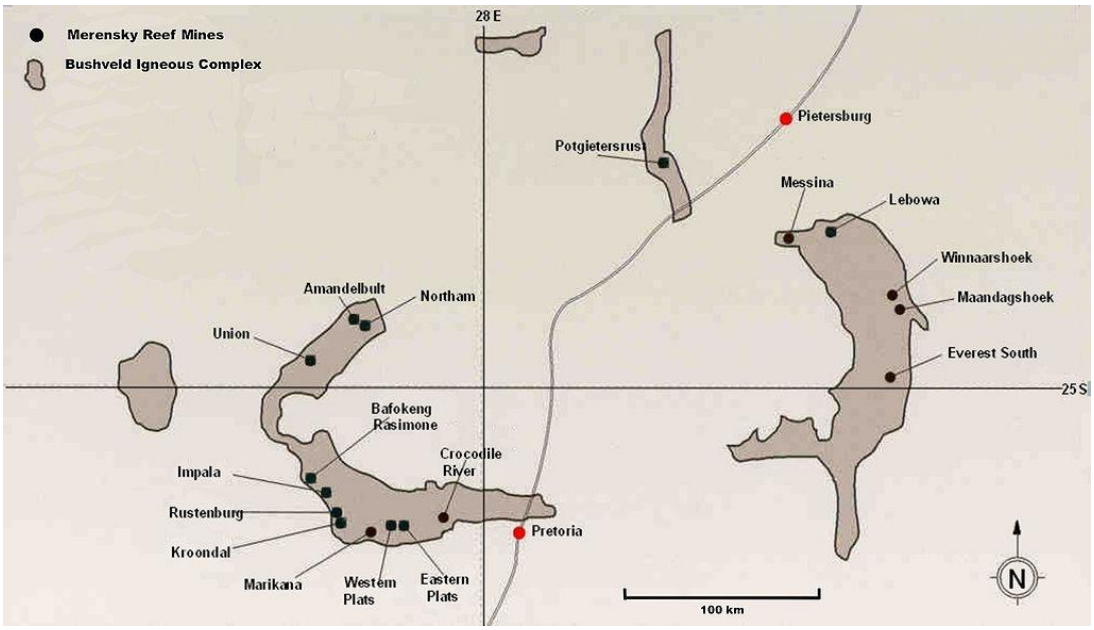

Figure 1.0.1: The Merensky Reef Mines and the Bushveld and Igneous Complex in South Africa and Zimbabwe

1.1.2 Historical Background of Platinum Group Metals (PGMs)

Julius Caesar Scaliger, an Italian humanist noted the first appearance of platinum in 1557, he described it as an unknown noble metal 'which no fire nor any Spanish artifice has yet been able to liquefy'(Weeks and Lind, 1946). The Spaniards called it platina which means silver, it was regarded as a worthless impurity only used in counterfeiting operations and filling the centres of hollowed out gold bars in the 16th and 17th century (Mulholland, 1983). A clear description of platinum was recorded by William Lewis FRS between 1755 and 1757, however it had few uses because it was arduous to work with. Until the experiments of W.H. Wollaston FRS, he established that platinum is malleable when strongly compressed and that it can be annealed and hammered. These finding increased the widespread usage of platinum (Weeks and Lind, 1946). In later years Wollaston discovered palladium and named it after the asteroid Pallas, followed by the discovery of rhodium in 1803. Osmium and iridium were discovered by Smithson Tennant in 1804, iridium was so called from the Greek iris (rainbow) in recognition of the striking variety of

the colours of its salts. Ruthenium was discovered in 1826 but isolated in 1844 by K.K Klaus, he named it after Ruthenia the Latin name for Russia where it was discovered (Hartley, 1991).

1.1.3 Anthropogenic Sources of Platinum Group Elements on Earth

There has been a growing interest in the recovery of PGMs because of their extensive use in various industries such as agriculture, medicine, electronics, energy and space industries (Iravani, 2014, Yong et al., 2002b). Economically, the metals are historically important as currency and remain important investment commodities (Das, 2010). However, due to their increased use, their availability has become limited and caused extreme price volatility (Corte et al., 2012). The price of palladium has increased from R 5 000 to R 26 000 per ounce over the past five years according to Gold Broker, with South Africa being the largest producer of platinum group metals (Table 1).

Table 1. 1: The world reserves of PMGs (Thethwayo, 2018).

Country	PGM reserves (kg)
United States	900 000
Canada	310 000
Russia	1 100 000
South Africa	63 000 000
Other countries	800 000
World total (rounded)	66 000 000

There has been an increase in the release of metal compounds into the environment directly or indirectly by various industrial and mining activities. Therefore, recovery of these metals from leachates of urban mines and liquid waste streams has become an economically attractive recycling process and important in detoxifying aquatic environments (Okibe et al., 2017). Conventional cycling techniques such as pyrometallurgical and hydrometallurgical processes that include adsorption by ion exchange resin, solvent extraction, and reduction of precious metal precipitate by reagents have been widely used to recover metals. However, these methods are not cost-effective as they are labour intensive and time consuming. Furthermore, they are not environmentally friendly as they generate large quantities of contaminants in the environment (Das, 2010).

The microbial reduction of metals has attracted recent interest because it is regarded as a clean alternative to the traditional chemical processes. Microbes offer an advantage in that they play a crucial role in the cycling of organic and inorganic species in the environment and if harnessed they may offer a wide range of innovative biotechnological processes (Lloyd, 2003). In addition, they are sensitive enough to recover metal concentrations at ppm concentrations which are below the economic threshold of traditional recovery methods (Zhang and Hu, 2017). Recent studies have demonstrated the ability of microorganisms to reduce metals through metal resistant mechanisms that incorporate changes in the oxidation state of the toxic metals. For example, the reduction of V(V) to V(IV) using *Shawanella oneidensis* (Carpentier et al., 2003); the reduction of Cr(VI) to Cr(III) by using chromium reducing organisms in the presence of Fe(II) where Fe(II) acted as a catalyst in the reduction processes (Bansal et al., 2019); biosorption and desorption potential of Au(II) by fresh water algae *Scenedesmus obliquus* AS-6-1 (Shen and Chirwa, 2018); biosorption of platinum onto a chitosan based biosorbant material (Guibal et al., 1999) and the reduction of Pd(II) to Pd(0) by *Desulfovibrio desulfuricans* (Guibal et al., 1999). The application of microbial metal reduction is endless.

SRB have drawn a great deal of attention because they have proven to have excellent metal reaction properties for a variety of metals in particular Pd. A great deal of research done on the bacteria has demonstrated that they have a broad metal reducing capability coupled to hydrogenases and cytochromes which results in metal deposition (Foulkes et al., 2016). This process has demonstrated the superiority of palladised whole cells or biominerals as catalyst over the carbon supported-palladium catalyst in important industrial reactions. Several studies have demonstrated the use of bio-Pd in remediative reactions such as the reduction of Cr(VI) to Cr(III) (Mabbett et al., 2006), dehalogenation of chlorophenol, polychlorinated biphenyl, polybrominated diphenyl ethers (Foulkes et al., 2016), and hydrogenation of itaconic acid (Creamer et al., 2007). When the bio-Pd was compared with the commercially produced Pd catalyst, the bio-Pd was more active than or at least as active as the latter.

1.2 Problem statement

The widespread usage of Pd and Pt in industrial processes has led to the production of diverse Pt and Pd loaded waste waters. Therefore, sustainable effective recovery strategies are needed for the treatment of low concentrated waste waters to prevent pollution and to stimulate recovery and reuse of these metals.

1.3 Aims

The study aims to investigate the crystallisation and deposition of Pd(0) and Pt(0) by *Desulfovibrio desulfuricans* and a consortium of SRB, respectively. The consortium is utilised because in environmental biotechnology it offers an advantage over a pure culture because it is less liable to contamination from other organisms and it can adapt to minor changes in its environment.

1.3.1 Specific objectives

- Identifying the optimum pH conditions for the bacteria to reduce the metal ions
- Evaluating to what degree can SRB and *Desulfovibrio desulfuricans* reduce Pd(II) and Pt(II) to their zero states at different Pd(II) and Pt(II) concentrations.
- Identifying the deposition sites and crystal size of the reduced metal ions on the bacteria
- Identifying the mechanisms used to reduce and crystalize the metal ions
- Model and stimulate the reduction process of these metals using kinetic parameters

1.4 Outline of Dissertation

The outline is listed as follows:

Chapter 1: Introduction

Provides background information and objectives of the study. The chapter looks at the history of PGMs and discusses the major concerns regarding the increased use of Pt and Pd to the environment and the economy, and the advantages of biotechnology as an alternative lucrative process to recover Pd and Pt,

Chapter 2: Literature review

Reviews previous work conducted on Pd and Pt. The different conventional recovery methods their limitations and available biotechnology methods. A detailed outline of the biotechnology mechanism and microorganism that drives recovery of the metals and lastly opportunities for future work are discussed.

Chapter 3: Methods and Material

Describes the materials and methods used in this study that is based on previous work on Pd and Pt reported in literature, with a few modifications. Results of this work are presented and discussed in detail in chapter 4.

Chapter 4: Results and Discussion

Presents experimental results and interpretation, where the results are compared against findings of previous works.

Chapter 5: Pd (II) and Pt (II) Reduction kinetic studies

Presents a proposed modified Monod Kinetic model to describe the rate of removal of Pd and Pt by SRB and *Desulfovibrio desulfuricans*.

Chapter 6: Conclusion and Recommendations

Reports major conclusions from findings of this study, in addition, recommendations are also made for future studies.

1.5 Research Significance

South Africa is a huge industrial producer of the platinum group metals. This can be correlated to high environmental pollutants in aqueous environments. During the refining of these metals, considerable amounts of waste is formed which can be toxic. Hence remediation strategies are of paramount importance. Conventional cycling techniques such as pyrometallurgical and hydrometallurgical processes that include adsorption by ion exchange resin, solvent extraction, and reduction of precious metal precipitate by reagents have been widely used to recover metals. However, these methods are costly as they require extensive labour, time, and they generate large quantities of secondary waste (Das, 2010). Thus, exploring bioremediation of these metals can be

an alternative to recover the Pd and Pt from waste streams in a cost-effective manner that will generate less harmful waste.

CHAPTER 2: LITERATURE REVIEW

2.1Platinum (Pt) and Palladium (Pd)

PGMs such as Pt and Pd together with gold (Au) and silver (Ag) are precious metals because they are in high demand and they are limited (Deplanche et al., 2011). PGMs are very valuable because they are resistant to corrosion and oxidation, they are good electrical conductors and have excellent catalytic activity and disinfection properties. Their high catalytic activity for a range of substrates has resulted in their use in many industrial synthetic processes from reforming reactions in the petroleum refining industry, hydrogenation and dehydrogenation reactions in the pharmaceutical industry (Bernardis et al., 2005), and in automotive catalytic converters to reduce gaseous emissions in vehicle exhausts to decrease the carbon footprint (Yong et al., 2002a). In environmental applications, its distinctive hydrogenation effect substantially accelerates the reductive degradation of many recalcitrant contaminants such as nitroaromatics, polychlorinated biphenyl, and azo dyes (Cheng et al., 2017). In addition, the metals are used to carve beautiful jewellery.

2.2 Recovery of Platinum Group Metals

PGM ore in South Africa is mined in the western and eastern limb of the Igneous Complex Bushveld in the Merensky Reef, the Platreef and Upper group 2 reef (Thethwayo, 2018). The Merensky Reef and Platreef have similar chemical and mineral compositions they have low sulfide content however, the Merensky reef is abundant in metal sulfides such as chalcopyrite and pyrrhotite which are associated with PGMs (Eksteen et al., 2011). These metals can be extracted using the following conventional methods: Pyrometallurgy and Hydrometallurgy.

2.2.1 Pyrometallurgy

One of the oldest extractive processes, it involves the thermal treatment of minerals or ores to bring about a physical and chemical change of the minerals to permit the recovery of precious metals the process involves roasting, smelting, and refining (Hiskey, 2000). A typical pyrometallurgy process is summarized in Figure 2.1. The ore initially undergoes comminution which is the crushing, milling, and gravity separation of the ore followed by concentration of the value minerals

via flotation (Thethwayo 2018). To further separate the sulfide PGM's from the silicate gangue mineral, the flotation concentrates are subjected to a high-temperature smelting process. Typically, electric arc furnaces are used to generate heat by passing an electric current through a resistive bath (Jones, 2005). After smelting, the furnace matte which consists of base metal sulfides is treated in converters where the iron sulfide is oxidized to ferrous oxide, and sulfide is oxidized to sulfur dioxide, which is removed as a gas, and iron oxide is removed as a fayalitic slag.

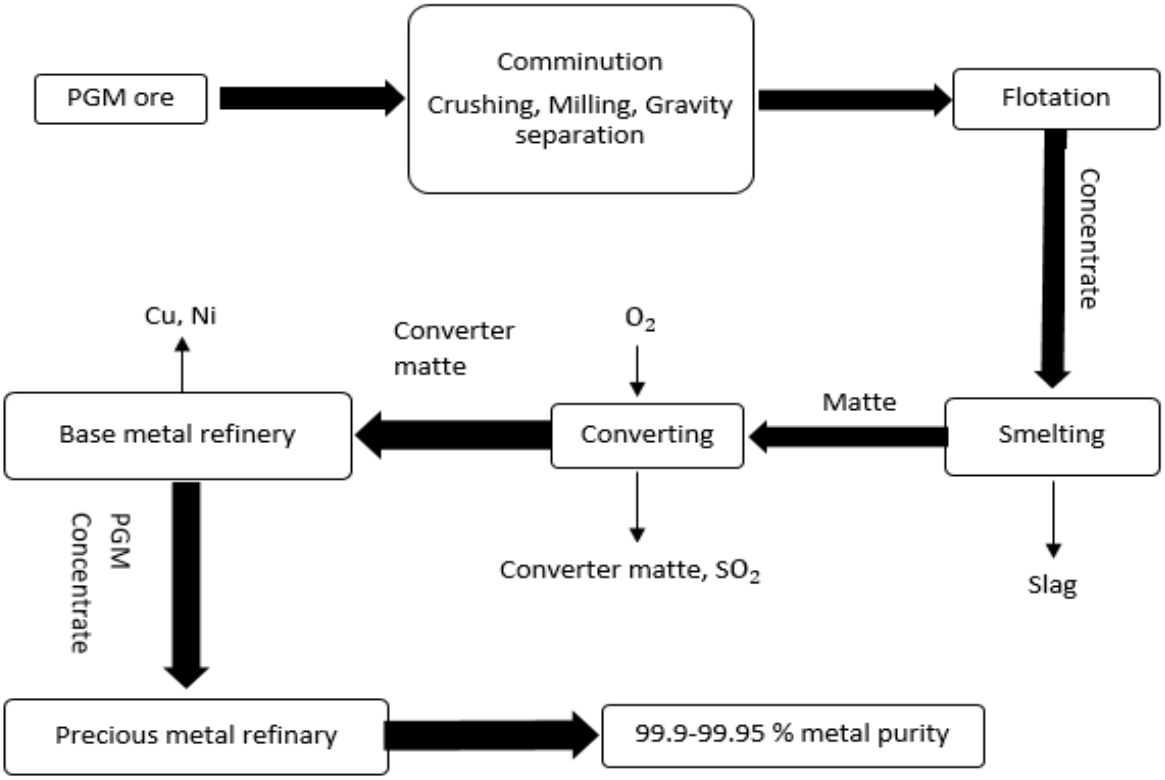

Figure 2.1: Flow diagram of a typical pyrometallurgy process

The slag phase typically consists of PGMs which are recycled back to the smelting furnace to recover the entrained metals, then refined with various solutions, extractions, and precipitation methods to separate individual metals (Thethwayo, 2018).

2.2.2 Hydrometallurgy

Hydrometallurgy is an extractive metallurgy process involved in the treatment of ores, concentrates, and other metal-bearing materials by aqueous chemistry to recover valuable metals from their ores. Hydrometallurgy is typically divided into the following areas shown in Figure 2.2: leaching, solid-liquid separation, purification, metal recovery, and refining (Habashi, 2009). Leaching involves the extraction of soluble metallic compounds from their ore by selectively dissolving them in a suitable solvent (Hiskey, 2000). The lixiviant solution conditions vary in terms of pH, oxidation-reduction potential, presence of chelating agents, and temperature, to optimize the rate, extent, and selectivity of dissolution of the desired metal component into the aqueous phase (Tasker et al., 2007). To achieve efficient leaching hydrometallurgy makes use of five basic leaching reactor designs; tank, in-situ, autoclave, vat, and heep. After leaching, undesirable solids are removed by screening, settling, filtration, and centrifugation. Purification involves the separation of undesirable metal ions either by precipitation, cementation, solvent extraction, ion exchange, gas reduction, or electrowinning. Followed by the recovery of the desired metal by electrolysis, gaseous reduction, or precipitation. Occasionally further refining is required to produce ultra-high purity metals.

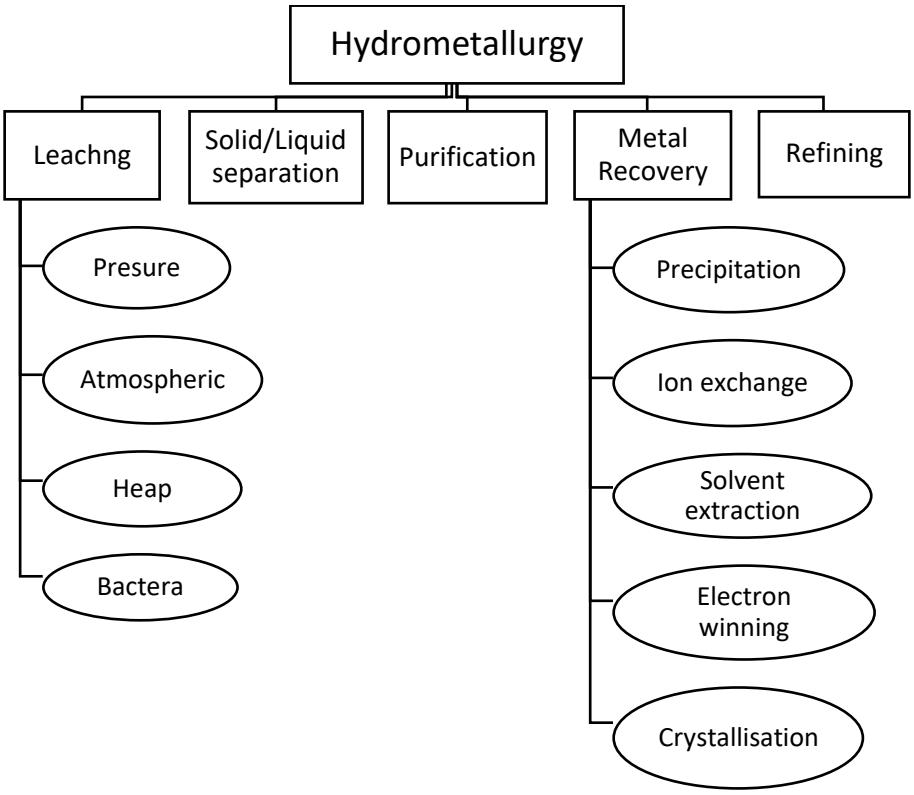

Figure 2.2: Overview of the hydrometallurgical process

Recovery of PGMs from secondary sources is becoming significant because the demand for the metals exceeds the availability of the metals. Albeit new catalysts are being investigated by researchers to substitute or decrease the use of PGMs in auto-exhausts, however, the net demand for the metal is still very high due to environmental pressures that lead to amplified usage (Dong et al., 2015). Therefore, recovery of the metals from secondary sources such as spent catalyst may be of benefit because spent catalysts have a high content of PGMs about seven kilograms per ton. Their composition is simple with the main impurities being Al_2O_3 cordierite and activated carbon. Therefore, recovery will include simple small-scale processes that are cost-effective, have less environmental pollution, and good economic benefits. Recovery of PGMs from waste includes conventional processes such as hydrometallurgy, pyrometallurgy, and non-conventional processes such as biohydrometallurgy (Dong et al., 2015). Hydrometallurgy and pyrometallurgy processes have been previously discussed in this document.

2.3.1 Biohydrometallurgy

Biohydrometallurgy is an extractive technique that uses microorganisms to recover certain metals from their ores (Newton, 2020). A process that covers cutting-edge areas of biotechnology such as bioleaching, biopreparation, biofloatation, bioflocculation, biooxidation, biosorption, bioreduction, and bioaccumulation (Sivasubramanian, 2016). The modern application of this techniques become a reality in the 1950s with copper bioleaching at the Kennecott Copper Bingham Mine in the United States, and expansion of biohydrometallurgy of other metals did not occur until the mid-1980s when the first commercial plant for pre-treatment of refractory gold-bearing concentrate was commissioned at the Fairview operation in South Africa, it has also been used to recover uranium and will eventually be used to recover other metals. (Brierley and Brierley, 2001, Newton, 2020). Biohydrometallurgy is relatively employed when conventional mining procedures are expansive or ineffective at recovering a metal for example dumps of unwanted waste material or run-of-mine material which till today dump bioleaching remains a very low-cost process for scavenging copper from rock that cannot be economically processed by any other methods (Brierley and Brierley 2001). Bioleaching involves the aqueous, inorganic chemistry of acidic sulfate solutions in contact with sulfide concentrates or ores containing valuable metals (Nancharaiah et al., 2016, Watling, 2016). As the acid seeps into the mine dump it creates a favourable environment for acid-loving microorganisms to grow thus attacking the ore. Metals are released into an aqueous solution through solubilization of ores or solid concentrates and processes such as biosorption, bioaccumulation, bioprecipitation, and bioreduction enrich the dissolved metals of leachate streams or diffuse metals of wastewaters as solid precipitates for further metallurgical processing (Figure 2.3) (Nancharaiah et al., 2016).

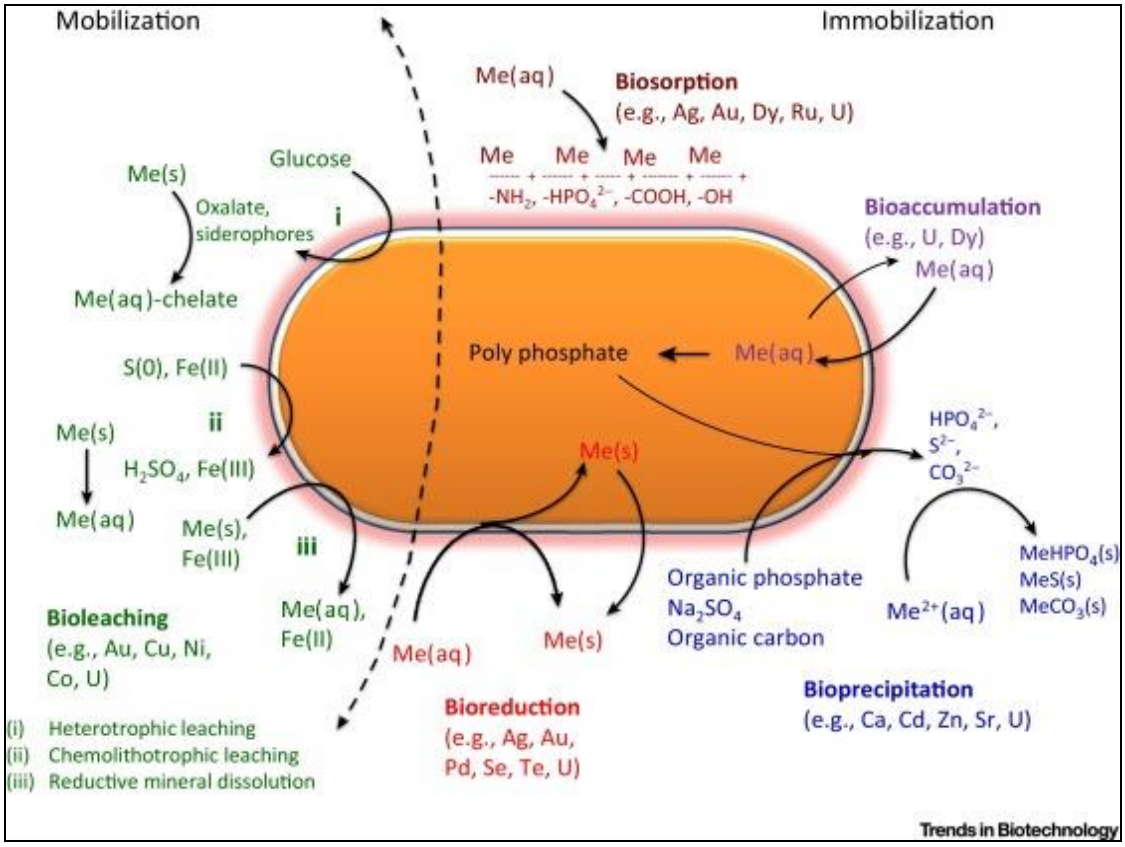

Figure2.3: Microbe–metal interactions depicting different mechanisms of metal solubilization and immobilization used for biorecovery (Nancharaiah et al., 2016).

The use of biohydrometallurgy has been widely used to extract precious metals from ore deposits (Chandraprabha et al., 2002, Sun et al., 2012). However, a recent sustainable application is receiving attention, the use of microbial biotechnology in the processing of industrial and other wastes to first recover precious metals from the waste and second to add value to a 'clean' or at least a less toxic waste product (Cui and Zhang, 2008, Maes et al., 2016). The is limited availability of precious metal high-grade ores, and the ongoing consumption of these resources will eventually lead to a rapid depletion of high-quality ores (He and Kappler, 2017). By viewing metal-containing waste as secondary 'ores', we can avoid exhausting natural resources (He and Kappler 2017).

Industries can enhance their profits by applying microbial biotechnology processes, which can be cost-effective and have a low energy requirement. In addition, several environmental benefits could be achieved by firstly, the treatment of waste by bioprocesses which can reduce the total amount of waste. In addition, land space for waste storage and disposal could be saved for other

human activities. Secondly, microorganisms can be used to break down toxic compounds (Akcil and Mudder, 2003), or perform bioprocesses that are more environmentally friendly as no or less toxic chemicals are employed (Zinke and Gabor, 2012). Thirdly, bioprocessing can effectively recover valuable metals and detoxify processed wastes simultaneously (Natarajan, 2018). Fourthly, once solid waste materials such as incineration solids, coal fly ash, municipal solid waste have been detoxified it can be reused for construction purposes (Hedrich et al., 2015). The sustainable usage of waste material can severely reduce the impact waste has on the environment.

2.3.2 Bioreduction

Bioreduction is a biochemical mechanism that reduces metals through specific enzymes and proteins in a microorganism. This biotechnological process has been known for over a century and it involves microorganisms that possess a metal resistant mechanism that would incorporate changes in the oxidation state of toxic metals. This has attracted recent interest as these transformations often play a crucial role in the cycling of organic and inorganic species in the environment. Therefore, if harnessed, they offer the basis for a wide range of innovative biotechnological processes. Such as the reduction of Cr(VI) to Cr(III) using a wide range of facultative anaerobes; *Escherichia coli, pseudomonads*, *Shewanella oneidensis*, and *Aeromonas species* (Lloyd, 2003). The reduction of Pd(II) to Pd(0) has also gained interest which has been driven by the widespread usage of PGMs in automotive catalytic converters to reduce gaseous emissions, for the synthesis of nano bioinorganic catalysts for commercial use, and the recovery of Pd(II) from industrial waste (Lloyd et al., 1998, Yong et al., 2002b). In addition, the application of bioreduction is documented in studies such as the reduction of Au(III) to Au(0) by a range of organisms such as Archaea *Pyrobacullum islandicum*, *Thermotoga maritima*, and *Shewanella alga* (Lloyd, 2003). In conclusion, the application of bioreduction for a wide range of metals is endless.

2.4 Obstacles in mining and recovery of precious metals from waste

Conventional recovery of precious metal is costly because of the high energy consumption and usage of chemicals for metal mobilization, and cementation (He and Kappler, 2017). To ensure profitability and minimize costs industries would utilise high-grade as raw material (Marsden and House, 2006). However, mining activities are recently more constrained due to limited high-grade ores because of depleted local resources and restrictions in the import of precious metals as a

result of laws and regulations of metal-exporting countries (Fleming, 1992, Reith et al., 2007)(Fleming, 1992). Therefore, recycling precious metals from waste streams is a possible solution that can alleviate the disparity between supply and demand.

Electronic wastes, tailing dumps accumulated at precious metal mine sites, and other unconventional resources can be used to extract and recover precious metals (Bao et al., 2010, Cui and Zhang, 2008, Kaya, 2016). However, tailings that contain low levels of gold-entrapped sulfides cannot be economically processed through conventional processes. In addition the recovery of gold particles trapped in host rocks by gravity or cyanidation challenging (Marsden and House, 2006). E-wastes can be profitability recovered because they relatively contain high levels of precious metals however, traditional pyrometallurgical and hydrometallurgical processes have several limitations. Pyrometallurgical processes (smelting) require high financial investments for energy and generate hazardous emissions (Cui and Zhang, 2008, Kaya, 2016). Cyanide leaching in hydrometallurgy is very toxic and has caused a series of environmental accidents at various gold mines around the world which has caused concerns regarding the utilisation of cyanide (Cui and Zhang 2008).

Industrial and household waste are commonly burned in incineration plants and subsequently disposed of in the environment or used as additives in construction such as cement. Consequently, waste disposal in the environment can cause leaching of toxic compounds into the surrounding areas and the loss of precious metals in the waste. Several attempts have been employed to recover precious metals from such wastes by conventional methods such aging, sieving, crushing, magnetic separation, density separation, and eddy current separation (Chandler et al., 1997).

However, these processes are poor at recovering precious metals from waste. The main hindrance is the low abundance of the metals in the municipal solid waste (MSW), and incineration residues (Morf et al., 2013). Waste streams also contain precious metals from hospitals (e.g. chemotherapeutic drugs containing Pt, plating processes, and automotive catalysts, and. The main limitation for recovering the metals from wastewaters is the low abundance of the metals (Bhagat et al., 2004, Ju et al., 2016). Conventional recovery methods such as solvent extraction, ion exchange resins, reduction and precipitation are not economically profitable. Hence, there is a strong need to develop a cost-effective and eco-friendly methods to recover precious metals. Such

as microbially assisted recovery which can potentially offer an affordable, sustainable approach to meeting the rising demands of precious metals (He and Kappler, 2017).

2.5 Biomineralization of metals

Biomineralization is the formation of minerals by living organisms, these minerals often form structural features such as seashells, bone in mammals and birds, copper, iron, and gold deposits by bacteria. For this reason, a wide range of organisms such as sponges, freshwater snails, and earthworms have been used to recover metals from the environment. Extensive research has been done on plants and plant extracts to produce metal nanoparticles however the most promising candidates for the recovery of metal nanoparticles are microorganisms (Foulkes et al., 2016). Microorganisms have been known to play a very important role in the environment. However, it is only in the last decade that we have come to understand the full extent of microbial processes that can control the solubility of metals and other elements through a molecular mechanism of biomineral formation (Lloyd et al., 2008). A wide variety of organisms have been exploited for the recovery of metals from fungi, yeast, algae, viruses and bacteria. Such as the use of fungi in the intracellular synthesis of Au and Ag (Castro-Longoria et al., 2011), the use of yeast cells (Saccharomyces cerevisiae) to produce cadmium telluride quantum dots (Bao et al., 2010) and the use of genetically modified tobacco mosaic virus to produce palladium nanoparticles (Castro-Longoria et al., 2011). According to literature biominerals are formed through indirect passive reactions others via enzymatic reductions (Lloyd et al., 2008). Enzymatic reduction involves enzymatically assisted metal precipitation from a high valance to a low or zero-valance (Deplanche et al., 2011). For example, the reduction of U(VI) to U(V) via unstable intermediates by *Micrococcus latilyticus* (Woolfolk and Whiteley, 1962), reduction of Au(III) to Au(0) nanoparticles by *Escherichia coli* and *Desulfovibrio desulfuricans* (Deplanche and Macaskie, 2008). Indirect passive reactions involve two pathways firstly it involves metal adsorption on to a large surface area of the charged cell walls whereby the extracellular layers lower the interfacial energies for heterogenous nucleation. This increases the local concentrations as they exceed the solubility product of the mineral causing it to precipitate. Secondly local geochemistry around the cell can be pushed by the microbial metabolism towards mineral forming conditions via the efflux of ligands including phosphate, sulfide or carbonate, or metabolism linked changes in pH (Konishi et al., 2007).

2.6 Sulfate-Reducing bacteria

Sulfate-Reducing Bacteria (SRB) are a diverse heterogeneous group of anaerobic microorganisms inhabiting various environmental conditions. SRB are one of the most important groups of microorganisms that participate in various nutritional cycles of the environment and cause degradation of various organic matters through the process of dissimilatory sulfate reduction (Das, 2010). They are known to be implicated in cases of microbially influenced corrosion arising in a wide range of natural and industrial circumstances. They have the capacity to reduce sulfate present indigenously in the environment and reduce it to poisonous hydrogen sulfide gas.

$$SO_4^{2-} + COD \rightarrow H_2S + CO_2 \quad (2.1)$$

(Sulfate) (Organic Substrate) (Sulfide) (Carbon Dioxide)

Typically, SRB are found mainly in marine and freshwater sediments where sulfate is present in abundance (Nielsen et al., 1999). But they are also found in agricultural and industrial wastewater systems, in oil fields and also in cooling towers (Dang et al., 1996, Rao et al., 2000). These microbial consortia can utilize sulfate, thiosulfate, sulfite and elemental sulfur as electron acceptors but cannot utilize nitrate, nitrite or formate (Azabou et al., 2007). They can also utilize environmental substances such as benzene, toluene, ethylbenzene, xylenes, naphthalene, phenanthrene and alkanes and halogenated compounds (Dang et al., 1996, Ensley and Suflita, 1995). The bacterial strains are also able to utilize peptone, asparagine, glycine, alanine, aspartic acid, ethanol, propanol, butanol, glycerol, glucose, lactate, succinate and malate. The complete genomes of different sulfate reducers have been, or are currently being, sequenced. Comparative analysis of these genome sequences will provide important information on their carbon and sulfur metabolism and open the possibility for functional genomics (Das, 2010).

2.7 Cell surface reactivity

The cell surface of bacteria is a highly reactive interface because of the abundance of reactive functional groups such as carboxyl, phosphoryl, and amine groups. These functional groups deprotonate with increasing pH, thus giving the bacteria a negative surface charge, which can react with cations (Beveridge and Murray, 1980, Cox et al., 1999). Charge properties and proton binding of bacterial surfaces have been studied in detail using acid-base titrations to determine the types

and abundance of these ligands to determine the capacity of bacteria to sorb cations from aqueous environments, with the view to use bacteria for toxic metal remediation (Cox et al., 1999, Daughney et al., 1998, Fein et al., 1997). Other studies have investigated how surface chemistry and charge properties may influence the hydrophobicity of microorganisms (Loosdrecht et al., 1987; Wilson et al., 2001), the resistance to predation by phagotrophs (Matz and Jürgens, 2001), the ability to adhere to solid surfaces and the resistance to toxins (Gimmler et al., 2001, Husmark and Rönner, 1990, Scott et al., 1996).

In a study conducted from native microbial communities and hydrous ferric oxide (HFO) minerals from several hot springs at Yellowstone National Park, USA, HFOs from acidic spring waters displayed surface functional groups typical of synthetic HFO and bound more cations. HFOs from natural spring water were characterized by a lower functional group density and retained more arsenic. When microbial biomass samples from acidic springs were analysed, it became apparent that some algal mats behaved similarly to HFO samples on a dry weight basis, while other thermophilic mats were considerably less reactive. Evidently, these studies have proven bacterial surface characteristics have significant influence on a variety of ecophysiological factors (Lalonde et al., 2007).

2.8 Biodeposition of Pd(0) and Pt(0) as nanoparticles

Reductive deposition of PGM is an important heterogenous reaction for synthesizing PGM nanoparticles and recovering PGM from waste. Chemical reductive methods have been widely used to deposit PGM from corresponding metal salt solutions with various reducing agents (Masala and Seshadri, 2004). However, chemical reductive methods require high temperatures to complete the reduction process. Bioreductive deposition of PGM is considered eco-friendly because it requires low energy consumption (Konishi et al., 2007). The process happens in two-phases, the first phase is a stoichiometric interaction between metal and reactive functional groups on the cell wall and internalization of the metal ions inside the cell, the second phase is an inorganic deposition of increased amounts of metal on the cell wall and/or in solution. (Beveridge and Murray, 1980). For the second phase to occur an electron donor such as formate or hydrogen is needed for the metals to be reduced, with the assistance of an enzyme (Equation 2.2). *Desulfovibrio*

desulfuricans was the first SRB to be reported with Pd-reducing capabilities (Lloyd et al., 1998), and subsequent studies have demonstrated the reduction and deposition of Pd(0) by the assistance of hydrogenases with formate or hydrogen as electron donors (Corte et al., 2012, Mabbett et al., 2006, Mikheenko et al., 2008).

$$Pd^{2+}_{(aq)} + COOH^{-}_{(aq)} + OH^{-}_{(aq)} \xrightarrow{\text{Enzyme (Bacteria)}} Pd_{(s)} + CO_{2(g)} + H_2O_{(l)} \quad (2.2)$$

2.9 Biocrystallization of platinum and palladium

Biocrystallization is the generation of metal precipitates and minerals by bacteria, it is a process that aims to reduce metal ions to their zero-valent state. This can be a stress response, a normal part of metabolism such as disposal of waste compounds, or pathology (Bunge et al., 2010). This mechanism has shown potential in the recovery of precious metals and in production of biosynthetic electrodes in microbial fuel cells (Yong et al., 2002b, Mabbett et al., 2006). In a study conducted by Yong et al. (2002a) crystal deposits of about 50nm were reported for the reduction of Pd(II) by *Desulfovibrio desulfuricans*. In addition, gram-negative bacteria such as *Cupriavidus necator*, *Pseudomonas putida*, and *Paracoccus denitrificans* were used to reduce Pd(II) with formate as an electron donor. The organisms formed aggregates of nanoparticles between 3 nm and 30 nm in size (Bunge et al., 2010). The formation was in the periplasmic space (Figure 2.4 b, e and h) and a maximum size of 1µm aggregates were extracellularly associated with the bacterial cell (Figure 2.4 a, d and g). In a study conducted by Simon-Pascual et al. (2019), Granular sludge was able to reduce Pt(II) to Pt(0) nanoparticles which were deposited intracellularly and extracellularly, and the deposits were reported to be between 2 nm to 5 nm. In addition, several studies have reported bioPd(0) particles to be in the nanometre range which is interesting since nanoscale particles often possess superior catalytic properties compared to their macroscale counterparts, owing to their higher surface-to-volume ratio. The catalytic properties of nanoparticles are strongly affected by the particle size; hence, agglomeration of the particle is important (Simon-Pascual et al., 2019). Therefore, the processes of biocrystallization will be of economic importance in the field of bio-purification and bio-recovery of many beneficial products from the energy conservation processes.

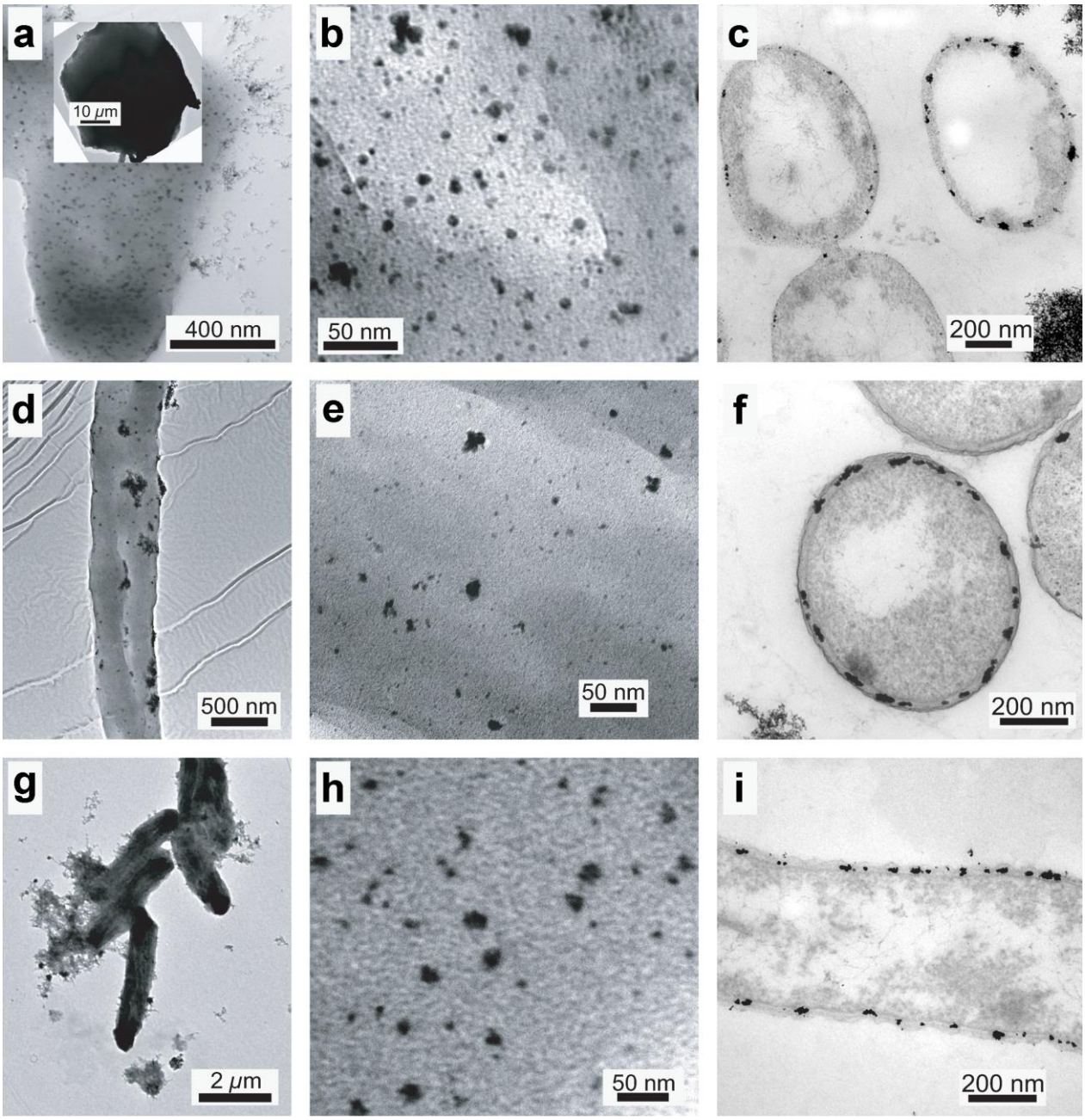

Figure 2.4: The association of Pd(0) at the single-cell scale. Transmission electron micrographs of Cupriavidus. necator (a–c), Pseudomonas. putida (d–f), and Paracoccus. denitrificans (g–i). Panel a depicts a chemically reduced Pd(0) particle. Panels c, f, and i are of ultrathin sectioned cells(Adapted from Bunge et al. (2010).

2.10 Bio-palladium and bio-platinum uses

Biogenic metals such as Pd and Pt have proven to have excellent catalytic and disinfection properties and they have been studied in the removal of a range of environmental contaminants for example Mabbett et al. (2006) reported the use of *Desulfovibrio desulfuricans* and *Escherichia. coli* in the recovery of Pd and other metals from industrial processed waste using an electro-bioreactor. The results showed that 79.22% of the palladium was removed by the resting cells of *Desulfovibrio desulfuricans* and the bio-Pd of *Desulfovibrio desulfuricans* gave a 100% removal of Cr(VI) within 2 hours of the Cr(VI) being in contact with the bio-Pd. *Escherichia coli* was just as effective as *Desulfovibrio desulfuricans* in removing Pd. However, the bio-Pd *(Escherichia coli*) generated from the processed waste had minimal Cr(VI) removal activity as compared to the bio-Pd (*Escherichia coli*) generated from pure commercial Pd solutions. The authors suggested the were other contaminants that inhibited the activity of the bio-Pd produced from wastewater that resulted in a decrease in catalytic activity. Cheng et al. (2017) demonstrated the electrochemical catalytic activity of palladised *Shewanella oneidensis* by hybridizing it with carbon nanotubes as an electron bridge. The results demonstrated an increase in voltage across the electrode with the palladised cells hybridized with carbon nanotubes the conductance was calculated to be 4.2 $k\Omega^{-1}$. Palladised cells without carbon nanotube hydridisation had a low conductance. This study demonstrated bio-Pd cells alone are poor conductors and thus need to be facilitated by a material of good conductance (Cheng et al., 2017). Nevertheless, this was a novel technology for microbial fuel cells. (De Gusseme et al., 2011) demonstrated the use of graphite coated palladised *Shewanella oneidensis* in the removal of diatrizoate from hospital wastewater using an electrolysis cell. The presence of bio-Pd in the cathode significantly reduced diatrizoate from the wastewater. Table 2.1 shows an overview of different environmental contaminants that were successfully degraded by bio-Pd catalyst. Biogenic platinum synthesized from seaweed (*Padna gymnospora*) has been recorded to have antibacterial effects against several pathogenic bacteria and enhanced anticancer effects against several types of cancers, and biogenic platinum synthesised from microorganisms has been recorded in the successful removal of pharmaceutical products such as ciprofloxacin, sulfamethoxazole, and 17β-estradiol (Martins et al., 2017, Puja and Kumar, 2019). In addition bio-Pt nanoparticles produced from *Desulfovibrio vulgaris* were reported to have high catalytic activity in removing pharmaceutical products, 95 % of 17β-etradiol was removed, 85%

and 70% of sulfamethoxazole and ciprofloxacin was removed respectively and the estrogenic effects of 17β-etradiol were reduced proving bio-Pt produced less toxic effects (Martins et al., 2017).

Table 2.1: Overview of different environmental contaminants that were successfully degraded with a bio-Pd catalyst, together with the reaction mechanism and the Pd-reducing species used in the study adopted from (Corte et al., 2012)

Compound	**Type of reaction**	**Polluted environment compartment**	**Pd-reducing species**
Cr(VI)	Reduction	Industrial wastewater	*Desulfovibrio desulfuricans* *Desulfovibrio vulgaris* *Escherichia coli* *Clostridium pasteurianum*
ClO_4^-	Reduction	Groundwater and drinking water	*Shewanella oneidensis*
Polychlorobifenyls (PCBs)	Dechlorination (1-10 Cl)	Air, water, soil, sediments	*Desulfovibrio desulfuricans* *Desulfovibrio vulgaris* *Shewanella oneidensis*
Chlorophenols	Dechlorination (1 Cl)		*Desulfovibrio desulfuricans* *Desulfovibrio vulgaris*
Lindane	Dechlorination (6 Cl)	Soil and groundwater	*Shewanella oneidensis*
Trichloroethylene (TCE)	Dechlorination (3 Cl)	Groundwater	*Shewanella oneidensis*

Polybrominated diphenyl ethers (PBDE)	Debromnation (1-10 Br)	Indoor air and dust	*Desulfovibrio desulfuricans*
Iodinated contrast media (ICM)	Deiodination (3 I)	Wastewaters and surface waters	*Shewanella oneidensis* *Citrobacter braakii*

2.11 Kinetic Studies

Monod based models have been frequently used for metal reduction kinetics (Liu et al., 2002, Lall and Mitchell, 2007, Sheng and Fein, 2014). Mathematically they are described in two ways. Firstly, by systematic coupling and solving of biochemical reactions and processes in reference to experimentally measured quantities or properties (Vlad and Ross, 2000). Secondly, by a microscopic approach, where the biochemical system is treated as a catalytic species to formulate a catalytic interaction model – a Monod bacterium-based model. The latter approach is used in microbial systems because of their complex biochemical nature; and has been used to design and control modern wastewater treatment plants (Rittmann and McCarty, 2001), and quantitatively describe substrate concentrations in microbial ecology (Liu et al., 2002).

CHAPTER 3: METHODOLOGY

3.1 Bacterial preparation

3.1.1 Pure isolate preparation

A pure isolate of *Desulfovibrio desulfuricans* (DSM620) was purchased from DSMZ a Gene bank in Braunschweig, Germany. The sample was freeze dried upon receipt. To get an active culture, 0.5 mL of modified Postgate medium C was transferred onto the specimen and allowed to stand for 30 min under oxygen free nitrogen (Afrox, Gauteng, South Africa) at room temperature (± 25°C. Once ready, 0.5 mL of the culture was transferred to 10 mL of Postgate medium C in a 10 mL test tube with a butyl rubber stopper under oxygen free nitrogen as shown in Figure 3.1. The culture was incubated at 30°C under 120 rpm shaking (Labotech, Gauteng, South Africa), until a black precipitate was visible which was after 3 days.

For metal reduction experiments, 10 mL of an actively growing culture was transferred to 90 mL of modified Postgate medium C in a 100 mL butyl-rubber sealed serum bottle, under oxygen free nitrogen and incubated at 30°C under 120 rpm shaking in the dark for 48 h to get midlogarithmic phase cultures (Ngwenya and Chirwa, 2015).

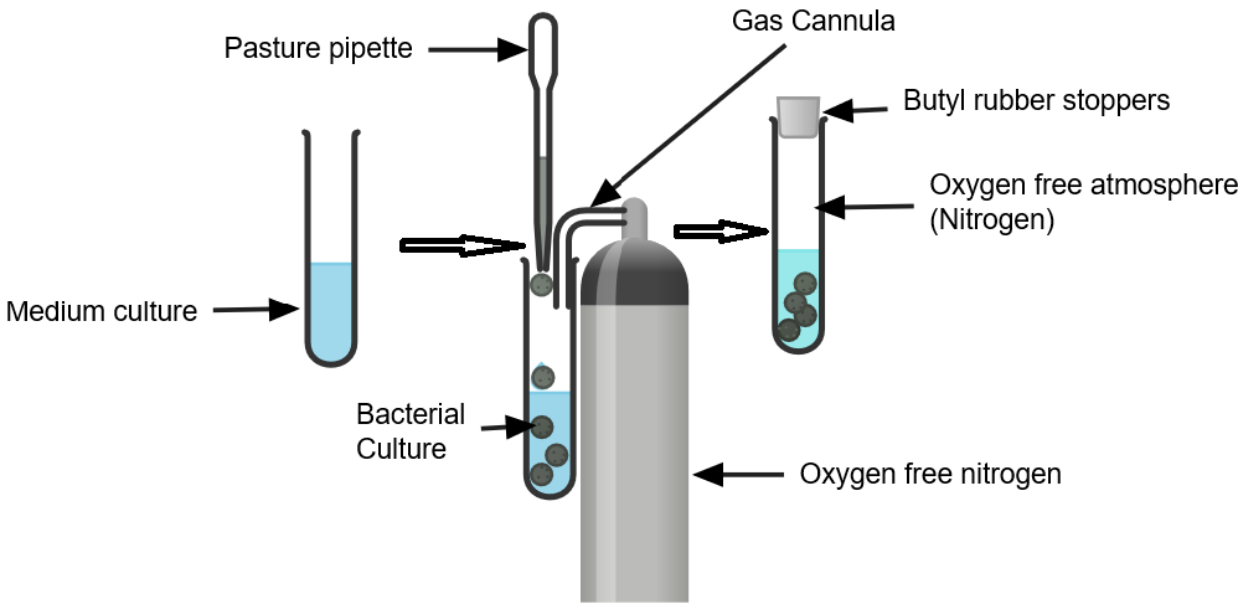

Figure 3. 1: Experimental set up for the activation of freeze-dried *Desulfovibrio desulfuricans*.

3.1.2 Cell isolation from sludge

Sludge was collected from the Brits wastewater treatment plant in the North West, South Africa. 0.2 g of the sample was placed in a 100 mL serum bottle, filled up to brim with Postgate medium C so that no air was trapped in the bottle and sealed with a butyl rubber stopper. The sample was incubated at 30ºC under 120 rpm shacking in the dark for 5 d (Molokwane and Nkhalambayausi-Chirwa, 2009). The presence of SRB was indicated by the blackening of the medium (production of FeS) (Postgate, 1979) as shown in Figure 3.2.

Figure 3. 2: Blackening of the medium due to SRB growth

3.1.3 Consortium preparation

The consortium of SRB was routinely maintained in a 100 mL of Postgate medium C in butyl rubber sealed 100 mL serum bottles. For experiments midlogarithmic phase cultures were prepared by anaerobic withdrawal of 10 mL of an actively growing culture into 90 mL of Postgate's medium C under oxygen free nitrogen, and grown at 30°C for 48 h (Ngwenya and Chirwa, 2015). Cells were harvested by centrifugation at 10ºC and 5000 rpm, kept on ice before and after centrifugation and washed with 20 mM MOPS-NaOH (Sigma-Aldrich, Gauteng, South Africa) buffer (pH 7.0) three times. Subsequently the cells were resuspended in 20 mM of MOPS buffer to provide the stock suspension for the preparation of the experiment, and stored at 4 °C until use (within 24 h) (Mabbett et al., 2006).

3.2 Bio-removal of Pd(II) metal ions from solution

3.2.1 pH experiment

A 2 mL concentrated cell suspension with an OD_{600} of 0.920 and 0.899 ($\pm$ 0.01) for *Desulfovibrio desulfuricans* and SRB respectively was diluted in a 5 mL buffer containing 2 mM of $Pd(NH_3)_4Cl_2$ (Sigma-Aldrich, Gauteng, South Africa) and 25 mM of formate solution, at a pH ranging from 1 -10 adjusted using NaOH and HCl (Glassworld, Gauteng, South Africa). The cell suspension was sparged with nitrogen for 6 min in a 100 mL serum bottle to form the headspace gas. This was

followed by incubation at 30ºC under 120 rpm shacking for 12 h. Thereafter, the sample was sparged with air immediately to stop the reduction and centrifuged at 5000 rpm for 5 min. Finally, the sample was analysed (Yong et al., 2002b).

3.2.2 Optimum cell concentration

For part 1 a concentrated cell suspension of 2 mL with an OD600 of 0.3 (± 0.1) was diluted in a 5 mL buffer containing 2 mM, 4 mM, and 8 mM of $Pd(NH_3)_4Cl_2$. For part 2 a concentrated cell suspension of 2 mL with an OD600 of 0.980 and 0.933 (±0.1) for *Desulfovibrio desulfuricans* and SRB respectively was utilised. The experiments were conducted at a pH of 4 and 25 mM of formate solution, sparged with nitrogen for 6 min to form the headspace gas in 100 mL serum bottles. Incubated at 30 ºC under 120 rpm shaking for 6 h. The samples were sparged with air immediately to stop the reduction, centrifuged at 5000 rpm for 5 min and analysed (Yong et al., 2002b).

3.2.3 Pd(II) Concentration experiment

A concentrated cell suspension of 2 mL with an OD_{600} of 0.980 and 0.930 (± 0.1) for *Desulfovibrio desulfuricans* and SRB respectively was diluted in a 30 mL buffer containing 2 mM, 4 mM, 6 mM, 8 mM 10 mM, 12 mM of $Pd(NH_3)_4Cl_2$ and 25 mM of formate solution. The pH was set at 4 and adjusted using HCl and NaOH. The concentrated cell suspension was sparged with nitrogen for 6 min to form the headspace gas in the serum bottles. followed by incubation at 30ºC under 120 rpm shaking for 6 h. Following incubation, time samples were taken hourly and sparged with air immediately to stop the reduction, centrifuged at 5000 rpm for 5 min then analysed.

3.3 Bio-removal of Pt(II) metal ions from solution

3.3.1 pH experiments

A 2 mL concentrated cell suspension with an OD600 of 1.13 and 1.18 (±0.1) *for Desulfovibrio desulfuricans* and SRB respectively was diluted in a 5 mL buffer containing 20 mg/L of a 1000 ppm Platinum standard solution with 25 mM of formate solution. The pH was adjusted from 1 - 10 using NaOH and HCl, sparged with nitrogen and incubated for 12 h similar to the Pd experiments.

3.3.2 Pt(II) Concentration experiments

A 2 mL concentrated cell suspension with an OD_{600} of 0.982 and 1.04 ($\pm$ 0.1) for *Desulfovibrio desulfuricans* and SRB respectively was diluted in a 30 mL buffer containing 20 mg/L, 50 mg/L, 80 mg/L, 110 mg/L and 140 mg/L of 1000 ppm Platinum standard solution (Glassworld), and 25 mM of formate solution. The pH was adjusted to 4 using HCl and NaOH, sparged with nitrogen and incubated for 7 h similar to the Pd experiments. Time samples were taken hourly and sparged with air immediately to stop the reduction, and centrifuged at 5000 rpm for 5 min then analysed.

3.4 Assay of metal ions

Pd(II) and Pt(II) levels in the supernatants were determined by Atomic Absorption Spectrometry, AAnalyst 400 spectrometer fitted with a S/N 201S8070301 Autosampler Model 510. The AA used an air-acetylene flame, Perkin-Elmer Lumina Pd hallow cathode lamp at a wavelength of 244.79 nm with a corresponding energy of 79 and Perkin-Elmer Lumina Pt hallow lamp at a wavelength of 265.95 with a corresponding energy of 73.

3.5 Analytical methods

3.5.1 Scanning Electron Microscopy (SEM) and Energy Dispersive Spectroscopy (EDS)

The morphology of Pd-loaded and Pt-loaded cells was determined using SEM and EDS, the cells were fixed in 2.5% (w/v) glutaraldehyde/formaldehyde fixative for 1 h, washed with 0.007 M phosphate buffer centrifuged three times and post fixed in 1 % osmium tetroxide for 30 min. Cells were washed with phosphate buffer again then dehydrated in 30 %, 50 %, 70 %, 90 %, and 100 % ethanol for 15 min each however left in 100 % ethanol for 30 min. Followed by a fixative of a 50:50 mixture of 100 % ethanol and Hexamethyldisilazane for 1 h, then resuspended in 100% Hexamethyldisilazane for 1 h. After preparation a drop of the cells was placed on a cover slip and allowed to dry overnight. Dry cover slips were coated with carbon and viewed using a Zeiss Ultra Plus FEG-SEM. Energy Dispersive Spectroscopy (EDS) analysis was done on Oxford instruments Aztec 3.0 SP1 software at 1.5 kV.

3.5.2 Transmission Electron Microscopy (TEM)

Pd-loaded and Pt-loaded cells were prepared using a similar procedure to that described for SEM until the dehydration stage. The cells were resuspended in a 50:50 mixture of 100 % ethanol and

epoxy resin for 1 h, then resuspended in 100 % epoxy resin for 4 h. After 4 h cells were centrifuged and embedded in fresh epoxy resin in a mould, placed in an oven to polymerize for 36 h. The resulting block was trimmed, sectioned and contrasted with uranyl acetate and lead citrate and viewed using JEOL JEM 2100F TEM

3.5.3 X-ray Diffraction (XRD)

XRD analysis was conducted on the Pd-loaded cells to determine the presence of Pd(0) and the quantity of the sample was adequate enough to quantify as compared to Pt- loaded cells- the sample quantity was significantly low (< 0.5 g) to perform XRD. The samples were dehydrated in 100 % ethanol and allowed to dry in an oven. After drying samples were analysed using a PANalytical X'Pert Pro powder diffractometer in θ–θ configuration with an X'Celerator detector and variable divergence and fixed receiving slits with Fe filtered Co-Kα radiation ($\lambda = 1.789$ Å). The phase identification was determined by selecting the best–fitting pattern from the ICSD database to the measured diffraction pattern, using X'Pert High score plus software.

3.5.4 Fourier-transform infrared spectroscopy (FTIR)

FTIR analysis was conducted to detect key functional groups on the cell surface of the organisms. Pd-loaded cells and Pt-loaded cells were air dried and analysed using PerkinElmer 100 Spectrometer with MIRacle ATR with Zn/Se.

3.6 16S rRNA sequence analysis for SRB

Metagenomic analysis of the full 16s gene amplicons was sequenced on the Sequel system by PacBio (www.pacb.com). Raw subreads were processed through the SMRTlink (v7.0.1) Circular Consensus Sequences (CCS) algorithm to produce highly accurate reads (>QV40). These highly accurate reads were then processed through vsearch (https://github.com/torognes/vsearch) and taxonomic information was determined based on QIMME2. Report generation command used: $create_vsearch_single_sample_pdf_report_pacbio.py200131_Cell1_ccs-lbc15-SRB1.Q20.otu_table.tsv LBC15 SRB1 r200131 16s.

CHAPTER 4: RESULTS AND DISCUSSION

4.1 Choice of bacteria for reduction studies

In this study SRB were isolated from sludge from a wastewater treatment plant in Brits, North West, South Africa. The site was chosen because of its proximity to a mining area (Figure 4.1). Therefore, it receives bulk domestic influent and mine influent. For this reason, microorganisms isolated from the plant sludge are hypothesized to have accumulated certain metal resistant mechanisms that can be exploited to reduced Pd(II) and Pt(II). The isolated consortium was compared against *Desulfovibrio desulfuricans* a well-studied model organism for metal reduction studies. Not much has been reported on SRB as a consortium in metal reduction studies. Hence it was chosen in this study to investigate its reduction potential. In addition, a consortium is said to be less liable to contamination from other organisms and offers adaptability to minor environmental changes therefore, it has an advantage over pure cultures in environmental biotechnology (Rashamuse and Whiteley, 2007).

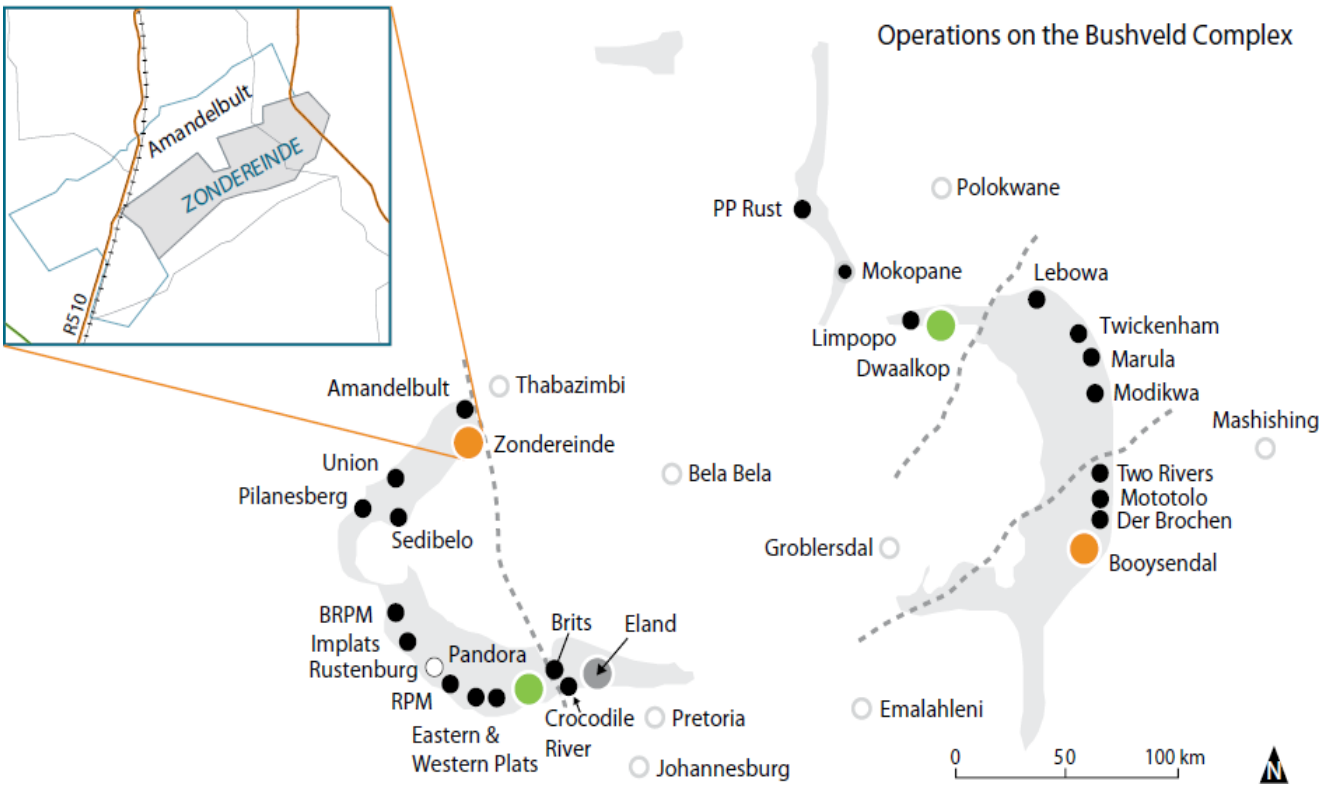

Figure 4.1: Depicting mine operations on the Bushveld complex, the black dots depict the different mines found on the complex

4.1.1 16S rRNA sequence analysis for the consortium

Metagenomics analysis was performed on the isolated consortium using 16S rRNA sequencing to identify the strains. The results revealed 62.22 % of the sample consisted of *Desulfosporia species*, 20.27 % an unknown bacterium, 9.68% *Desulfotomaculum aeronauticum* and 0.079% *Clostridium tetani*, in total 15 possible Pd and Pt reducing strains were identified (Figure 4.2), (Table 4.1).

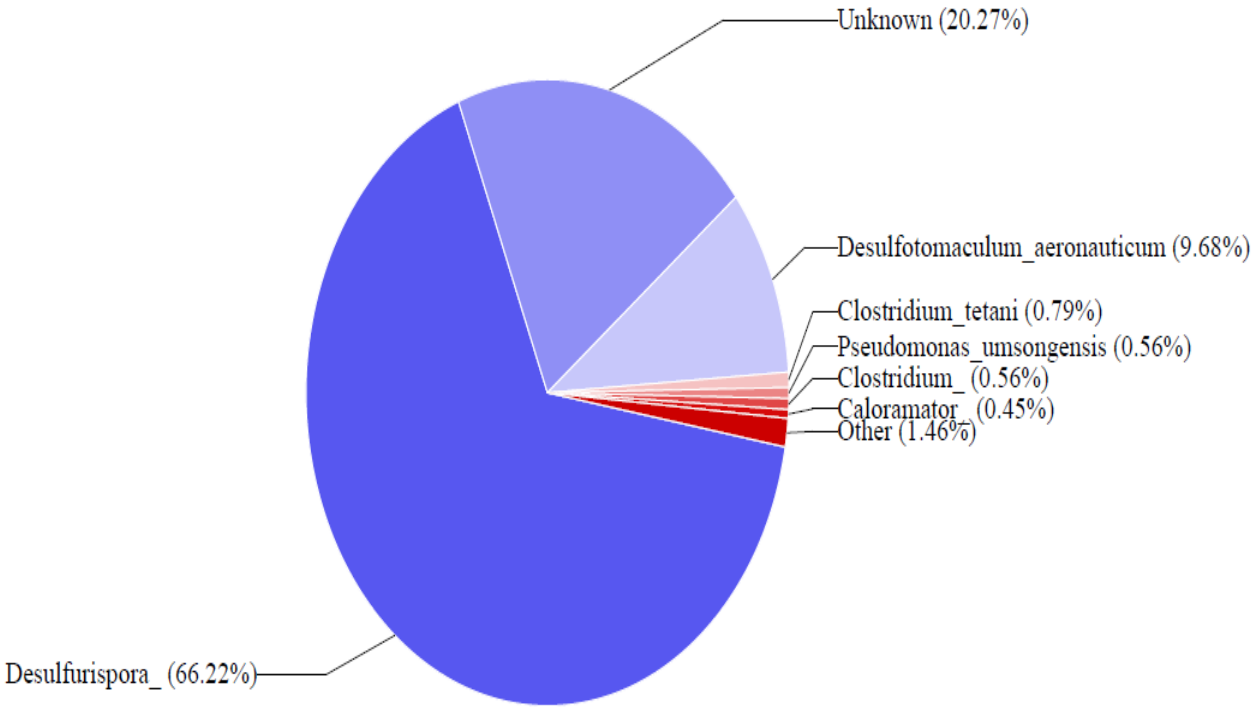

Figure 4.2: Chart depicting species of SRB identified from the Brits wastewater treatment sludge.

Table 4.1: Metagenomics data on the 16S rRNA sequencing of SRB isolated from sludge

Species	Read Count	Percentage %
Desulfurispora	588.0	66.22
Unknown	180.0	20.27
Desulfotomaculum aeronauticum	86.0	9.68

Clostridium tetani	7.0	0.79
Pseudomonas umsongensis	5.0	0.56
Clostridium	5.0	0.56
Caloramator	4.0	0.45
Clostridium subterminale	3.0	0.34
Clostridium cellulovorans	2.0	0.23
Clostridium celatum	1.0	0.11
Acidopila rosea	1.0	0.11
Clostridium botulinum	1.0	0.11
Pseudomonas veronii	1.0	0.11
Unknown	1.0	0.11
Clostridium thermopalmarium	1.0	0.11
Streptococcus alactolyticus	1.0	0.11
Clostridium gasigenes	1.0	0.11

4.2 The influence of medium pH on Pd(II) removal from solution

Bacterial organisms in this study were observed to be active at very low pH values. SRB were able to remove 48% and 58% of Pd(II) at pH 1 and 2 respectively, *Desulfovibrio desulfuricans* removed 38% and 49% of Pd(II) at pH 1 and 2 respectively as shown in Figure 4.3. With an increase in pH there was an increase in removal of Pd(II) until a maximum of 90% and 83% for SRB and *Desulfovibrio desulfuricans* respectively at a pH of 4. Followed by a decrease in removal reaching a minimum of 68% and 64% at pH 10 for SRB and *Desulfovibrio desulfuricans* respectively (Figure 4.3). The percentages removed were calculated using the following formula:

$$\%\text{removed} = \frac{C_i - C_f}{C_i} \times 100 \quad (4.1)$$

- C_I = initial concentration
- C_f = Final concentration,

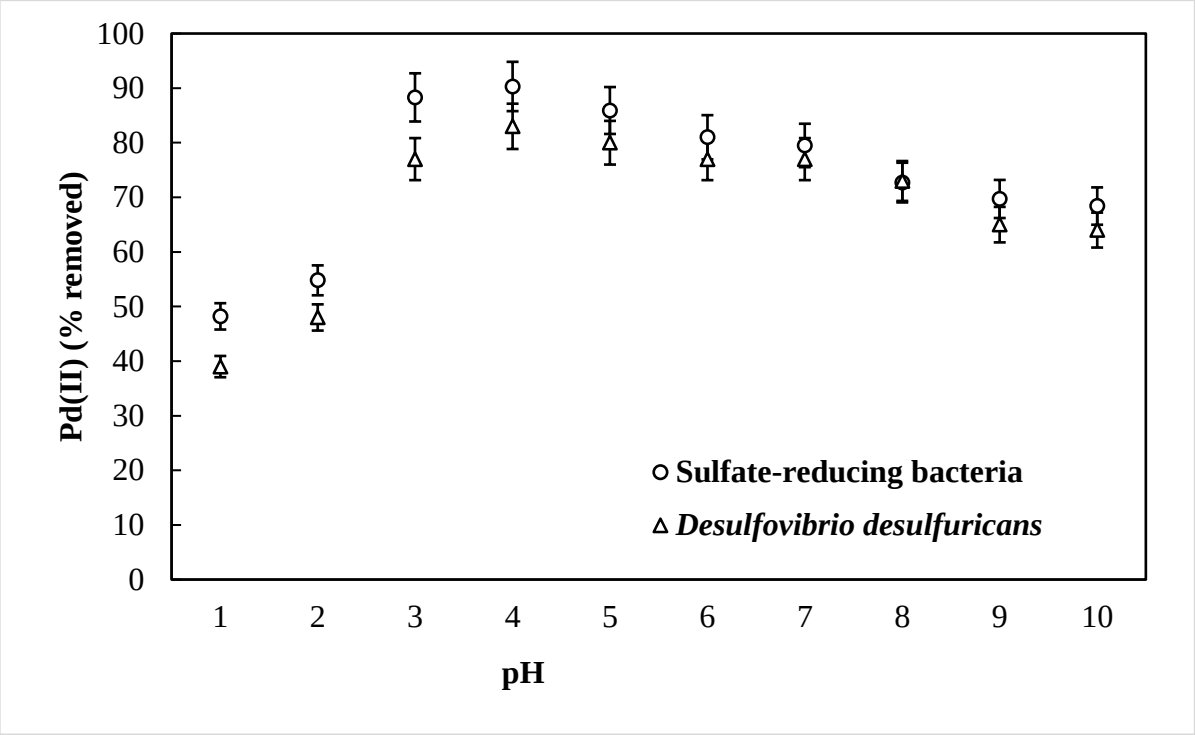

Figure 4.3: The effects of pH on Pd(II) removal from solution by SRB and *Desulfovibrio desulfuricans* after 12 h of incubation.

The dependency of microbial Pd(II) removal on the pH of the environment could be due to various functional groups on the bacterial cell wall and the chemistry of the Pd particle. Functional groups capable of metal sorption are usually basic, for example carboxyl, phosphate and amine groups, which are deprotonated at high pH values. Therefore, as the pH increases more functional groups dissociated and become available for ion reduction due to less competition from protons (Rashamuse and Whiteley, 2007). Hence, minimal removal was observed at low pH values of 1 and 2 in this study. Another factor to consider is the influence of the solution media at a given pH. Pd speciation is strongly related to pH and chloride concentration conditions (Vargas et al., 2004). When chloride concentrations are high above 10 mmol/dm^3 approximately 75% of anionic species such as $PdCl^-$ and $PdCl^{2-}$ are present at low pH values, and metal hydroxylation becomes

significant at pH values higher than 3.5 (Ruiz et al., 2000). When chloride concentrations are lower than 0.5 mmol/dm^3 approximately 90% of cationic species such as $PdCl_2$, $PdCl^+$ and $Pd^{2+}$are predominant at low pH values and hydroxyl complexes such as $Pd(OH)^+$, $Pd(OH)_2$, and $Pd(OH)_4^{2-}$ appear at a pH above 2.5. This phenomenon could also explain the high removal percentage of Pd(II) observed at pH 4 instead of 2(Vargas et al., 2004). Chloride concentrations were above 10 mmol/dm^3 at low pH values because of chloride anions from the HCl used to adjust the pH in this study. Therefore, it is likely that cationic species favourable for Pd biosorption/reduction were predominant at pH values higher than 3.5.

4.3 Influence of pH on microbial biomass

Microbial biomass provides polymers as ligand groups on to which metal species can bind; polymers such as proteins, nucleic acids, and polysaccharides, which would give the biomass a charge on its surface in the form of insoluble functional groups (Niu and Volesky, 1999, Vargas et al., 2004).

In this study, FTIR analysis was used to determine which functional groups are responsible for binding Pd(II) species and to predict the influence of media pH on those functional groups. SRB and Desulfovibrio desulfuricans cells treated with Pd(II) were compared against SRB and Desulfovibrio desulfuricans cells that did not receive treatment (control). The results showed a peak at 1650 cm^{-1} for both cell types and a peak at 2300 cm^{-1} for SRB (Figure 4.4), and according to Table 4.2 and 4.3 adapted from Coates (2006), 1650 cm^{-1} is characteristic of an amine functional group and 2300 cm^{-1} is characteristic of a nitrile functional group.

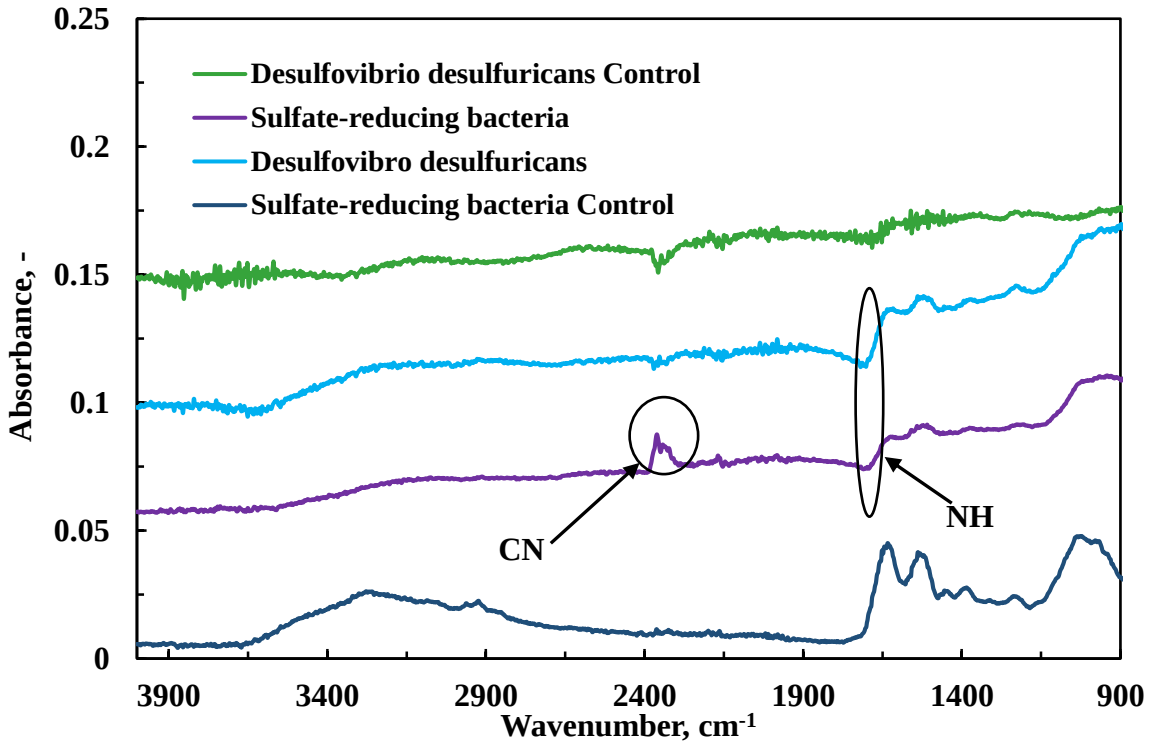

Figure 4.4: FTIR results showing the wavenumber of absorption bands that correspond to certain functional groups involved in metal sorption on SRB and *Desulfovibrio desulfuricans*.

In addition, *Desulfovibrio species* are gram negative bacteria which contain about 5 - 10% of peptidoglycan in their cell wall. Peptidoglycan is a polymer that contains two sugar derivatives; *N*-acetylglucosamine and *N*-acetylmuramic acid which mainly provides carboxyl and amine groups (Beveridge, 1999). The pKa of carboxyl groups in the cell wall is usually 4.8 while the amine groups have a pKa of approximately 7–10 (Fein et al., 1997). As the pH decreases, the negatively charged carboxyl groups and the neutral weak base amine groups become protonated, offering positive binding sites (Niu and Volesky, 1999). However, at low pH values due to HCl, the surface presents protonated groups which attract Cl anions electrostatically and positions them as counter anions that are exchanged with anionic $PdCl_2$ species, resulting in decreased Pd biosorption (Vargas et al., 2004). Indeed in this study HCL was used in pH adjustments which could explain the observed low reduction of Pd(II) at low pH values of 1 and 2 (Figure 4.3).

Table 4.2 Amine and amino compound group frequencies. Adopted from (Coates, 2006)

Origin	Group frequency wavenumber (cm^{-1})	Assignment
		Primary amino
N-H	3400–3380 +3345–3325	Aliphatic primary amine, NH stretch
N-H	3510–3460 +3415–3380	Aromatic primary amine, NH stretch
N-H	1650–1590	Primary amine, NH bend
C-H	1090–1020	Primary amine, CN stretch
		Secondary amino
>N-H	3360–3310	Aliphatic secondary amine, NH stretch
>N-H	~3450	Aromatic secondary amine, NH stretch
>N-H	3490–3430	Heterocyclic amine, NH stretch
=N-H	3350–3320	Imino compounds, NH stretch
>N-H	1650–1550	Secondary amine, NH bend
C-N	1190–1130	Secondary amine, CN stretch
		Tertiary amino
C-N	1210–1150	Tertiary amine, CN stretch
		Aromatic amino
C-N	1340–1250	Aromatic primary amine, CN stretch
C-N	1350–1280	Aromatic secondary amine, CN stretch

C-N	1360–1310	Aromatic tertiary amine, CN stretch

Table 4.3: Examples of nitrogen multiple and cumulated double bond compound group frequencies. Adapted from (Coates, 2006)

Group Frequency ($\boldsymbol{cm}$)$^{-1}$	**Functional groups**
2280–2240	Aliphatic cyanide/nitrile
2240–2220	Aromatic cyanide/nitrile
2260–2240/1190–1080	Cyanate (-OCN and C-OCN stretch)
2276–2240	Isocyanate (-N=C=O asymmetrical stretch)
2175–2140	Thiocyanate (-SCN)
2150–1990	Isothiocyanate (-NCS)
1690–1590	Open-chain imino (-C=N-)
1630–1575	Open-chain azo (-N=N-)

4.4 Removal of Pd(II) from solution

4.4.1 Optimum cell concentration

Two different cell concentrations were investigated to determine the optimum cellular concentration for Pd(II) removal from solution. Cell concentration with an OD_{600} of 0.3 (0.0028 g/L), tested with $Pd(NH_3)_4Cl_2$ solution produced a black precipitate after 12h of incubation (Figure 4.5). A precipitate which is suggested to be made up of Pd(0) nanoparticles attached to the cell walls and is produced through a reduction process that is mediated by hydrogenase enzymes (Lloyd et al., 1998, Yong et al., 2002b). In addition 90% of 2mM of Pd(II) was removed by SRB however, with an increase in Pd(II) concentration from 4mM to 8Mm the percentage decreased to 74% and 72% respectively. The same trend was observed for *Desulfovibrio desulfuricans* (Figure 4.6).

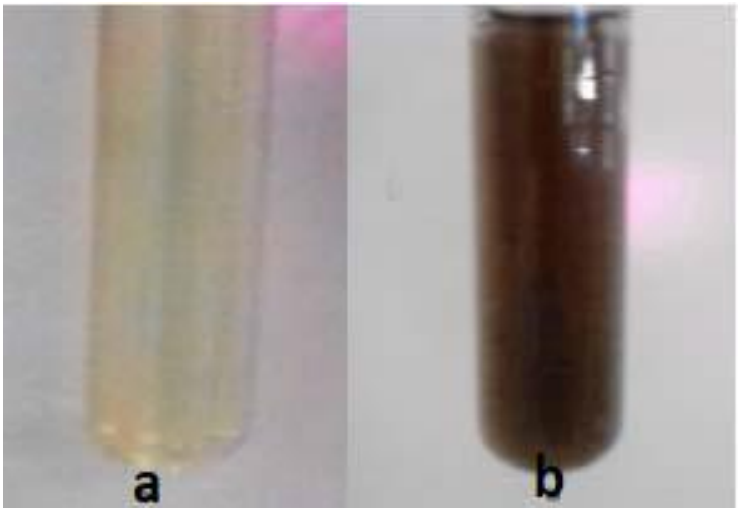

Figure 4.5: (a) buffer containing $Pd(NH_3)_4Cl_2$, and formate before inoculation with bacteria, (b) Blackening of the buffer possibly due to Pd nanoparticle formation by SRB.

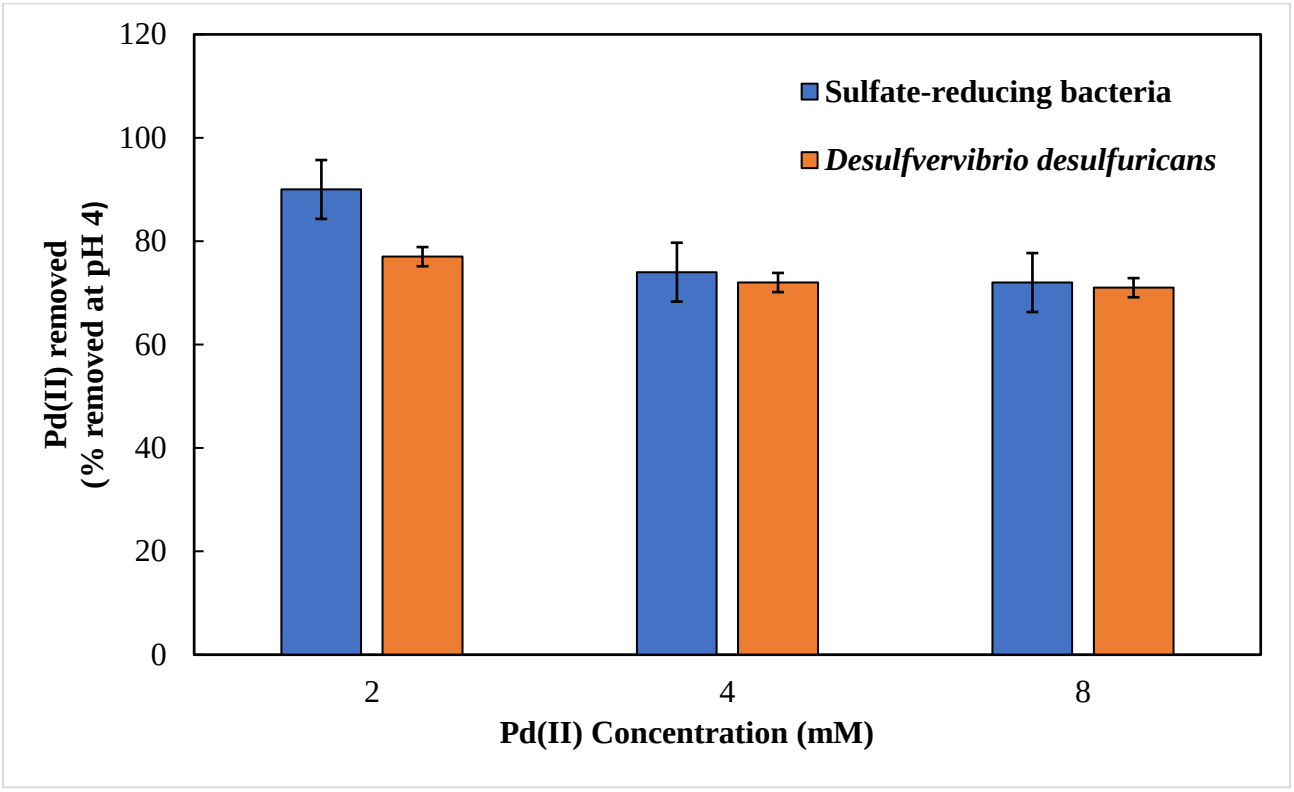

Figure 4.6: The effects of Pd(II) concentration on the removal of Pd(II) by SRB and *Desulfovibrio desulfuricans* with an OD_{600} of 0.3 at a pH 4 after 12 h of incubation.

When the concentration of cells was increased to an OD_{600} of 0.980 (0.085 g/L) and 0.933 (0.06 g/L) for *Desulfovibrio desulfuricans* and SRB respectively, the results showed an improved percentage of Pd(II) removal. An optimum of 96% of Pd(II) was removed at 2mM followed by 95.9% and 95.1% at concentrations 4 mM and 8 Mm respectively. An optimum of 99.3% was removed by *Desulfovibrio desulfuricans* at 2 mM which decreased to 93.1% at 8 mM (Figure 4.7). Increasing the cell concentration increased the percentage of reduction, therefore, the increased cell concentration was used for further Pd reduction experiments.

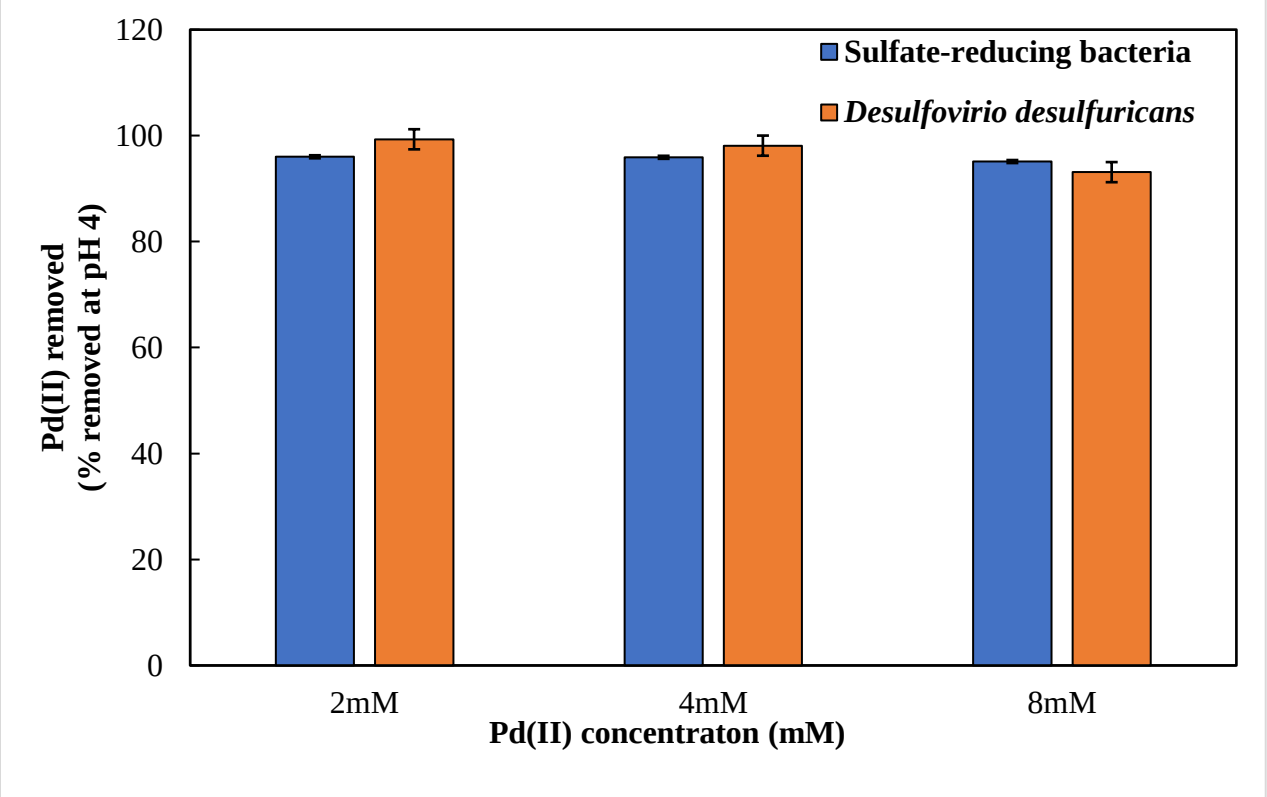

Figure 4.7: The effects of Pd(II) concentration on the removal of Pd(II) by SRB and *Desulfovibrio desulfuricans* with an OD_{600} of 0.9 at pH 4 after 12 h of incubation.

4.4.2 Batch experiments

The concentration of Pd(II) was converted from mM to mg/L (Table 4.4). Cells tested with $Pd(NH_3)_4Cl_2$ produced a black precipitate after 6 h of incubation, however a black and silver precipitate was observed from 6 mM (964.3 mg/L) (Figure 4.8).

Table 4.4: Conversion of initial Pd(II) concentration mM to mg/L

Concentration (Mm)	Concentration in (mg/L)
2	356.3
4	631.4
6	964.3
8	1094.2
10	1607.1
12	1928.5

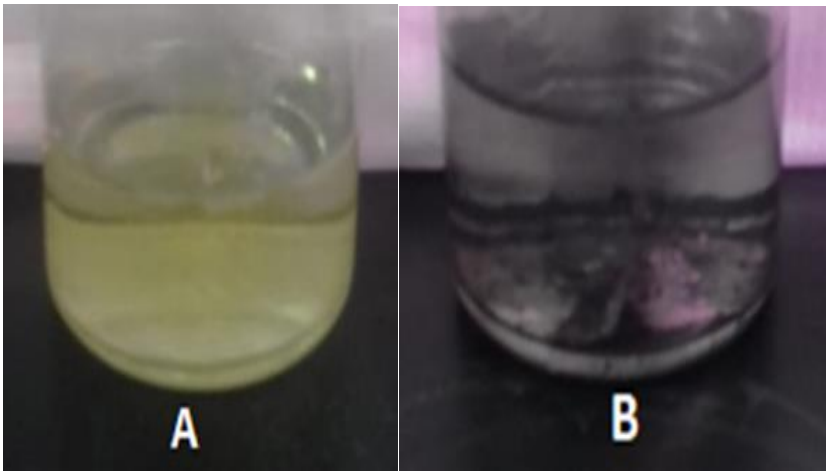

Figure 4.8: Removal of 6 mM Pd(II) metal ions by SRB; A) The control contains Pd($N{H_3}$)$_4$Cl_2 solution and formate, B) The experimental, consisting of SRB, possible Pd(0), and water.

Approximately above 95 % of Pd(II) was removed from solution in 6 h across all concentrations by SRB as shown in Table 4.5. *Desulfovibrio desulfuricans* performed exceptionally well at low Pd(II) concentrations; as the concentration increased the percentage removed decreased slightly, from of 99.3% at a concentration of 356.3 mg/L to 83.5% at a concentration of 1928.5 mg/L (Table 4.6). Data analysis revealed significant difference in the treatment of the Pd(II) solution with SRB and *Desulfovibrio desulfuricans* as compared to their respective controls ($p < 0.05$). However, there was no significant difference in the percentage removal efficiencies between the two treatments ($p > 0.05$) demonstrating efficient reduction of Pd by both treatments.

Table 4.5: Effects of different concentrations of Pd(II) at various exposure times on the percentage reduction of Pd(II) by SRB.

Time (h)	**Concentration (mg/L)**					
	356.3	631.4	964.3	1094.2	1607.1	1928.5
(%) Removed						
0	0	0	0	0	0	0
1	93.5	91.8	94.8	86.4	36.4	75.8
2	89.6	89.6	85.5	58.3	31	66.9
3	93.3	99.1	92.5	82.9	69.9	76.1
4	92.4	99.5	91.4	96.4	69.7	76
5	93	99.8	93.9	93.3	79.5	86.9
6	96	95.9	96	95.1	93	94.3

Table 4.6: Effects of different concentrations of Pd(II) at various exposure times on the percentage reduction of Pd (II) by *Desulfovibrio desulfuricans.*

Time (h)	**Concentration (mg/L)**					
	356.3	631.4	964.3	1094.2	1607.1	1928.5
(%) Removed						
0	0	0	0	0	0	0
1	77.1	86.1	88	81.6	81.5	35.4
2	60.8	66.6	85.5	68.3	79.7	35.2

3	86.1	95.4	89.5	97	85.8	69.2
4	99.6	96.7	89.2	96.8	85.8	69
5	99	98	90.3	97.6	91.8	78.4
6	99.3	98.1	98.3	93.1	93.6	83.5

However, before maximum removal was achieved there were fluctuations observed for the first 2 h of incubation for both treatments (Figure 4.9 and 4.10). The fluctuations could be attributed to pH changes discussed earlier in this chapter, caused by interactions with ions in solution and complexes formed at the bacterial cell surface (Capeness et al., 2015, Sethuraman and Kumar, 2011).

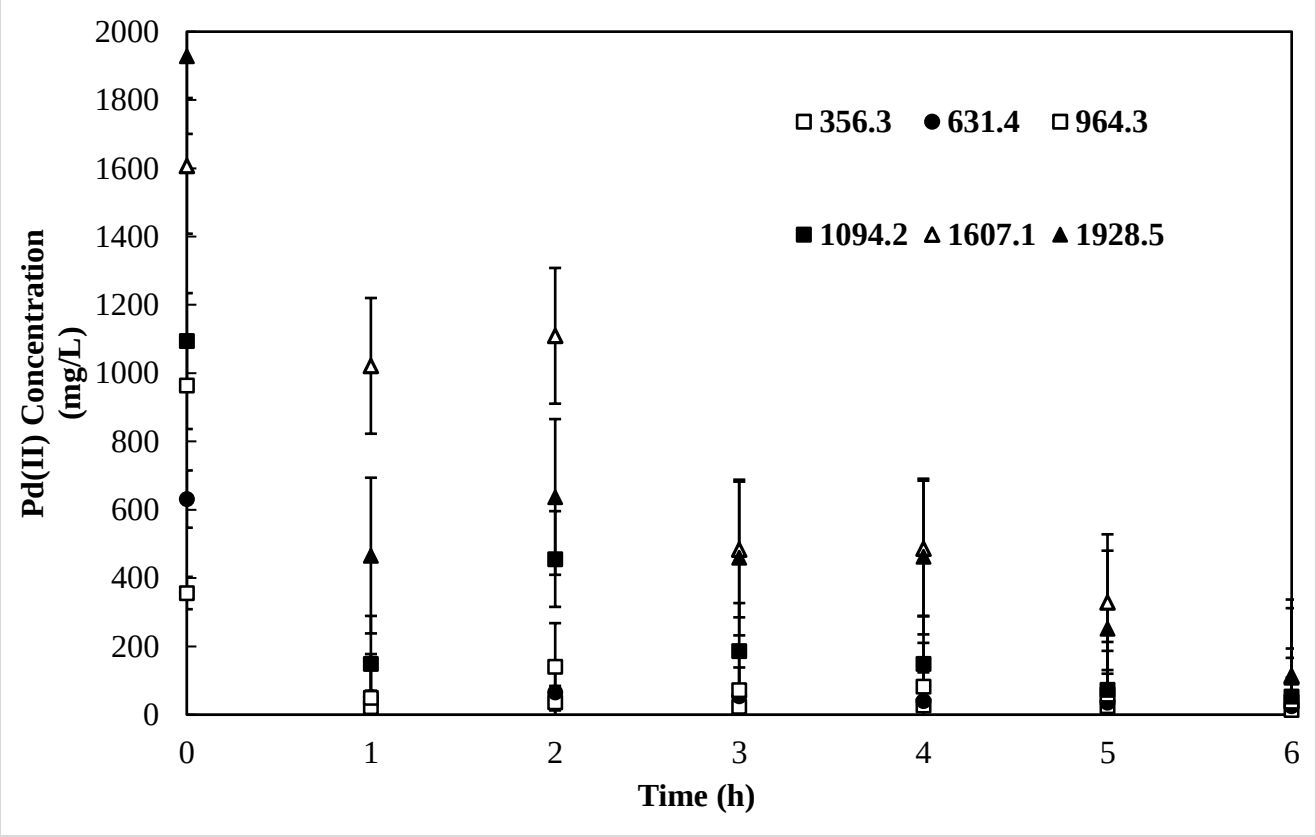

Figure 4.9: Pd(II) reduction by SRB at different concentrations over a 6 h incubation period.

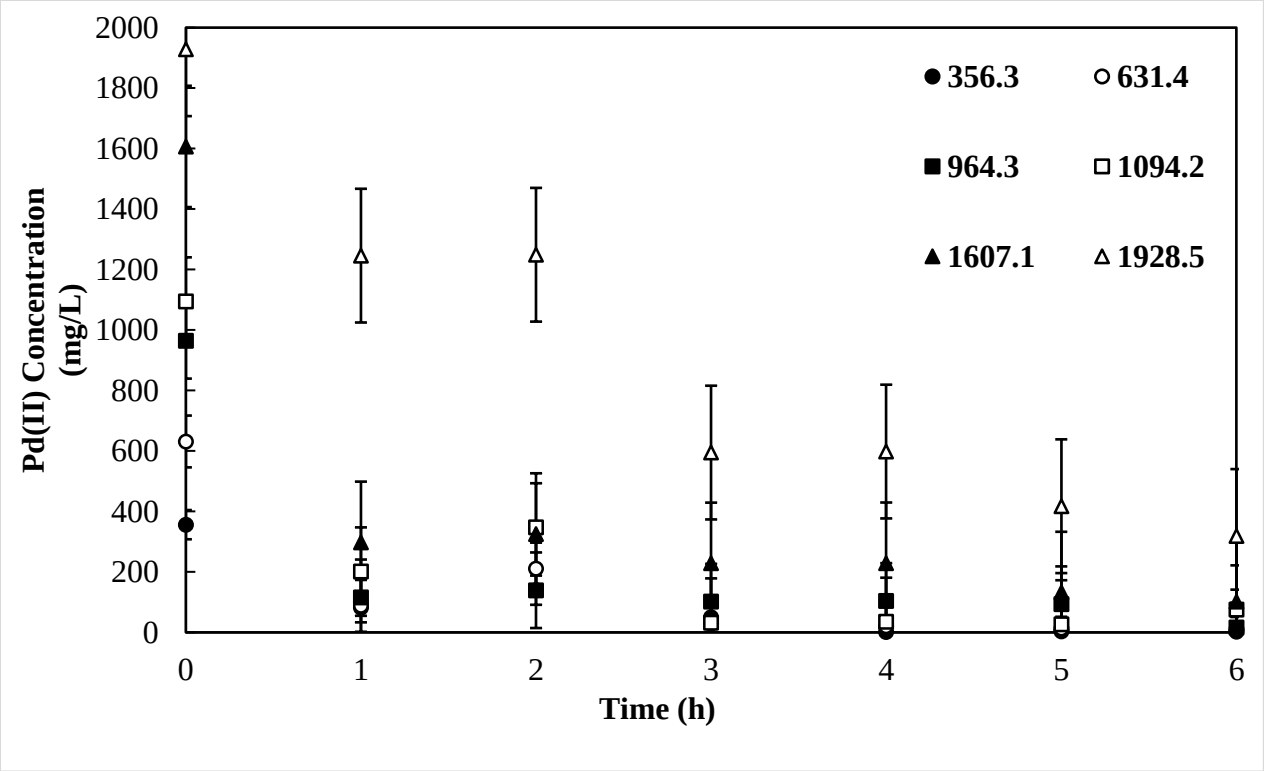

Figure 4.10: Pd(II) reduction by *Desulfovibrio desulfuricans* at different concentrations over a 6 h incubation period.

4.4.3 Biodeposition

Post incubation a black and silver precipitate formed which was suggested to be made up of Pd(0) nanoparticles attached to the cell walls, produced through a reduction process that is mediated by hydrogenase enzymes. Pd(II) bioreduction can be described as an enzymatically accelerated biomineralization process in which the activation energy for nucleation is lowered by the interfacial energy. Leading to target ions forming crystal nuclei that interact initially with local size binding sites resulting into reduction via hydrogen using the reducing power focused by hydrogenase activity as previously reported for the reduction of Tc(VII) and Pd(II) (De Luca et al., 2001, Lloyd et al., 1997, Lloyd et al., 1998). In addition, Pd reducing cells play a tri-functional role. Firstly, as enzyme catalysts where formate hydrogenase or hydrogenase activity provide electrons. Secondly, as nucleation sites for foci of Pd(0) metal deposition for subsequent crystal growth. Thirdly, as a scaffold for crystals of Pd(0) able to autocatalyze further reaction by acting as a sink for formate and hydrogen trapping and production of highly active H^+ from formate or hydrogen (Figure 4.11), (Wahl et al., 2001).

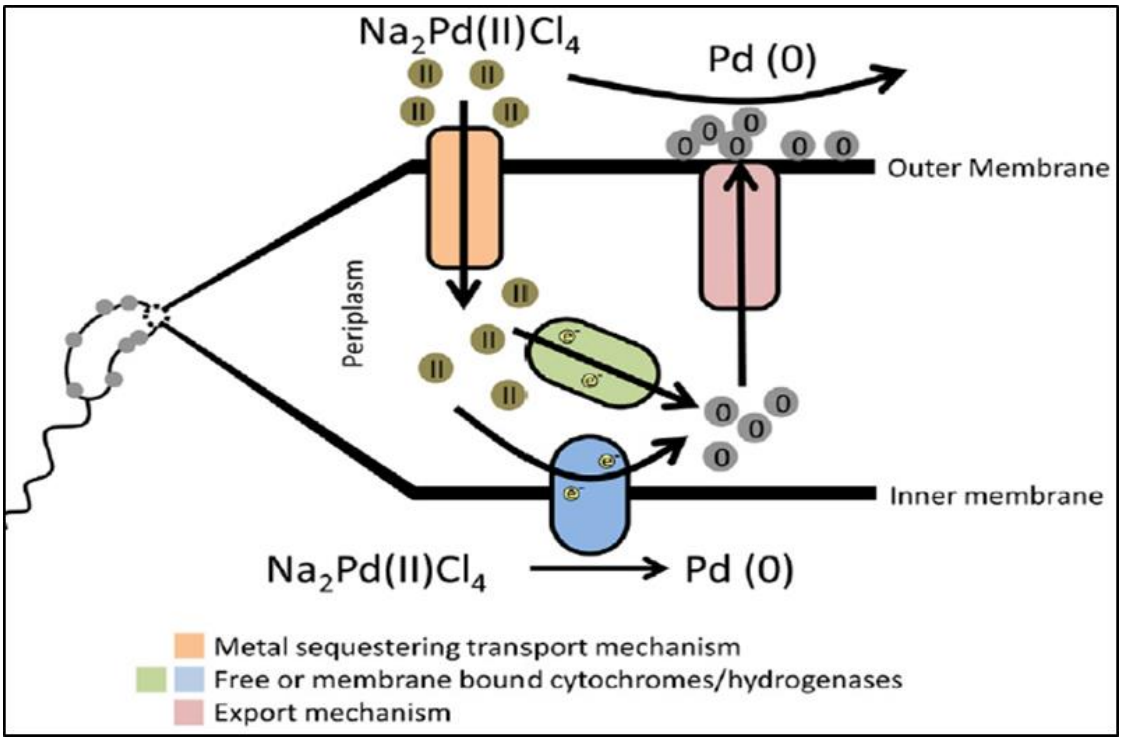

Figure 4.11: Proposed method for palladium reduction to Pd(0) in the periplasm of *Desulfovibrio desulfuricans*. Pd(II) ions are taken by the bacterium across the outer membrane to the periplasm where they are reduced by cytochromes and hydrogenases to form Pd(0) (Capeness et al., 2015).

Having the above in mind, TEM and SEM-EDX results showed deposits on the surface of the Palladium challenged bacteria (Figure 4.12 and 4.13). This is in accordance with observations by Yong et al. (2002a), where deposits were found to be between 40 nm and 50 nm in size. Therefore, it can be assumed that Pd(II) in this study was absorbed by cells and the reduction happened via a periplasmic hydrogenase as reported previously for the reduction of Pd(II) by Lloyd et al. (1998). In addition, the cell surface of the bacteria provides a template for the organisation of the growing crystals, which present a larger surface area which may function as an enhanced chemical catalyst as illustrated in Figure 4.11. This phenomenon can also be observed on the TEM results where crystal like structures can be seen in and on the cell wall of the bacteria as clearly defined dark black deposits (Figure 4.12).

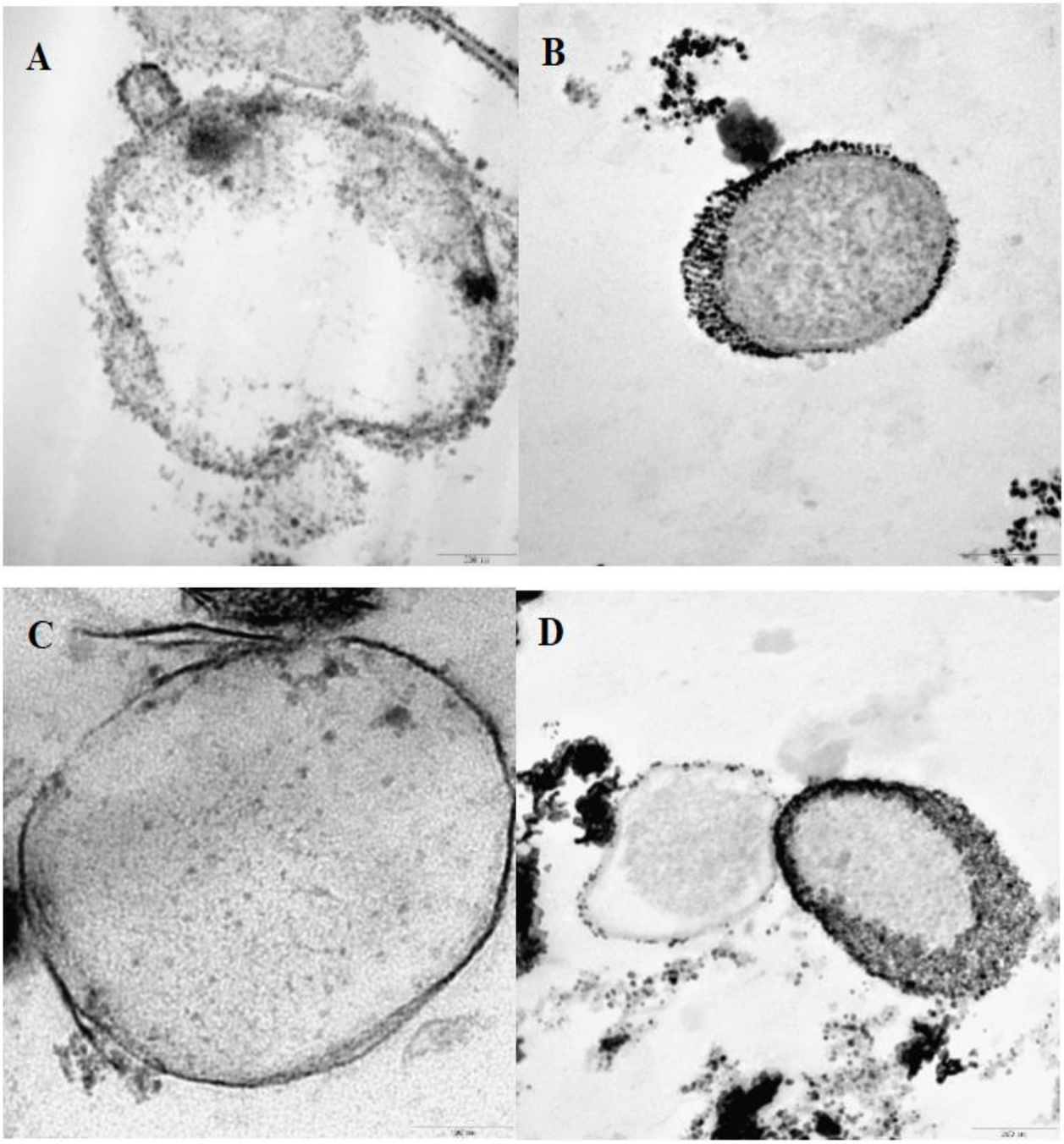

Figure 4.12: TEM images of Pd(0) deposited on the cell wall. A) unchallenged SRB control, B) SRB challenged with Pd(II), C) unchallenged *Desulfovibrio desulfuricans* control, D) *Desulfovibrio desulfuricans* challenged with Pd(II)

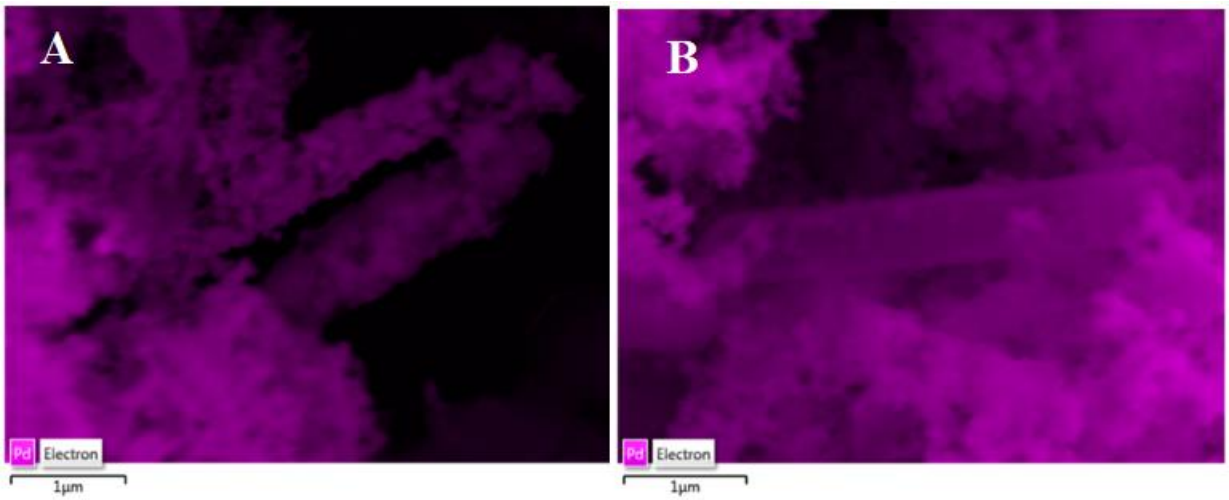

Figure 4.13: SEM-EDX images showing the presence of Pd on the cell wall. A) elemental map of Pd on SRB; B) elemental map of Pd on *Desulfovibrio desulfuricans.*

Further analysis revealed the presence of other elements; the major four being Pd at 82.79 Wt%, Fe at 2.94 Wt%, Os at 2.98 Wt% and S at 2.79 Wt% for SRB (Table 4.10). 8.76 Wt% O, 3.05 Wt% S, 3.45 Wt% Fe and 74.42 Wt% Pd for *Desulfovibrio desulfuricans* (Table 4.7 and 4.8). Osmium tetraoxide was used as a fixative during cell preparation for SEM analysis which could explain the presence of O and Os in both samples. Fe and S are one of the products formed during cell respiration meaning they were produced during cell culture.

Table 4.7: EDS elemental analysis of SRB challenged with Pd(II)

Element	Weight%	Weight% Sigma
O	2.52	0.07
Na	0.17	0.03
Si	0.13	0.02
P	0.41	0.02
S	2.78	0.03
Fe	2.94	0.07
Pd	82.79	0.36
Os	2.98	0.08
Ac	2.65	0.30
Th	2.63	0.26
Total:	100.00	

Table 4.8: EDS elemental analysis of *Desulfovibrio desulfuricans* challenged with Pd(II)

Element	Weight%	Weight% Sigma
N	2.65	0.12
O	8.76	0.07
Na	0.64	0.02
Si	0.12	0.01
P	0.99	0.02
S	3.05	0.02
Fe	3.45	0.05
Zn	0.03	0.05
Pd	74.42	0.19
Os	2.88	0.06
Ac	1.67	0.17
U	1.34	0.09
Total:	100.00	

4.4.4 Biocrystalization

XRD analysis was performed on the black and silver precipitates from the experiment. The results that the precipitate contains elemental Pd particles. The graph in Figure 4.14 shows clearly defined peaks of the sample that correspond to Pd(0) peaks. The crystal size of the particle was determined using scherrer's formula:

$$t = \frac{K\lambda}{BCos\theta_B} \tag{4.2}$$

- t – Thickness of crystallite
- K – constant dependent on crystal shape
- λ – X-ray wavelength
- B – FWHM (full with at half maximum) of the peak in radians 2θ
- θ – Bragg angle

The formula is generally used to relate the size of sub-micrometer crystallites in a solid to the broadening of a peak in a diffraction pattern. In this study the first three peaks were used to determine the crystallite size. The calculated sizes ranged from 16.9 nm ,11.1 nm and 9.6 nm (Table 4.9)

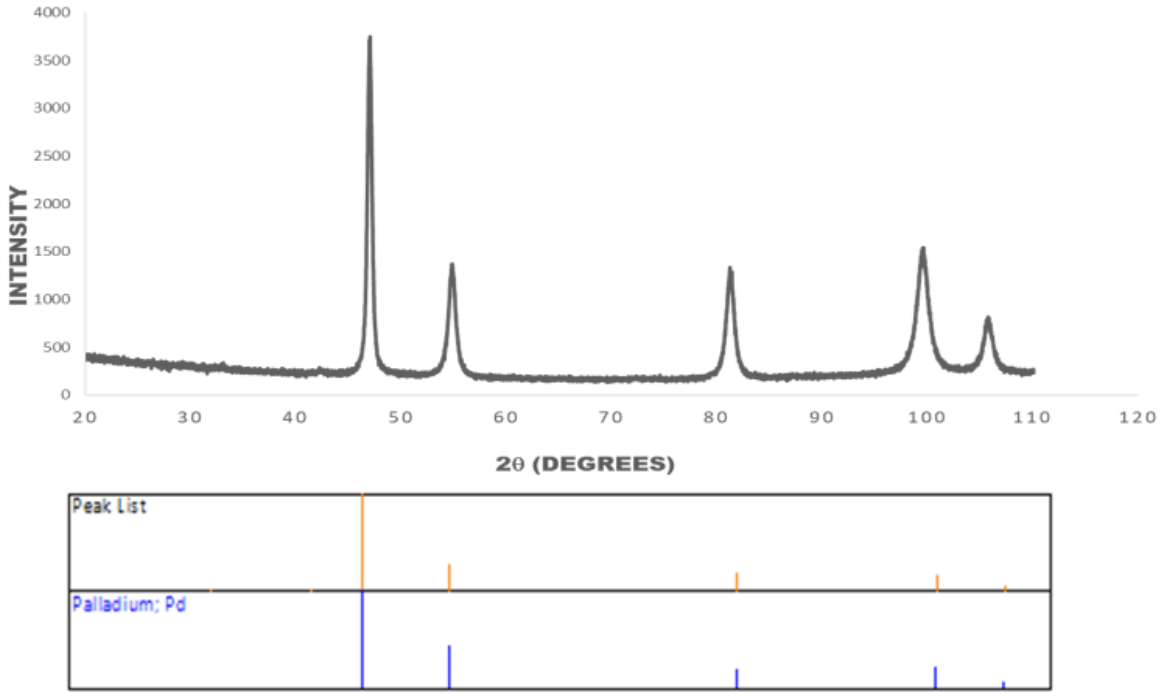

Figure 4.14: XRD graph showing clearly defined peaks of the experimental sample that correspond to Pd(0) peaks.

Table 4.9: Calculated thickness of the Pd (0) Nano particles formed based on the first three peaks

Peak number	Thickness of crystal (nm)
1	16.86188
2	11.10759
3	9.560395

Which is much lower than 50 nm reported by Yong et al. (2002b). However, smaller crystals offer an advantage over bulky crystals because they present a larger surface area and may subsequently function as enhanced chemical catalyst (Yong et al., 2002a). In a study conducted by Redwood et al. (2008), Pd(0) deposits of approximately 20 nm were reported as having clusters of approximately 5 nm -10 nm Pd(0) nanoparticles. Upon catalytic activity evaluation, bio-Pd was significantly catalytically more active than the chemical one in a hypophosphite test. In a study

conducted by Mabbett et al. (2006), bio-Pd was able to reduce 100% Cr (VI) in the 2 hours with 50 % reduction in 10 min, while chem-Pd gave 20 % reduction in 10 minutes. Therefore, the bio-Pd nanoparticles in this study have the potential to be recycled and reused in other processes as biocatalysts. However further tests would have to be conducted to explore the use of bio-Pd as a catalyst.

SRB have demonstrated that they can efficiently reduce palladium. However, ensuring the long-term stability of the product (bio-Pd or bio-Pd) for future use is a topic that requires more in-depth studies. The greatest limitation that poses a threat to bio-Palladium is poisoning of the catalyst. Sulfides are known to have a strong affinity for the Pd metal and may block the active sites of the catalyst via formation of strong Pd–S bonds and layers of sulfide around the Pd clusters (Alfonso et al., 2003). Thus, sulfide induced catalyst deactivation is a crucial challenge which hinders the full exploitation of the catalyst potential as a treatment technology for remediation of water. Therefore, a possible approach to prevent sulfide poisoning is the oxidative removal of sulfide prior to any contact with the noble metal (Angeles-Wedler et al., 2009).

4.5 Removal of Pt(II) from solution

SRB have proven to efficiently remove and reduce soluble Pd(II) into elemental Pd(0) just as *Desulfovibrio desulfuricans*. However, the formation of Pt nanoparticles by biological methods has not been fully investigated. Therefore, since platinum is just as valuable as palladium the second part of this study was to evaluate the ability of SRB and *Desulfovibrio desulfuricans* in reducing Pt(II) from aqueous solutions.

4.5.1 Influence of Medium pH on Pt(II) removal from solution.

The results suggested that a pH of 4 was the optimum condition for Pt(II) removal for SRB because an optimum of 40 % Pt(II) was removed from solution in 12 hours, and an optimum pH that ranged between 4 – 5 was desirable for *Desulfovibrio desulfuricans* which reached a maximum of 23 % removal at that pH (figure 4.15).

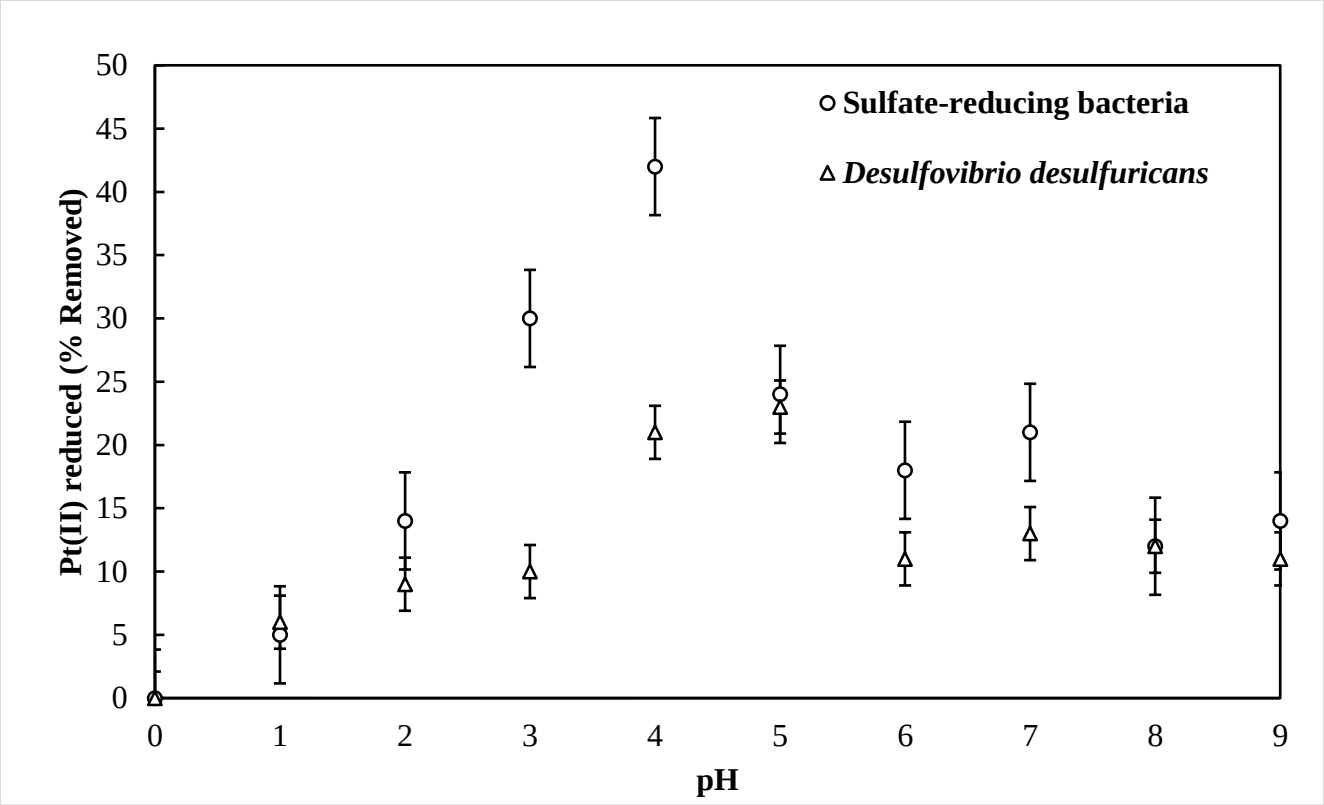

Figure 4.15: The effects of pH on Pt(II) removed by SRB and of *Desulfovibrio desulfuricans* after a 12 h incubation period.

These findings are not surprising since the removal of Pd(II) in this study was also achieved at an optimum pH of 4 by these organisms (Figure 4.3). Therefore, like Pd(II), the removal of Pt(II) could be due to various functional groups on the bacterial cell walls. Functional groups which are basic such as carboxyl, phosphate and amine groups discussed earlier under Pd(II) removal studies. Therefore, as the pH increases more functional groups dissociate and become available for ion reduction due to less competition from protons (Riddin et al., 2006, Rashamuse and Whiteley, 2007). FTIR results showed the presence of these functional groups on the cell surface of the organisms. An amine group and a carboxylate group (Figure 4.16), which is assumed became deprotonated at pH values between 4 and 5. Therefore, for further Pt(II) removal investigations a pH of 4 was used.

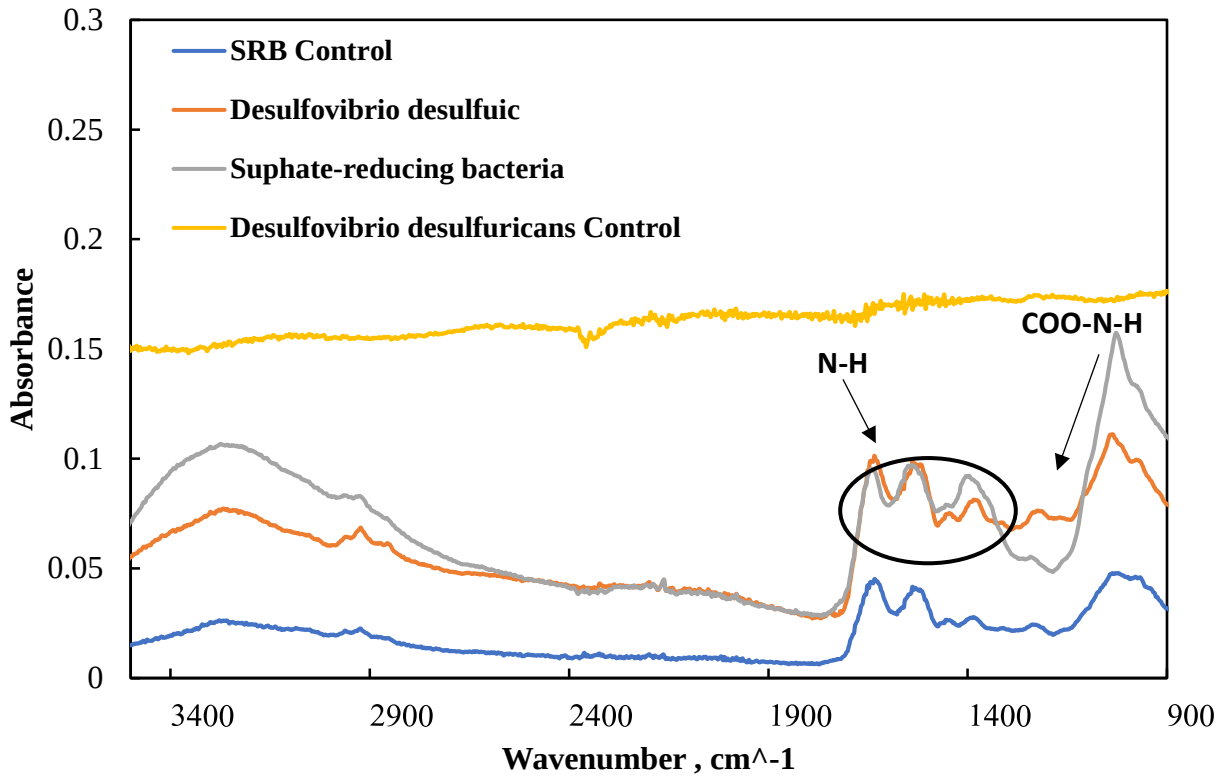

Figure 4.16: FTIR results showing wavenumber of absorption bands that correspond to certain functional groups on SRB and *Desulfovibrio desulfuricans* that are involved in Pt(II) sorption and removal from solution.

4.5.2 Batch experiments

To test the stability and efficiency of the organisms in removing Pt(II), the cells were tested with increasing concentrations of a standard solutions of platinum. Concentrations ranged from 20 mg/L to 140 mg/L. After 1 h of incubation at 30°C about 60 % of Pt(II) was removed across all concentrations, 95 % removal of 50 mg/L being the highest recorded after 1 h for SRB (Table 4.10) and a maximum of 85 % removal for 140 mg/L Pt(II) was recorded for *Desulfovibrio desulfuricans* (Table 4.11). However, after the second hour of incubation there seemed to be dissolution of Pt(II) back in solution, thereafter, irregularities could be seen till the 5^{th} h of incubation (Figure 4.17 and 4.18). This suggested that Pt(II) removal happened through a different mechanism than the one reported for palladium. After 5 h of incubation equilibrium was reached, this trend was observed in both treatments (Figure 4.17 and 4.18). Nevertheless, data analysis revealed a significant difference in the treatment of Pt(II) solution with SRB and *Desulfovibrio desulfuricans* as compared to their respective controls ($p < 0.05$). When both treatments were

compared with each other, no significant difference was observed between the two treatments ($p > 0.05$). Therefore, there is strong statistical evidence that both treatments could remove Pt(II) from solution.

Table 4.10: Effects of different concentrations of Pt(II) at various exposure times on the percentage of Pt(II) removed by SRB

Time (h)	**Concentration (mg/L)**				
	20	50	80	110	140
(%) Removed					
0	0	0	0	0	0
1	92	95	71	61	67
2	52	57	71	71	56
3	54	65	79	83	59
4	47	84	80	79	59
5	55	56	58	58	59
6	53	57	58	58	59
7	54	56	58	58	59

Table 4.11: Effects of different concentrations of Pt(II) at various exposure times on percentage of Pt(II) removed by *Desulfovibrio desulfuricans*

Time (h)	**Concentration (mg/L)**				
	20	50	80	110	140
(%) Removed					

0	0	0	0	0	0
1	55	65	67	72	85
2	52	55	63	63	68
3	62	55	61	68	76
4	78	66	63	74	80
5	48	47	48	43	43
6	53	50	46	49	48
7	56	55	54	53	53

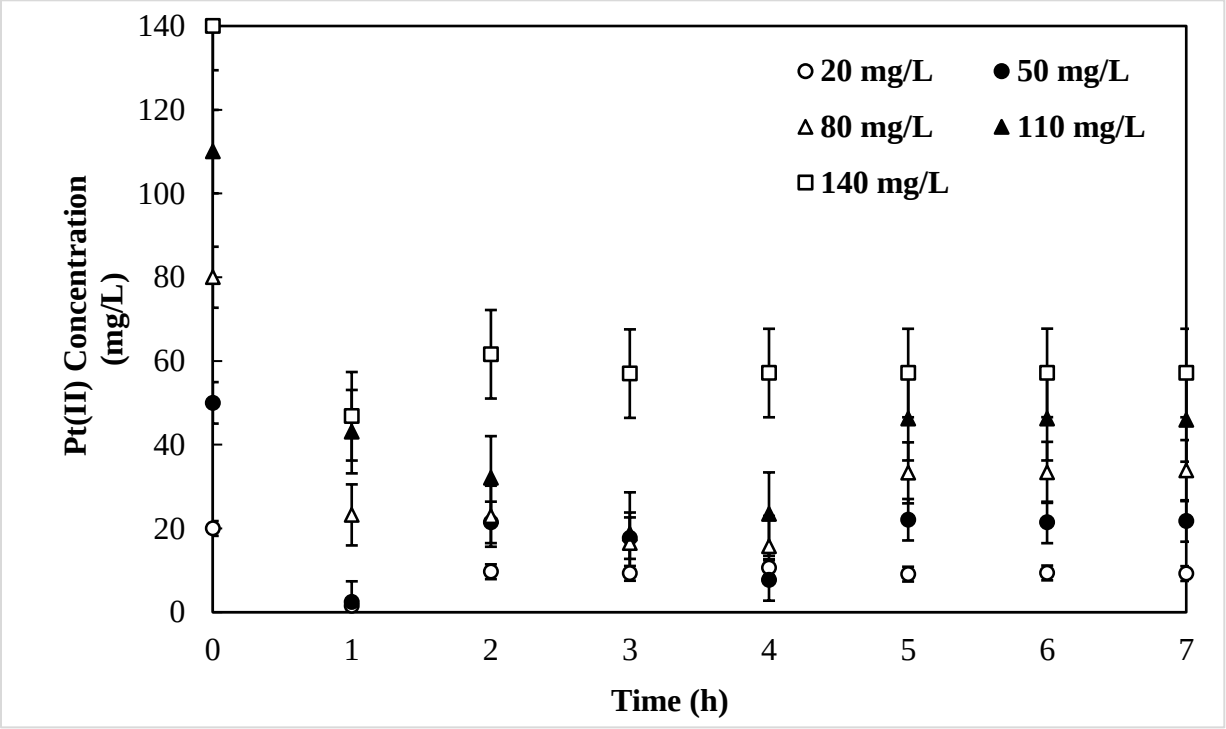

Figure 4.17: Removal of Pt(II) by SRB at different concentrations over a 4 h incubation period

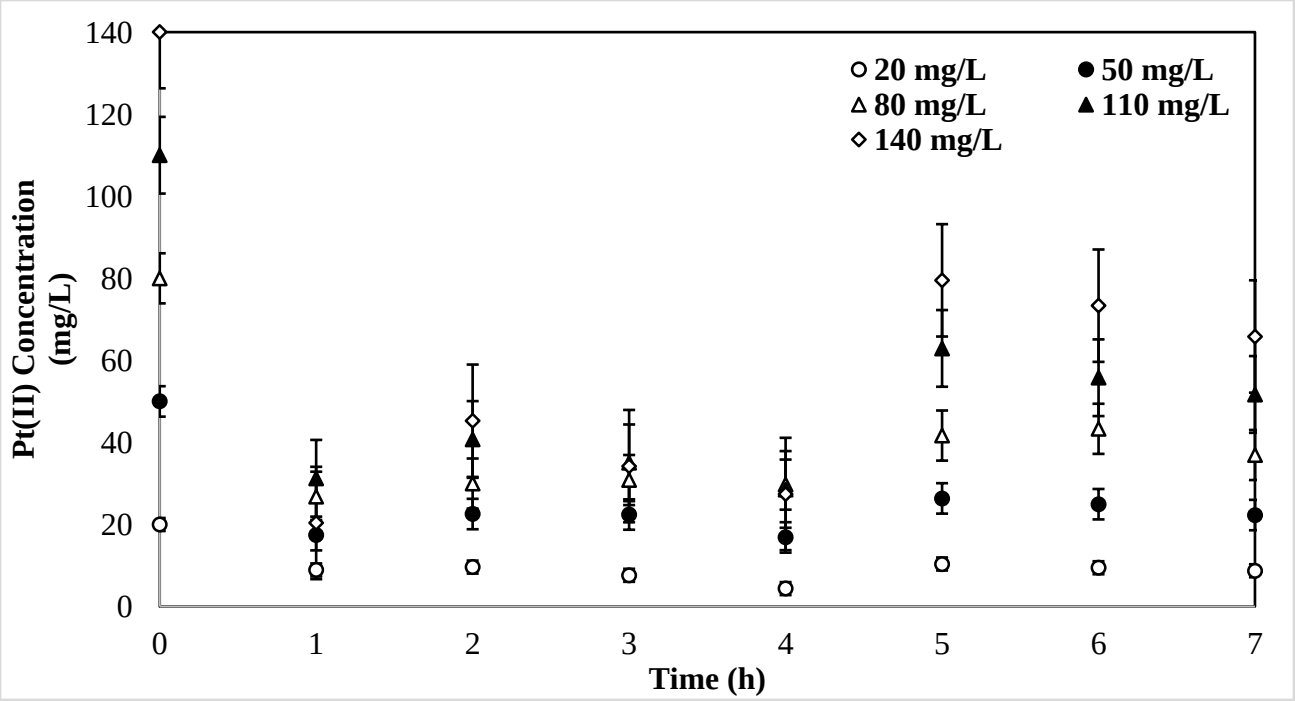

Figure 4.18: Removal of Pt(II) by *Desulfovibrio desulfuricans* at different concentrations over a 4 h incubation period

Literature has reported the reduction of Pd(II) by *Desulfovibrio desulfuricans* through hydrogenases at the expanse of hydrogen or formate as an electron donor (Lloyd et al., 1998, Yong et al., 2002c). Therefore, hydrogenase enzyme may be responsible for Pt(II) reduction and nanoparticle formation (Riddin et al., 2006). Although enzymatic transformation of metal ions to produce nanoparticles appears to be more lucrative over other processes it has its limitations. Firstly, enzymes work best at specific optimum conditions is one major problem associated with the use of this technique. Metal salts at different pH and temperatures tend to inhibit the activity of the redox enzyme. Another controlling factor is the electro chemical potential that reflect the ability of reducing or oxidizing equivalents. Other liquids that may be present in metal salt preparation may also affect the activity of the enzyme, such as the presence of HCl or more particularly a high concentration of chloride ions which could retard the reduction of the platinum complex to form metallic platinum nanoparticles. Which could explain the instability of the organisms in removing/reducing Pt(II) from time 1 h to 5 h because apart from using HCl and NaOH to adjust the pH the platinum standard solution had a high concentration of HCl. Lastly, hydrogenase enzymes are highly sensitive to oxygen (Kamachi et al., 1995). Which explains why the study was conducted in anaerobic conditions.

4.5.3 Biodeposition

The assumption is that the reduction and deposition of Pt(0) follows the same mechanism as the reduction and deposition of Pd(0), because TEM analysis of the cells challenged with Pt(II) showed black oblique deposit on the cell wall, in suspension and the cytoplasm (Figure 4.19 b and d) similar to Pd in part 4.3.3. However, in a previous study about formate-dependent Pd(II) bioreduction by *Desulfovibrio fructosvorans*. The deletion of Periplasmic hydrogenase caused Pd(0) nanoparticles to be relocated in the cytoplasmic membrane site of the remaining hydrogenases. Which means hydrogenases are partially involved in the bioreduction process (Mikheenko et al., 2008). This could explain the deposition of Pt particles in the cytoplasm observed in this study. In addition, energy dispersive spectrometer revealed the presence of Pt particles in both samples (Figure 4.20).

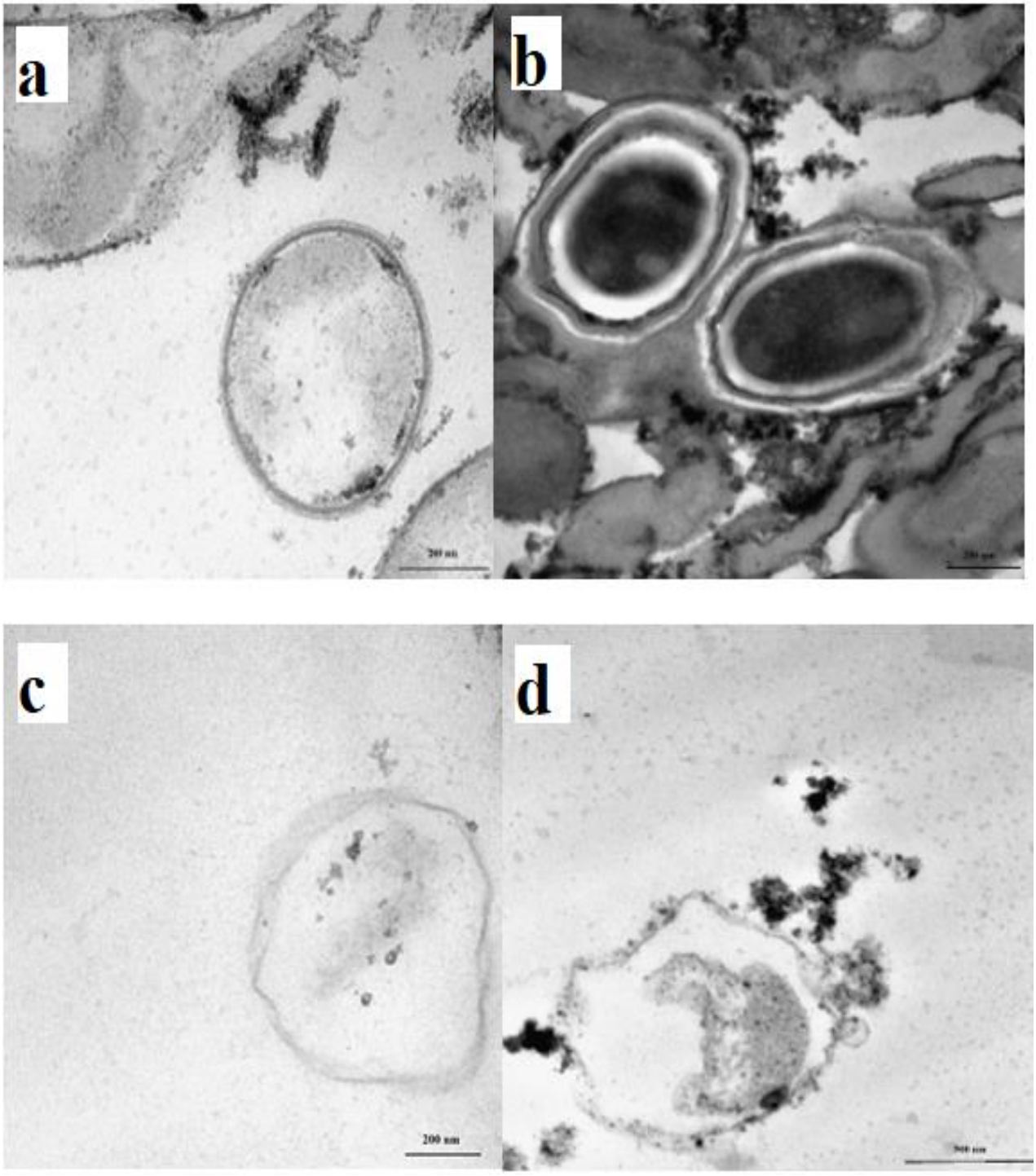

Figure 4.19: TEM images of Pt(0) deposited on the cell wall. a) *Desulfovibrio desulfuricans* control, b) *Desulfovibrio desulfuricans* challenged with Pt(II), c) SRB control, d) SRB challenged with Pt(II)

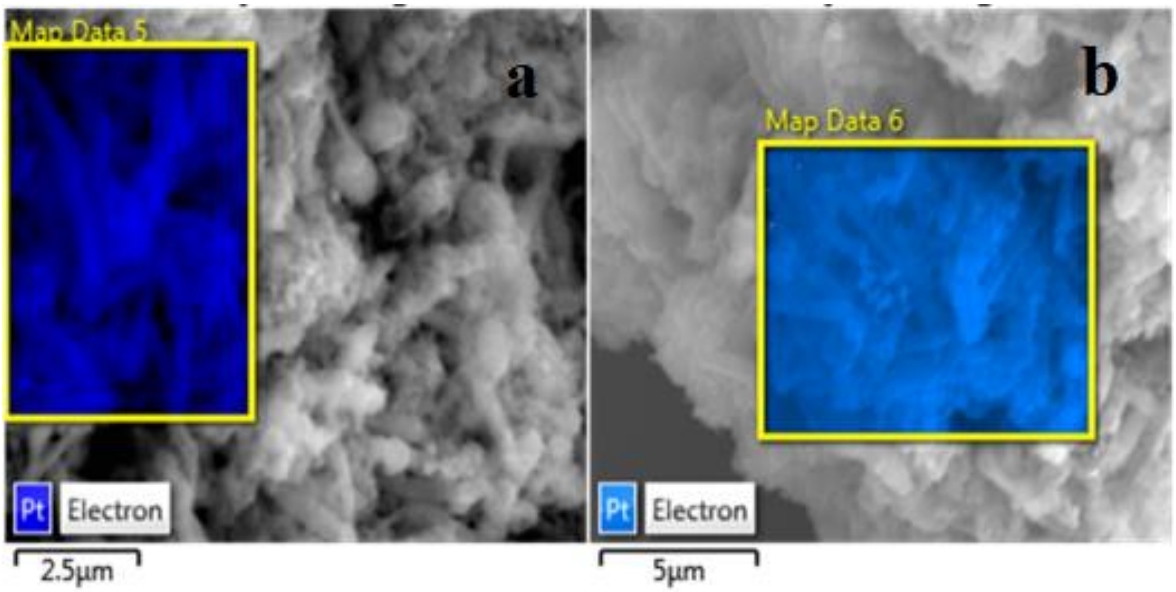

Figure 4.20: SEM-EDX images showing the presence of Pt particles deposited on the cell wall. a) elemental map of Pt on SRB b) elemental map of Pt on *Desulfovibrio desulfuricans.*

Further analysis revealed the presence of other elements; the major four being O at 20.79 Wt%, Fe at 11.16 Wt%, Os at 26.37 Wt% and Pt at 23.96 Wt% for SRB (Table 4.12). 13.73 Wt% O, 15.49 Wt% S, 17.22 Wt% Os and 38.43 Wt% Pt for *Desulfovibrio desulfuricans* (Table 4.13). Osmium tetraoxide was used as a fixative during cell preparation for SEM analysis which could explain the presence of O and Os in both samples. Fe and S are one of the products formed during cell respiration meaning they were produced during cell culture. This means Pt ions could have formed complexes with Fe or S, however the wt% ratio of Fe and Pt, S and Pt are not equal - Pt can gain 2 electrons to make it elemental Fe and S can donate 2 electrons. Therefore, for every 10 wt% of Fe or S produced 10wt% of Pt should be produced for the complexes to form. Therefore, the Pt produced was assumed to be Pt(0). However, further tests such as XRD and XPS would have to be conducted to have a final conclusion. XRD studies could not be performed in this study because the sample size was too small $<$ 0.5g for XRD analysis which was a limitation in this study.

Table 4.12: EDS elemental analysis of SRB challenged with Pt(II)

Element	Weight%	Weight% Sigma
O	20.79	0.08
Na	5.62	0.03
Si	0.94	0.02
P	4.50	0.04

S	5.77	0.03
Cl	0.54	0.02
Ca	0.34	0.02
Fe	11.16	0.06
Ag	0.01	0.05
Re	0.00	0.00
Os	26.37	0.11
Pt	23.96	0.13
Total:	100.00	-

Table 4.13: EDS elemental analysis of *Desulfovibrio desulfuricans* challenged with Pt(II)

Element	**Weight%**	**Weight% Sigma**
O	13.73	0.12
Na	3.35	0.06
Si	2.33	0.04
S	15.49	0.10
Fe	9.13	0.12
Zn	0.33	0.13
Ag	0.00	0.00
Os	17.22	0.20
Pt	38.43	0.25
Total:	100.00	-

CHAPTER 5: REDUCTION KINETICS OF Pd(II) AND Pt(II)

Monod based models have been frequently used to mathematically describe microbial behavior in metallic environments (Liu et al., 2002, Lall and Mitchell, 2007, Sheng and Fein, 2014). For this reason a Monod bacterium-based model was used in this study to describe Pd(II) and Pt(II) reduction kinetics by SRB and *Desulfovibrio desulfuricans*. The model was developed to evaluate the feasibility of the batch cultures in reducing Pd(II) and Pt(II) by examining the maximum amount of metal a batch culture can reduce – its' maximum reduction capacity. Parameters were estimated using the following computer programs AQUASIM 2.0 a simulation program for aquatic systems and Sigma Plot 11.

5.1 Pd(II) reduction kinetics

The previous chapter outlined how Pd(II) and Pt(II) reduction is facilitated by enzymes such as hydrogenases and cytochromes which are bound to the cell membrane. Therefore, a model based on the Monod/Michaelis-Menten equation was proposed - where the enzymatic activity is the driving force for metal reduction (Wang and Shen, 1997). In addition this model was formally used to describe Cr(VI) in *Bacillus* species, and a consortium culture from the Brits wastewater treatment plant, North west, South Africa (Chirwa and Wang, 1997, Molokwane et al., 2008, Igboamalu and Chirwa, 2016). The following Monod model was proposed with a few modifications.

$$Pd(II) + Z \underset{k_{-1}}{\overset{k_1}{\rightleftharpoons}} [Z * Pd(0)] \quad (5.1)$$

$$[Z * Pd(0)] \xrightarrow{k_2} Z + Pd(0) \quad (5.2)$$

- Where; Pd(II) = Palladium(II) concentration
- Z = Enzyme
- [Z * Pd(0)] = Enzyme Pd(0) complex
- Pd(0) = Pd(0) concentration
- k_1 = Rate constant for the forward reaction

- k_{-1}= Rate constant for reverse reaction
- k_2 = Rate constant for third reaction

Therefore, the enzyme rate equation from equation 5.1 and 5.2 becomes;

Let C represent Pd(II) concentration,

$$\frac{dZ}{dt} = k_1 C Z_T \quad (5.3)$$

$$\frac{dZ^*}{dt} = k_{-1} C Z^* \quad (5.4)$$

Therefore,

$$\frac{dZ^*}{dt} = \frac{dC}{dt} k_2 Z^* \quad (5.5)$$

Combining equation 5.3,5.4,5.5 gives the rate of Z^* formation represented as,

$$\frac{dZ^*}{dt} = k_1 C(Z_T) - k_{-1}(Z^*) - k_2(Z^*) \quad (5.6)$$

$$Z_T = Z - Z^* \quad (5.7)$$

Where,

Z_T = Total available complex

Z^* = Enzyme complex

Combining equation 5.6 and 5.7,

$$\frac{dZ^*}{dt} = k_1 C(Z - Z^*) - k_{-1}(Z^*) - k_2(Z^*) \quad (5.8)$$

At steady state conditions enzyme formation $\frac{dZ^*}{dt} = 0$, therefore the equation becomes,

$$k_1 C(Z - Z^*) - k_{-1}(Z^*) - k_2(Z^*) = 0 \quad (5.9)$$

Solving for Z^* gives,

$$Z^* = \frac{CZ}{C+(\frac{k_{-1}+k_2}{k_1})} \quad (5.10)$$

Therefore, the rate of Pd(II) reduction can be represented as,

$$-\frac{dC}{dt} = \frac{CZ}{C+(\frac{k_{-1}+k_2}{k_1})} \quad (5.11)$$

The Monod equation is represented as,

$$-\frac{dC}{dt} = \left(\frac{u_{max}C}{C+K}\right)X \quad (5.12)$$

Comparing equation 5.11 and 5.12,

u_{max} = maximum specific removal rate (mg/L/h)

E is equivalent to X (biomass concentration) (mg/L)

$\frac{k_{-1}+k_2}{k_1}$ is equivalent to K (half velocity concentration) (mg/L)

From equation 5.12 the rate and extend of Pd(II) reduction in a bacterial system is proportional to the number of cells in the system and the capacity of reduction. Therefore, X can be represented as,

$$X = X_0 - \left(\frac{C_0-C}{K_c}\right) \quad (5.13)$$

Where, C_0 = initial Pd(II) concentration

C = Pd(II) concentration at time (t)

X_0 = Initial biomass concentration (mg)

K_c = maximum Pd(II) reducing capacity (mg/mg)

Combining equation 12 and 13 generates the following proposed equation,

$$-\frac{dC}{dt} = \left(\frac{u_{max}C}{C+K}\right)\left(X_0 - \left(\frac{C_0-C}{K_c}\right)\right) \quad (5.14)$$

The model, equation 5.14, was fitted on AQUASIM and the following Parameters (u_{max}, K, K_c) were estimated by performing simulations for best fit of the equation against the experimental data to obtain the curves in Figure 5.1 and 5.2. Good fits between the simulated model and experimental data with concentrations ranging from 356 mg/L – 964 mg/L were noted, for both treatments of SRB and *Desulfovibrio desulfuricans* (Figure 5.1, and 5.2). K_c (Pd(II) reduction capacity) was observed to increase with increasing initial Pd(II) concentrations (Table 5.1). Suggesting the rate of Pd(II) reduction by SRB/ *Desulfovibrio desulfuricans* increases with increasing Pd(II) concentration. A similar trend was observed for Cr(VI) in a study conducted by Igboamalu and Chirwa (2016), the reduction capacity of Cr(VI) was observed to be directly proportional to the concentration of Cr(VI). However, in this study a decrease in K_c was observed at 1607 mg/L of Pd(II) for SRB and at 1928 mg/L of Pd(II) for *Desulfovibrio desulfuricans* (Table 5.1). Suggesting the are other factors and limitations mentioned in the previous chapter such as chloride and sulphides interference that were a hinderance in the efficient reduction of Pd(II) at those concentrations. Evidently u_{max} was low at 356 mg/L and high at 964 mg/L compared to the other concentrations for *Desulfovibrio desulfuricans*. A low maximum specific reduction rate may also be an attribute of chloride inhibition which could also explain the increasing K values. An enzyme with a high K value has a low affinity for its substrate in this case Pd(II). Therefore, looking at the individual concentrations the bacteria performed considerably well at removing the metal from solution according to the model. However, looking at the whole experiment holistically it is evident as the concentration increased the was a decrease in Pd(II) removal.

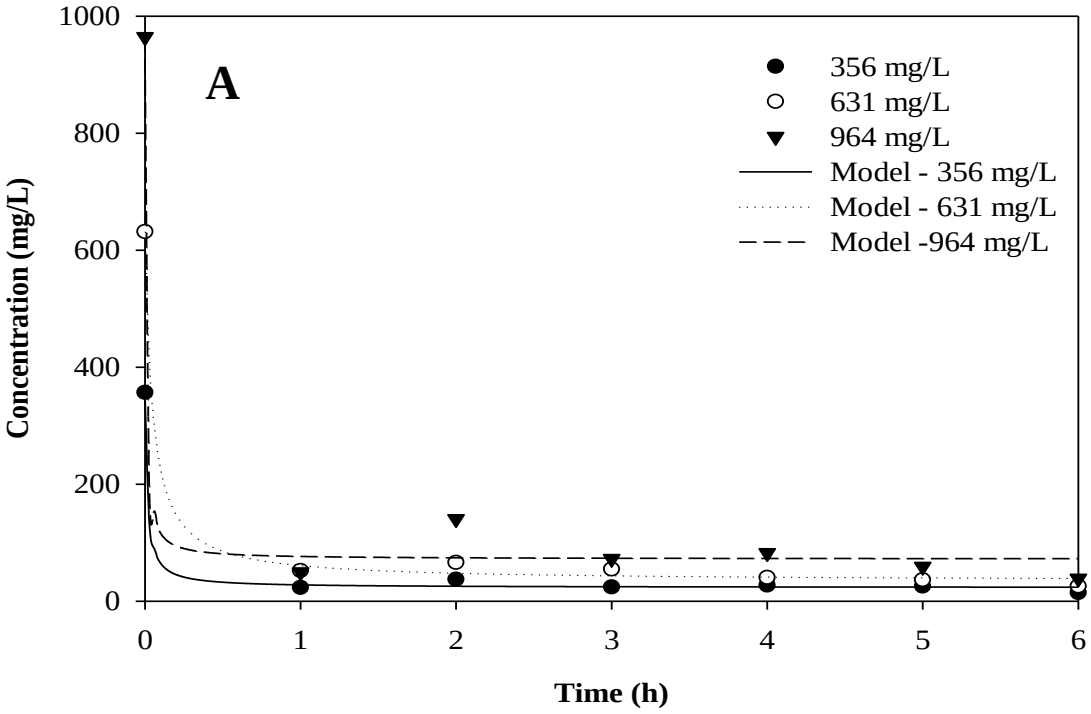
A
356 mg/L
631 mg/L
964 mg/L
Model - 356 mg/L
Model - 631 mg/L
Model -964 mg/L
Concentration (mg/L)
Time (h)
0
200
400
600
800
1000
0
1
2
3
4
5
6

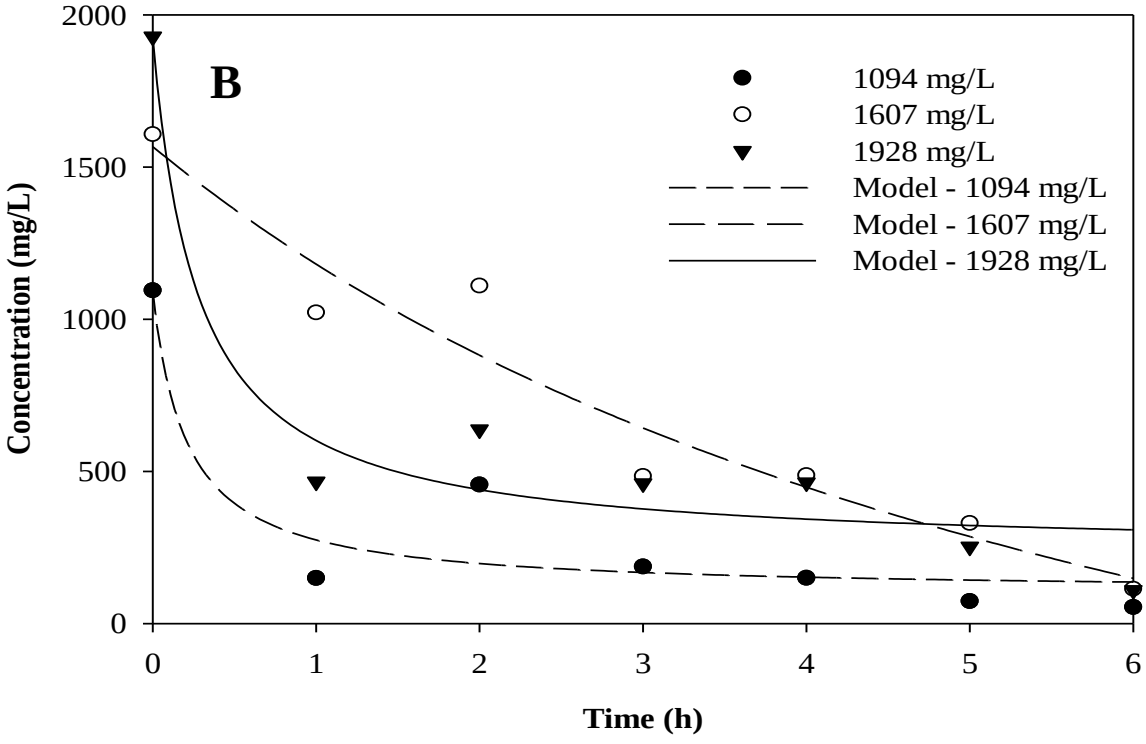
B
1094 mg/L
1607 mg/L
1928 mg/L
Model - 1094 mg/L
Model - 1607 mg/L
Model - 1928 mg/L
Concentration (mg/L)
Time (h)
0
500
1000
1500
2000
0
1
2
3
4
5
6

Figure 5.1: Pd(II) reduction by SRB from the following initial Pd(II) concentrations; 356 mg/L - 164 mg/L (A),1094 mg/L - 1928 mg/L (B).

Table 5.1: Kinetic parameters for Pd(II) reduction by SRB and *Desulfovibrio desulfuricans*

Concentration (mg/L)	**u_{max}(mg/L/h)**	**K (mg/L)**	**K_c (mg/mg)**	**R^2**
SRB				
356	48.9538	12.006	5.521	0.997
631	48.938	34.505	9.799	0.998
964	48.9538	448.699	16.014	0.990
1094	48.9538	499.385	17.550	0.872
1607	48.9538	860.488	12.583	0.934
1928	48.9538	989.167	29.501	0.944
Desulfovibrio desulfuricans				
356	12.099	229.556	6.304	0.918
631	49.029	576.849	10.395	0.928
964	88.986	343.799	14.675	0.990
1094	49.029	558.661	17.753	0.942
1607	49.029	999.611	27.948	0.990
1928	41.490	993.149	16.347	0.952

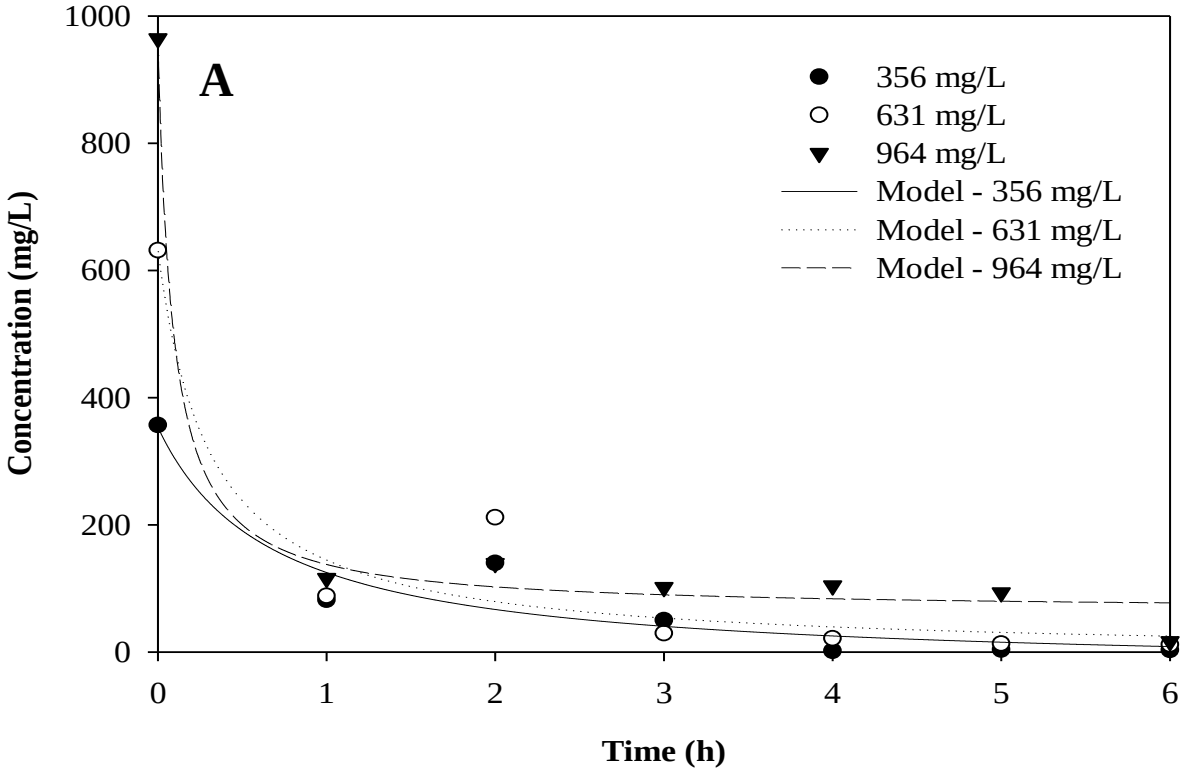
A
356 mg/L
631 mg/L
964 mg/L
Model - 356 mg/L
Model - 631 mg/L
Model - 964 mg/L
Concentration (mg/L)
Time (h)
0
200
400
600
800
1000
0
1
2
3
4
5
6

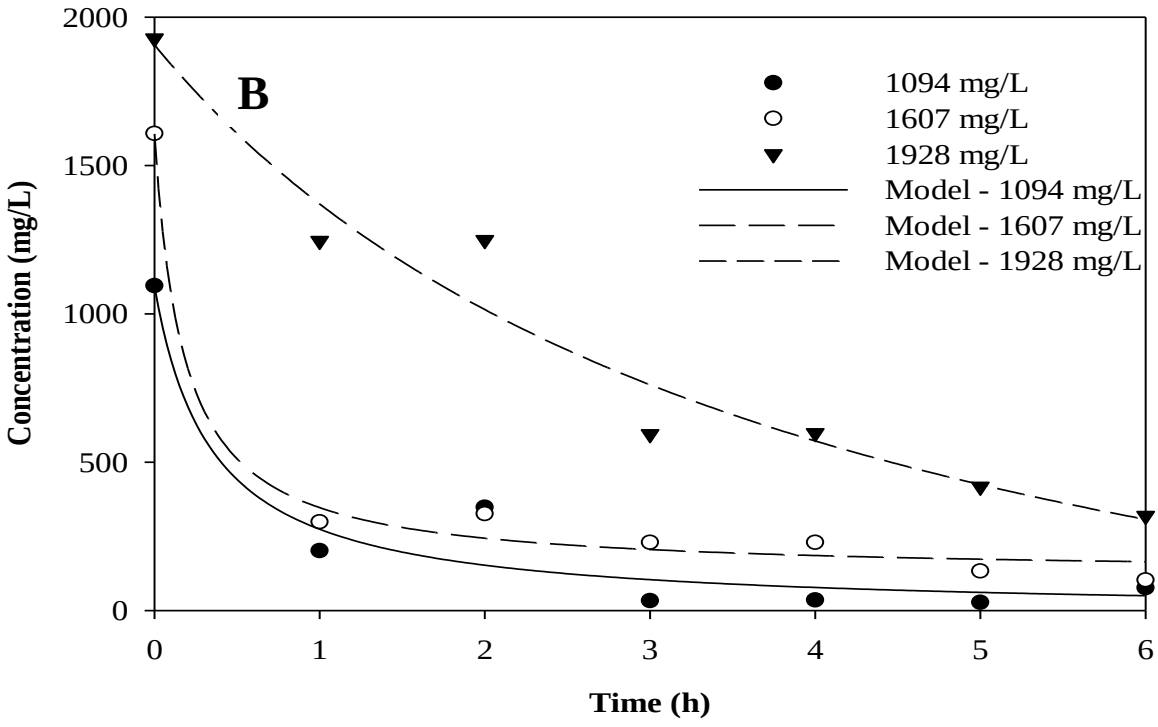
B
1094 mg/L
1607 mg/L
1928 mg/L
Model - 1094 mg/L
Model - 1607 mg/L
Model - 1928 mg/L
Concentration (mg/L)
Time (h)
0
500
1000
1500
2000
0
1
2
3
4
5
6

Figure 5.2: Pd(II) reduction by *Desulfovibrio desulfuricans* from the following initial Pd(II) concentrations; 356 mg/L - 964 mg/L (A) , 1094 mg/L - 1928 mg/L (B).

5.2 Pt(II) reduction kinetics

Pt(II) reduction was characterised by irregular readings of adsorption and desorption, however, significant amounts of Pt(II) were removed from solution after incubation. Therefore, the following modified Monod model was proposed;

$$Pt(II) + Z \underset{k_{-1}}{\overset{k_1}{\rightleftharpoons}} [Z * Pt(0)] \quad (5.15)$$

$$[Z * Pt(0)] \overrightarrow{k_2} Z + Pt(0) \quad (5.16)$$

The biomass concentration was constant throughout the study therefore $X = X_0$ which is the initial biomass concentration. The Km value was assumed to be much larger than the Pt(II) concentration such that the whole denominator term is dominated by Km (Roestorff and Chirwa, 2018) to give equation 5.17, modified from equation 5.12

$$\frac{-dPt(II)}{dt} = \frac{k_2.X_0.Pt(II)}{Km} \quad (5.17)$$

- Where, Pt(II) = Platinum(II) concentration.
- X_0 = Enzyme (Microbial mass).
- [X + Pt(II)] = Enzyme Pt(II) complex.
- k_2 = Rate constant for third reaction.

Upon integration: $Pt(II) = Pt(II)_0 e^{-\frac{k_2.X_0}{Km}t}$ (5.18)

The results show rapid reduction in the first section from t=0 and t = 4 meaning the Pt(II) is readily accessible and absorbed on the cell surface. In the second section, a portion of the Pt(II) appears to desorb back into solution until equilibrium is reached (Figure 5.3 and 5.4). Therefore, the following equation was proposed for the removal of Pt(II) the first term represents the first removal and the second term represents desorption. with α and β as the corresponding fractions.

$$Pt(II)_{Total} = \gamma + \alpha\,[Pt(II)]_{Removal} + \beta\,[Pt(II)]_{desorption} \times t \quad (5.19)$$

The term $\frac{k_2.X_0}{Km}$ from equation 5.17 can be simplified as k, (rate constant). Equation 5.18 can be substituted in equation 5.19 to give.

$$Pt(II)_{Total} = \gamma + \alpha\,Pt(II)_0 e^{-kt} + \beta\,Pt(II)_0 \times t \quad (5.20)$$

γ = Initial Pt(II) concentration (mg/L)

α = maximum specific reducing constant (mg/L/h)

k = rate constant (h^{-1})

β = desorption constant (h^{-1})

t = time (h)

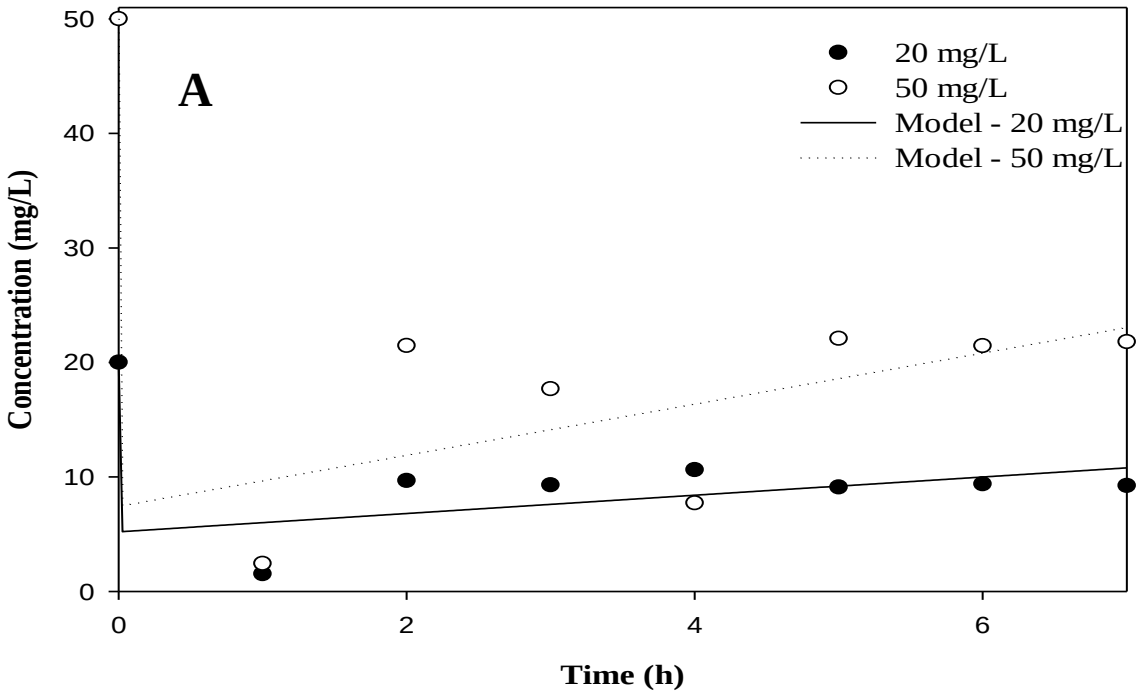

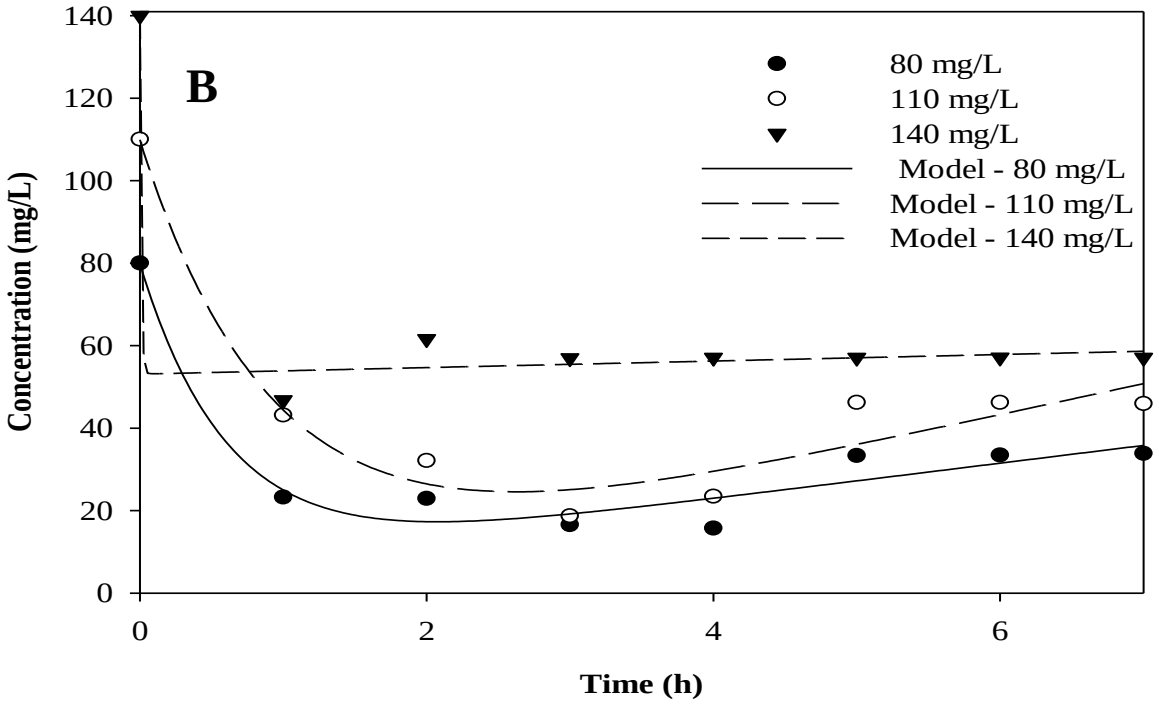

Figure 5.3: Pt(II) reduction by SRB from a concentration of 20 mg/L – 50 mg/L (A) to 80 mg/L – 140 mg/L (B)

Table 5.2: Kinetic parameters for Pt(II) bioreduction by SRB and *Desulfovibrio desulfuricans*.

Pt(II) Concentration (mg/L)	$k(h^{-1})$	a **(mg/L/h)**	$\beta(h^{-1})$	R^2
SRB				
20	17.49×10^6	14.79	0.79	0.77
50	87.21×10^3	42.55	2.23	0.82
80	1.60	74.18	4.31	0.95
110	1.04	113.00	7.63	0.95

140	114.00	86.90	0.79	0.98
Desulfovibrio desulfuricans				
20	1.49	13.82	0.44	0.84
50	2262	31.51	0.83	0.92
80	35.35	55.55	2.44	0.96
110	4.59	83.82	4.35	0.89
140	166.20	124.00	8.49	0.88

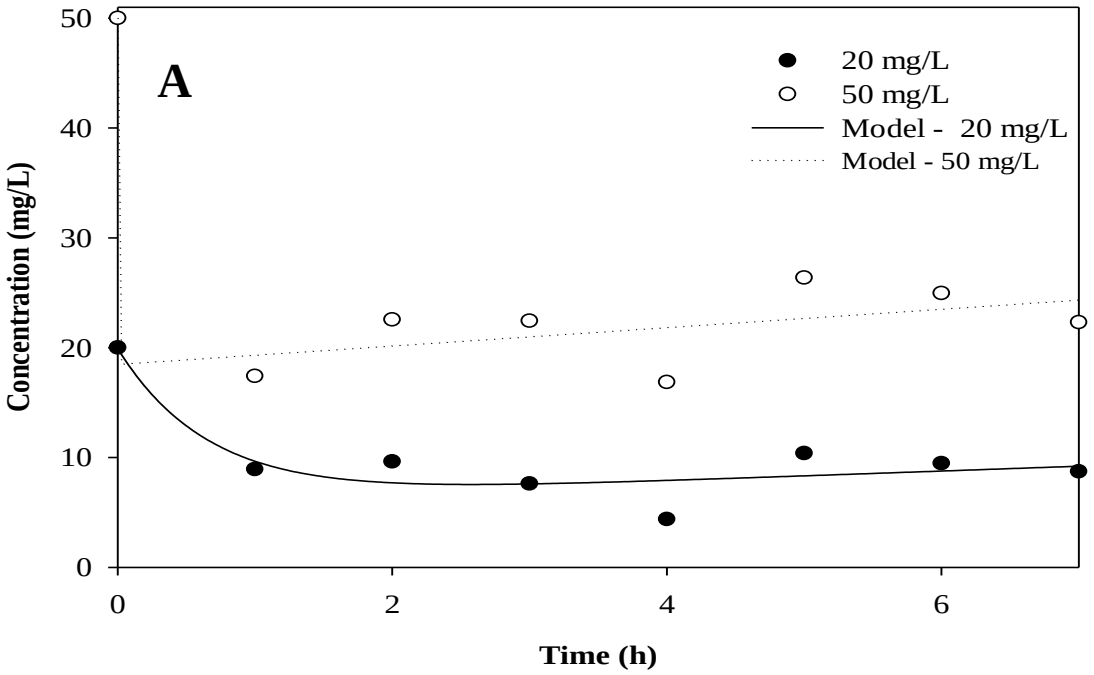

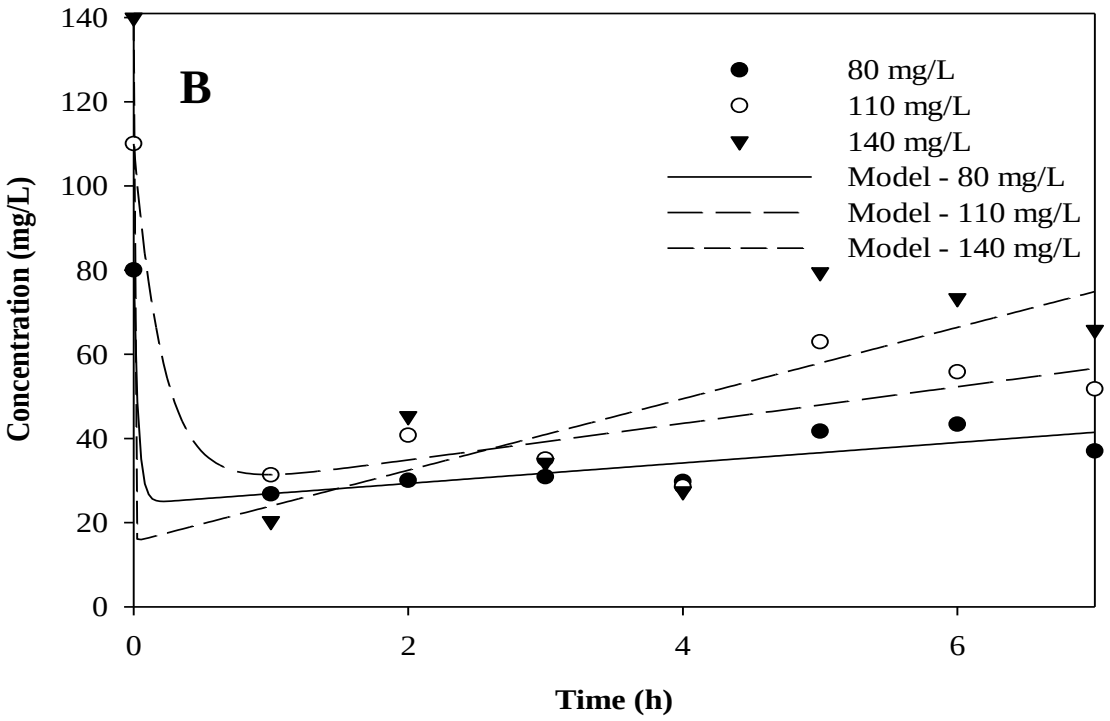

Figure 5.4: Pt(II) reduction by *Desulfovibrio desulfuricans* from a concentration of 20 mg/L – 50 mg/L (A) to 80 mg/L – 140 mg/L (B)

The proposed model did not adequately fit the data set; however, this is not surprising because the biochemical nature of enzymes and electron transport systems is usually complex and is altered by different environments (Liu et al., 2002). The maximum specific reducing constant (a) and deposition constants (B) were observed to increase with increasing concentrations of Pt(II), and a higher reducing constant in comparison to the deposition constant is evidence of the affinity Pt(II) ions have to the cell wall. In addition, the rate constant was extremely high at 20 mg/L and 50 mg/L for SRB, which means the rate of reduction at these concentrations happened rapidly or the parameter is sensitive to the data set (Table 5.3).

The findings in this kinetic study demonstrated Both treatments are capable of removing Pd(II) and Pt(II) efficiently, however extensive kinetic studies of theses metals is still needed to better elucidated the mechanisms that drive biosorption or reduction. These interventions will assist in the modelling systems for pilot scale PGM recovery.

CHAPTER 6: CONCLUSION AND RECOMMENDATION

6.1 Conclusion

- SRB were chosen because they can adapt to minor environmental changes. and literature has shown *Desulfovibrio desulfuricans* is resilient against most metals and is effective at reducing them. In addition, metagenomic analysis on SRB revealed 17 possible Pd(II) and Pt(II) reducing bacteria with *Desulfosporia species*, *Desulfotomaculum aeronauticum* and *Clostridium* as novel Pd(II) and Pt(II) reducers.
- The removal of Pd(II) by SRB and *Desulfovibrio desulfuricans* at different pH values, revealed significant activity of the bacteria at a pH of 3, with 4 being the optimum pH- 90% and 83% of Pd(II) was removed by SRB and *Desulfovibrio desulfuricans* respectively. However, a competitive effect of chloride ions was discovered at low pH levels, resulting in 54% and 48% of the palladium being reduced by SRB and *Desulfovibrio desulfuricans*. This study demonstrated that the pH of an environment collates strongly with microbial communities across a wide range of biogeochemical conditions, it shapes microbial metabolism by affecting environmental conditions that are needed for microbial growth and survival and It defines the chemical activity of protons which are a key player in redox reactions, mineral dissolution and precipitation.
- Microbial concentration is also a vital parameter that influences the rate of Pd or Pt removal from solution. The study revealed 0.0028 g/L of cell concentration was inadequate until increased to 0.085 g/L ($\pm$ 0.1). 90% of Pd(II) was removed by all three metal concentrations of 2 mM, 4mM and 8Mm. Therefore, a concentration of 0.085 g/L and a pH of 4 was used to carry out subsequent experiments.
- Both treatments removed at least 90% of Pd(II) in 6 h through a metabolic activity which happens via a formate hydrogenase complex. Reduction was confirmed for Pd(II), the microbes utilised the reductive power of electron donors such as formate to form crystalline Pd(0) deposits on the cell surface. Hence, black deposits were detected on the cell membrane by TEM and XRD confirmed crystallite sizes in the nano range, which is an advantage because the biogenic Pd can be reused as a catalyst.

- Both treatments could remove at least 56% of Pt(II) in 7 hours. The pattern of removal was irregular which could be attributed to environmental conditions that interfered with enzyme activity. Nevertheless, deposition was detected by TEM on the cell wall, in solution and inside the cell wall. In addition, Statistical evidence proved both treatments could effectively remove Pt(II) from solution.
- Modified Monod kinetics models were proposed, and the maximum removal capacity was recorded to increase with increasing initial concentration (5.521 mg/mg – 29.501 mg/mg). Meaning the rate of reduction increased with increasing concentration the same trend was observed for Pt(II).
- However, to fully reap the rewards of the application - SRB in the remediation and reduction of PGMs, the reported limitations need to be solved for the application to be potentially viable.

6.2 Recommendations

- The greatest limitation that poses a threat to bio-Palladium is poisoning of the catalyst by sulfides therefore, a possible approach to prevent sulfide poisoning is the oxidative removal of sulfide prior to any contact with the noble metal
- To limit the interference of chloride ions in the reduction process the experiment can be carried out in a buffer that is inert to any possible complex formation with either the platinum or palladium salt or nanoparticles
- Future work is required to fully understand reduction kinetics of the biomass for future applications in pallidum and platinum bioremediation and recovery.
- Biogenic palladium and platinum reduced can be evaluated as a catalyst in remediating other water contaminants and as a biogenic cathode in microbial fuel cells.

REFERENCES

AKCIL, A. & MUDDER, T. 2003. Microbial destruction of cyanide wastes in gold mining: process review | SpringerLink.

ALFONSO, D. R., CUGINI, A. V. & SHOLL, D. S. 2003. Density functional theory studies of sulfur binding on Pd, Cu and Ag and their alloys. *Surface Science,* 546**,** 12-26.

ANGELES-WEDLER, D., MACKENZIE, K. & KOPINKE, F.-D. 2009. Sulphide-induced deactivation of Pd/Al2O3 as hydrodechlorination catalyst and its oxidative regeneration with permanganate. *Applied Catalysis B: Environmental,* 90**,** 613-617.

AZABOU, S., MECHICHI, T., PATEL, B. K. C. & SAYADI, S. 2007. Isolation and characterization of a mesophilic heavy-metals-tolerant sulfate-reducing bacterium Desulfomicrobium sp. from an enrichment culture using phosphogypsum as a sulfate source. *Journal of Hazardous Materials,* 140**,** 264-270.

BANSAL, N., COETZEE, J. J. & CHIRWA, E. M. N. 2019. In situ bioremediation of hexavalent chromium in presence of iron by dried sludge bacteria exposed to high chromium concentration. *Ecotoxicology and Environmental Safety,* 172**,** 281-289.

BAO, H., HAO, N., YANG, Y. & ZHAO, D. 2010. Biosynthesis of biocompatible cadmium telluride quantum dots using yeast cells. *Nano Research,* 3**,** 481-489.

BERNARDIS, F. L., GRANT, R. A. & SHERRINGTON, D. C. 2005. A review of methods of separation of the platinum-group metals through their chloro-complexes. *Reactive and Functional Polymers,* 65**,** 205-217.

BEVERIDGE, T. J. 1999. Structures of Gram-Negative Cell Walls and Their Derived Membrane Vesicles. *Journal of Bacteriology,* 181**,** 4725-4733.

BEVERIDGE, T. J. & MURRAY, R. G. 1980. Sites of metal deposition in the cell wall of Bacillus subtilis. *Journal of Bacteriology,* 141**,** 876-887.

BHAGAT, M., BURGESS, J. E., ANTUNES, A. P. M., WHITELEY, C. G. & DUNCAN, J. R. 2004. Precipitation of mixed metal residues from wastewater utilising biogenic sulphide. *Minerals Engineering,* 17**,** 925-932.

BOTTKE, W. F., VOKROUHLICKÝ, D., MARCHI, S., SWINDLE, T., SCOTT, E. R. D., WEIRICH, J. R. & LEVISON, H. 2015. Dating the Moon-forming impact event with asteroidal meteorites. *Science,* 348**,** 321-323.

BRIERLEY, J. A. & BRIERLEY, C. L. 2001. Present and future commercial applications of biohydrometallurgy. *Hydrometallurgy,* 59**,** 233-239.

BUNGE, M., SØBJERG, L. S., ROTARU, A.-E., GAUTHIER, D., LINDHARDT, A. T., HAUSE, G., FINSTER, K., KINGSHOTT, P., SKRYDSTRUP, T. & MEYER, R. L.

2010. Formation of palladium(0) nanoparticles at microbial surfaces. *Biotechnology and Bioengineering,* 107**,** 206-215.

CAPENESS, M. J., EDMUNDSON, M. C. & HORSFALL, L. E. 2015. Nickel and platinum group metal nanoparticle production by Desulfovibrio alaskensis G20. *New Biotechnology,* 32**,** 727-731.

CARPENTIER, W., SANDRA, K., SMET, I. D., BRIGÃ¯Â¿Â½, A., SMET, L. D. & BEEUMEN, J. V. 2003. Microbial Reduction and Precipitation of Vanadium by Shewanella oneidensis. *Applied and Environmental Microbiology,* 69**,** 3636-3639.

CASTRO-LONGORIA, E., VILCHIS-NESTOR, A. R. & AVALOS-BORJA, M. 2011. Biosynthesis of silver, gold and bimetallic nanoparticles using the filamentous fungus Neurospora crassa. *Colloids and Surfaces B: Biointerfaces,* 83**,** 42-48.

CHANDLER, A. J., EIGHMY, T. T., HJELMAR, O., KOSSON, D. S., SAWELL, S. E., VEHLOW, J., SLOOT, H. A. V. D. & HARTLÉN, J. 1997. *Municipal Solid Waste Incinerator Residues,* Elsevier.

CHANDRAPRABHA, M. N., MODAK, J. M., NATARAJAN, K. A. & RAICHUR, A. M. 2002. Strategies for efficient start-up of continuous biooxidation process for refractory gold ores. *Minerals Engineering,* 15**,** 751-753.

CHENG, H.-Y., HOU, Y.-N., ZHANG, X., YANG, Z.-N., XU, T. & WANG, A.-J. 2017. Activating electrochemical catalytic activity of bio-palladium by hybridizing with carbon nanotube as “e ? Bridge”. *Scientific Reports,* 7**,** 1-9.

CHIRWA, E. M. N. & WANG, Y.-T. 1997. Hexavalent Chromium Reduction by Bacillus sp. in a Packed-Bed Bioreactor. *Environmental Science & Technology,* 31**,** 1446-1451.

COATES, J. 2006. Interpretation of Infrared Spectra, A Practical Approach. *Encyclopedia of Analytical Chemistry.* American Cancer Society.

CORTE, S. D., HENNEBEL, T., GUSSEME, B. D., VERSTRAETE, W. & BOON, N. 2012. Bio-palladium: from metal recovery to catalytic applications. *Microbial Biotechnology,* 5**,** 5-17.

COX, J. S., SMITH, D. S., WARREN, L. A. & FERRIS, F. G. 1999. Characterizing Heterogeneous Bacterial Surface Functional Groups Using Discrete Affinity Spectra for Proton Binding. *Environmental Science & Technology,* 33**,** 4514-4521.

CREAMER, N. J., MIKHEENKO, I. P., YONG, P., DEPLANCHE, K., SANYAHUMBI, D., WOOD, J., POLLMANN, K., MERROUN, M., SELENSKA-POBELL, S. & MACASKIE, L. E. 2007. Novel supported Pd hydrogenation bionanocatalyst for hybrid homogeneous/heterogeneous catalysis. *Catalysis Today,* 128**,** 80-87.

CUI, J. & ZHANG, L. 2008. Metallurgical recovery of metals from electronic waste: A review. *Journal of Hazardous Materials,* 158**,** 228-256.

DANG, P. N., DANG, T. C. H., LAI, T. H. & STAN-LOTTER, H. 1996. Desulfovibrio vietnamensissp.nov., a Halophilic Sulfate-Reducing Bacterium from Vietnamese Oil Fields. *Anaerobe,* 2**,** 385-392.

DAS, N. 2010. Recovery of precious metals through biosorption ― A review. *Hydrometallurgy,* 103**,** 180-189.

DAUGHNEY, C. J., FEIN, J. B. & YEE, N. 1998. A comparison of the thermodynamics of metal adsorption onto two common bacteria. *Chemical Geology,* 144**,** 161-176.

DE GUSSEME, B., HENNEBEL, T., VANHAECKE, L., SOETAERT, M., DESLOOVER, J., WILLE, K., VERBEKEN, K., VERSTRAETE, W. & BOON, N. 2011. Biogenic Palladium Enhances Diatrizoate Removal from Hospital Wastewater in a Microbial Electrolysis Cell. *Environmental Science & Technology,* 45**,** 5737-5745.

DE LUCA, G., DE PHILIP, P., DERMOUN, Z., ROUSSET, M. & VERMÉGLIO, A. 2001. Reduction of Technetium(VII) by Desulfovibrio fructosovorans Is Mediated by the Nickel-Iron Hydrogenase. *Applied and Environmental Microbiology,* 67**,** 4583-4587.

DEPLANCHE, K. & MACASKIE, L. E. 2008. Biorecovery of gold by Escherichia coli and Desulfovibrio desulfuricans. *Biotechnology and Bioengineering,* 99**,** 1055-1064.

DEPLANCHE, K., MURRAY, A., MENNAN, C., TAYLOR, S. & MACASKIE, L. 2011. Biorecycling of Precious Metals and Rare Earth Elements. *Nanomaterials*.

DONG, H., ZHAO, J., CHEN, J., WU, Y. & LI, B. 2015. Recovery of platinum group metals from spent catalysts: A review. *International Journal of Mineral Processing,* 145**,** 108-113.

EKSTEEN, J. J., VAN BEEK, B. & BEZUIDENHOUT, G. A. 2011. Cracking a hard nut: an overview of Lonmin's operations directed at smelting of UG2-rich concentrate blends. *Journal of the Southern African Institute of Mining and Metallurgy,* 111**,** 681-690.

ELVIS, M. 2013. Prospecting Asteroid Resources. *In:* BADESCU, V. (ed.) *Asteroids: Prospective Energy and Material Resources.* Berlin, Heidelberg: Springer Berlin Heidelberg.

ENSLEY, B. D. & SUFLITA, J. M. 1995. Metabolism of Environmental Contaminants by Mixed and Pure Cultures of Sulfate-Reducing Bacteria. *In:* BARTON, L. L. (ed.) *Sulfate-Reducing Bacteria.* Boston, MA: Springer US.

FEIN, J. B., DAUGHNEY, C. J., YEE, N. & DAVIS, T. A. 1997. A chemical equilibrium model for metal adsorption onto bacterial surfaces. *Geochimica et Cosmochimica Acta,* 61**,** 3319-3328.

FLEMING, C. A. 1992. Hydrometallurgy of precious metals recovery. *Hydrometallurgy,* 30**,** 127-162.

FOULKES, J. M., DEPLANCHE, K., SARGENT, F., MACASKIE, L. E. & LLOYD, J. R. 2016. A Novel Aerobic Mechanism for Reductive Palladium Biomineralization and Recovery by Escherichia coli. *Geomicrobiology Journal,* 33**,** 230-236.

GIMMLER, H., DE JESUS, J. & GREISER, A. 2001. Heavy metal resistance of the extreme acidotolerant filamentous fungus Bispora sp. *Microbial Ecology,* 42**,** 87-98.

GUIBAL, E., LARKIN, A., VINCENT, T. & TOBIN, J. M. 1999. Platinum recovery on chitosan-based sorbents. *In:* AMILS, R. & BALLESTER, A. (eds.) *Process Metallurgy*. Elsevier.

HABASHI, F. 2009. Recent trends in extractive metallurgy. *Journal of Mining and Metallurgy, Section B: Metallurgy,* 45**,** 1-13.

HARTLEY, F. R. 1991. CHAPTER 1 - The Occurrence, Extraction, Properties and Uses of the Platinum Group Metals. *In:* HARTLEY, F. R. (ed.) *Studies in Inorganic Chemistry*. Elsevier.

HE, J. & KAPPLER, A. 2017. Recovery of precious metals from waste streams. *Microbial Biotechnology,* 10**,** 1194-1198.

HEDRICH, S., BELLENBERG, S., KERMER, R., GEHRKE, T., SAND, W., SCHIPPERS, A., REICHEL, S., GLOMBITZA, F. & JANNECK, E. 2015. Biotechnological Recovery of Valuable Metals from Lignite Ash. *Advanced Materials Research*.

HISKEY, B. 2000. Metallurgy, Survey. *Kirk-Othmer Encyclopedia of Chemical Technology*. American Cancer Society.

HUSMARK, U. & RÖNNER, U. 1990. Forces involved in adhesion of Bacillus cereus spores to solid surfaces under different environmental conditions. *Journal of Applied Bacteriology,* 69**,** 557-562.

IGBOAMALU, T. & CHIRWA, E. 2016. - Kinetic Study of Cr(VI) Reduction in an Indigenous Mixed Culture of Bacteria in the Presence of As(III). - 49.

IRAVANI, S. 2014. Bacteria in Nanoparticle Synthesis: Current Status and Future Prospects. *International Scholarly Research Notices*.

JONES, R. T. 2005. An overview of Southern African PGM smelting. 32.

JU, X., IGARASHI, K., MIYASHITA, S.-I., MITSUHASHI, H., INAGAKI, K., FUJII, S.-I., SAWADA, H., KUWABARA, T. & MINODA, A. 2016. Effective and selective recovery of gold and palladium ions from metal wastewater using a sulfothermophilic red alga, Galdieria sulphuraria. *Bioresource Technology,* 211**,** 759-764.

KAMACHI, T., UNO, S., HIRAISHI, T. & OKURA, I. 1995. Purification and properties of intact hydrogenase from Desulfovibrio vulgaris (Miyazaki). *Journal of Molecular Catalysis A: Chemical,* 95**,** 93-98.

KAYA, M. 2016. Recovery of metals and nonmetals from electronic waste by physical and chemical recycling processes. *Waste Management,* 57**,** 64-90.

KONISHI, Y., OHNO, K., SAITOH, N., NOMURA, T., NAGAMINE, S., HISHIDA, H., TAKAHASHI, Y. & URUGA, T. 2007. Bioreductive deposition of platinum nanoparticles on the bacterium Shewanella algae. *Journal of Biotechnology,* 128**,** 648-653.

LALL, R. & MITCHELL, J. 2007. Metal reduction kinetics in Shewanella. *Bioinformatics,* 23**,** 2754-2759.

LALONDE, S. V., AMSKOLD, L., MCDERMOTT, T. R., INSKEEP, W. P. & KONHAUSER, K. O. 2007. Chemical reactivity of microbe and mineral surfaces in hydrous ferric oxide depositing hydrothermal springs. *Geobiology,* 5**,** 219-234.

LIU, C., GORBY, Y. A., ZACHARA, J. M., FREDRICKSON, J. K. & BROWN, C. F. 2002. Reduction kinetics of Fe(III), Co(III), U(VI), Cr(VI), and Tc(VII) in cultures of dissimilatory metal-reducing bacteria. *Biotechnology and Bioengineering,* 80**,** 637-649.

LLOYD, J. R. 2003. Microbial reduction of metals and radionuclides. *FEMS Microbiology Reviews,* 27**,** 411-425.

LLOYD, J. R., COLE, J. A. & MACASKIE, L. E. 1997. Reduction and removal of heptavalent technetium from solution by Escherichia coli. *Journal of Bacteriology,* 179**,** 2014-2021.

LLOYD, J. R., PEARCE, C. I., COKER, V. S., PATTRICK, R. A. D., LAAN, G. V. D., CUTTING, R., VAUGHAN, D. J., PATERSON?BEEDLE, M., MIKHEENKO, I. P., YONG, P. & MACASKIE, L. E. 2008. Biomineralization: linking the fossil record to the production of high value functional materials. *Geobiology,* 6**,** 285-297.

LLOYD, J. R., YONG, P. & MACASKIE, L. E. 1998. Enzymatic Recovery of Elemental Palladium by Using Sulfate-Reducing Bacteria. *Applied and Environmental Microbiology,* 64**,** 4607-4609.

MABBETT, A. N., SANYAHUMBI, D., YONG, P. & MACASKIE, L. E. 2006. Biorecovered Precious Metals from Industrial Wastes:? Single-Step Conversion of a Mixed Metal Liquid Waste to a Bioinorganic Catalyst with Environmental Application. *Environmental Science & Technology,* 40**,** 1015-1021.

MAES, S., CLAUS, M., VERBEKEN, K., WALLAERT, E., DE SMET, R., VANHAECKE, F., BOON, N. & HENNEBEL, T. 2016. Platinum recovery from industrial process streams by halophilic bacteria: Influence of salt species and platinum speciation. *Water Research,* 105**,** 436-443.

MARSDEN, J. & HOUSE, I. 2006. *The Chemistry of Gold Extraction*, SME.

MARTINS, M., MOURATO, C., SANCHES, S., NORONHA, J. P., CRESPO, M. T. B. & PEREIRA, I. A. C. 2017. Biogenic platinum and palladium nanoparticles as new catalysts for the removal of pharmaceutical compounds. *Water Research,* 108**,** 160-168.

MASALA, O. & SESHADRI, R. 2004. Synthesis Routes for Large Volumes of Nanoparticles. *Annual Review of Materials Research,* 34**,** 41-81.

MATZ, C. & JÜRGENS, K. 2001. Effects of Hydrophobic and Electrostatic Cell Surface Properties of Bacteria on Feeding Rates of Heterotrophic Nanoflagellates. *Applied and Environmental Microbiology,* 67**,** 814-820.

MIKHEENKO, I. P., ROUSSET, M., DEMENTIN, S. & MACASKIE, L. E. 2008. Bioaccumulation of Palladium by Desulfovibrio fructosivorans Wild-Type and Hydrogenase-Deficient Strains. *Applied and Environmental Microbiology,* 74**,** 6144-6146.

MOHAN, D. & PITTMAN, C. U. 2006. Activated carbons and low cost adsorbents for remediation of tri- and hexavalent chromium from water. *Journal of Hazardous Materials,* 137**,** 762-811.

MOLOKWANE, P. E., MELI, K. C. & NKHALAMBAYAUSI-CHIRWA, E. M. 2008. Chromium (VI) reduction in activated sludge bacteria exposed to high chromium loading: Brits culture (South Africa). *Water Research,* 42**,** 4538-4548.

MOLOKWANE, P. E. & NKHALAMBAYAUSI-CHIRWA, E. M. 2009. Microbial culture dynamics and chromium (VI) removal in packed-column microcosm reactors.

MORF, L. S., GLOOR, R., HAAG, O., HAUPT, M., SKUTAN, S., LORENZO, F. D. & BÖNI, D. 2013. Precious metals and rare earth elements in municipal solid waste – Sources and fate in a Swiss incineration plant. *Waste Management,* 33**,** 634-644.

MULHOLLAND, J. 1983. A History of Platinum and Its Allied Metals. Donald McDonald , Leslie B. Hunt. *Isis,* 74**,** 430-431.

NANCHARAIAH, Y. V., MOHAN, S. V. & LENS, P. N. L. 2016. Biological and Bioelectrochemical Recovery of Critical and Scarce Metals. *Trends in Biotechnology,* 34**,** 137-155.

NATARAJAN, K. A. 2018. *Biotechnology of Metals: Principles, Recovery Methods and Environmental Concerns,* Elsevier.

NEWTON, D. 2020. Biohydrometallurgy | Encyclopedia.com.

NGWENYA, N. & CHIRWA, E. M. N. 2015. Characterisation of surface uptake and biosorption of cationic nuclear fission products by sulphate-reducing bacteria. *Water SA,* 41**,** 314-324.

NIELSEN, J. T., LIESACK, W. & FINSTER, K. 1999. Desulfovibrio zosterae sp. nov., a new sulfate reducer isolated from surface-sterilized roots of the seagrass Zostera marina. *International Journal of Systematic and Evolutionary Microbiology,* 49**,** 859-865.

NIU, H. & VOLESKY, B. 1999. Characteristics of gold biosorption from cyanide solution. *Journal of Chemical Technology & Biotechnology,* 74**,** 778-784.

OKIBE, N., NAKAYAMA, D. & MATSUMOTO, T. 2017. Palladium bionanoparticles production from acidic Pd(II) solutions and spent catalyst leachate using acidophilic Fe(III)-reducing bacteria. *Extremophiles,* 21**,** 1091-1100.

POSTGATE, J. R. 1979. *The Sulphate-Reducing Bacteria*, CUP Archive.

PUJA, P. & KUMAR, P. 2019. A perspective on biogenic synthesis of platinum nanoparticles and their biomedical applications. *Spectrochimica Acta Part A: Molecular and Biomolecular Spectroscopy,* 211**,** 94-99.

RAO, T. S., SAIRAM, T. N., VISWANATHAN, B. & NAIR, K. V. K. 2000. Carbon steel corrosion by iron oxidising and sulphate reducing bacteria in a freshwater cooling system. *Corrosion Science,* 42**,** 1417-1431.

RASHAMUSE, K. J. & WHITELEY, C. G. 2007. Bioreduction of Pt (IV) from aqueous solution using sulphate-reducing bacteria. *Applied Microbiology and Biotechnology,* 75**,** 1429-1435.

REDWOOD, M. D., DEPLANCHE, K., BAXTER?PLANT, V. S. & MACASKIE, L. E. 2008. Biomass-supported palladium catalysts on Desulfovibrio desulfuricans and Rhodobacter sphaeroides. *Biotechnology and Bioengineering,* 99**,** 1045-1054.

REITH, F., ROGERS, S. L., MCPHAIL, D. C. & BRUGGER, J. 2007. Potential for the Utilisation of Micro-Organisms in Gold Processing. 9.

RIDDIN, T. L., GERICKE, M. & WHITELEY, C. G. 2006. Analysis of the inter- and extracellular formation of platinum nanoparticles byFusarium oxysporumf. sp.lycopersiciusing response surface methodology. *Nanotechnology,* 17**,** 3482-3489.

RITTMANN, B. E. & MCCARTY, P. L. 2001. *Environmental Biotechnology: Principles and Applications,* New York, McGraw-Hill Education.

ROESTORFF, M. M. & CHIRWA, E. M. N. 2018. Comparison of the Performance of Chlorococcum Ellipsoideum and Tetradesmus Obliquus as a Carbon Source for Reduction of Cr(VI) with Bacteria. *Chemical Engineering Transactions,* 70**,** 463-468.

RUIZ, M., SASTRE, A. M. & GUIBAL, E. 2000. Palladium sorption on glutaraldehyde-crosslinked chitosan. *Reactive and Functional Polymers,* 45**,** 155-173.

SCOTT, C., FLETCHER, R. L. & BREMER, G. B. 1996. Observations on the mechanisms of attachment of some marine fouling blue?green algae. *Biofouling,* 10**,** 161-173.

SETHURAMAN, P. & KUMAR, M. D. 2011. Biosorption kinetics of Cu (II) ions removal from aqueous solution using bacteria. *Pakistan Journal of Biological Sciences : PJBS,* 14**,** 327-335.

SHEN, N. & CHIRWA, E. M. N. 2018. Biosorption and desorption potential of gold(III) by freshwater microalgae scenedesmus obliquus as-6-1.

SHENG, L. & FEIN, J. B. 2014. Uranium Reduction by Shewanella oneidensis MR-1 as a Function of NaHCO3 Concentration: Surface Complexation Control of Reduction Kinetics. *Environmental Science & Technology,* 48**,** 3768-3775.

SIMON-PASCUAL, A., SIERRA-ALVAREZ, R. & FIELD, J. A. 2019. Platinum(II) reduction to platinum nanoparticles in anaerobic sludge. *Journal of Chemical Technology & Biotechnology,* 94**,** 468-474.

SIVASUBRAMANIAN, V. 2016. *Environmental Sustainability Using Green Technologies*, CRC Press.

SUN, L.-X., ZHANG, X., TAN, W.-S. & ZHU, M.-L. 2012. Effect of agitation intensity on the biooxidation process of refractory gold ores by Acidithiobacillus ferrooxidans. *Hydrometallurgy,* 127-128**,** 99-103.

TASKER, P. A., TONG, C. C. & WESTRA, A. N. 2007. Co-extraction of cations and anions in base metal recovery. *Coordination Chemistry Reviews,* 251**,** 1868-1877.

THETHWAYO, B. M. Extraction of Platinum Group Metals. 2018 2018.

VARGAS, I. D., MACASKIE, L. E. & GUIBAL, E. 2004. Biosorption of palladium and platinum by sulfate-reducing bacteria. *Journal of Chemical Technology & Biotechnology,* 79**,** 49-56.

VLAD, M. O. & ROSS, J. 2000. Statistical Ensemble Approach and Fluctuation−Dissipation Relations for Multivariable Chemical Systems Far from Equilibrium. *The Journal of Physical Chemistry A,* 104**,** 3159-3176.

WAHL, R., MERTIG, M., RAFF, J., SELENSKA?POBELL, S. & POMPE, W. 2001. Electron-Beam Induced Formation of Highly Ordered Palladium and Platinum Nanoparticle Arrays on the S Layer of Bacillus sphaericusNCTC 9602. *Advanced Materials,* 13**,** 736-740.

WANG, Y.-T. & SHEN, H. 1997. Modelling Cr(VI) reduction by pure bacterial cultures. *Water Research,* 31**,** 727-732.

WATLING, H. 2016. Microbiological Advances in Biohydrometallurgy. *Minerals,* 6**,** 49.

WEEKS, M. E. & LIND, S. C. 1946. Discovery of the Elements. *The Journal of Physical Chemistry,* 50**,** 286-286.

WOOLFOLK, C. A. & WHITELEY, H. R. 1962. REDUCTION OF INORGANIC COMPOUNDS WITH MOLECULAR HYDROGEN BY MICROCOCCUS LACTILYTICUS I. : Stoichiometry with Compounds of Arsenic, Selenium, Tellurium, Transition and Other Elements. *Journal of Bacteriology,* 84**,** 647-658.

YONG, P., ROWSON, N. A., FARR, J. P., HARRIS, I. R. & MACASKIE, L. E. 2002a. Bioreduction and biocrystallization of palladium by Desulfovibrio desulfuricans NCIMB 8307. *Biotechnol Bioeng,* 80**,** 369-79.

YONG, P., ROWSON, N. A., FARR, J. P. G., HARRIS, I. R. & MACASKIE, L. E. 2002b. Bioaccumulation of palladium by Desulfovibrio desulfuricans. *Journal of Chemical Technology & Biotechnology,* 77**,** 593-601.

YONG, P., ROWSON, N. A., FARR, J. P. G., HARRIS, I. R. & MACASKIE, L. E. 2002c. Bioreduction and biocrystallization of palladium by Desulfovibrio desulfuricans NCIMB 8307. *Biotechnology and Bioengineering,* 80**,** 369-379.

ZHANG, H. & HU, X. 2017. Rapid production of Pd nanoparticle by a marine electrochemically active bacterium Shewanella sp. CNZ-1 and its catalytic performance on 4-nitrophenol reduction. *RSC Advances,* 7**,** 41182-41189.

ZINKE, H. & GABOR, E. 2012. *Green mining: process of cyanide-free bioleaching and bioadsorption of precious metals*. EP09735954A. 2012-10-31.

Appendix A

Postgate Medium C Formulation

The following chemicals were added in 1 L ultra-pure water from a Milli-Q, Millipore Direct Q3 Unit supplied by Microsep, Johannesburg, South Africa. Chemicals were purchased Sigma Aldrich unless otherwise stated.

K_2HPO_4 (Glassworld, South Africa)	0.5 g
NH_4Cl (Glassworld, South Africa)	1.0 g
Na_2SO_4,	1.0 g
$CaCl_2$ x 2 H_2O	0.1 g
$MgSO_4$ x 7 H_2O	2.0 g
Na-DL-lactate	2.0 g
Yeast extract (Merck, South Africa)	1.0 g
Na-resazurin solution (0.1% w/v)	0.5 mL

- The solution was brought to a boil while stirring, using a magnetic stirrer;
- Then remove from the heat and cooled to room temperature ($\pm$ 25℃) while being sparged with oxygen free nitrogen.
- Once cooled the following chemicals were added;

$FeSO_4$ x 7 H_2O	0.5 g
Na-thioglycolate	0.1 g
Ascorbic acid	0.1 g

- The solution was distributed in sterile serum bottles and sealed with a stopper and and cap, autoclave (Hlclave HV 50 Hivayama, South Africa) for 15 min at 121 ℃ at an atmospheric pressure of 1 psi, once cooled to room temperature $\pm$25 ℃ the medium was ready for inoculation.

Appendix B

Statistical analysis: t-test results

Table 1.1: p-value for the removal of Pd(II) from solution.

Concentration (mg/L)	P-value		
	(SRB vs control)	(*Desulfovibrio desulfuricans* vs control)	SRB vs *Desulfovibrio desulfuricans*
356.3	0.000972	0.001518	0.791454
631	0.000978	0.001273	0.907854
964.3	0.000989	0.000999	0.919979
1094.2	0.001377	0.001245	0.808877
1607.1	0.004647	0.001025	0.281609
1928.5	0.001199	0.003626	0.377917

Table 1.2: p-value for the removal of Pt (II) from solution

Concentration mg/L	P-value		
	SRB vs Control	(*Desulfovibrio desulfuricans* vs control)	SRB vs *Desulfovibrio desulfuricans*
20	0.000697	0.000373	0.987605
50	0.000576	0.000291	0.453358
80	0.000323	0.000314	0.440694
110	0.000348	0.000443	0.652002
140	0.000225	0.000672	0.734808

Appendix C

SEM Analysis for palladium

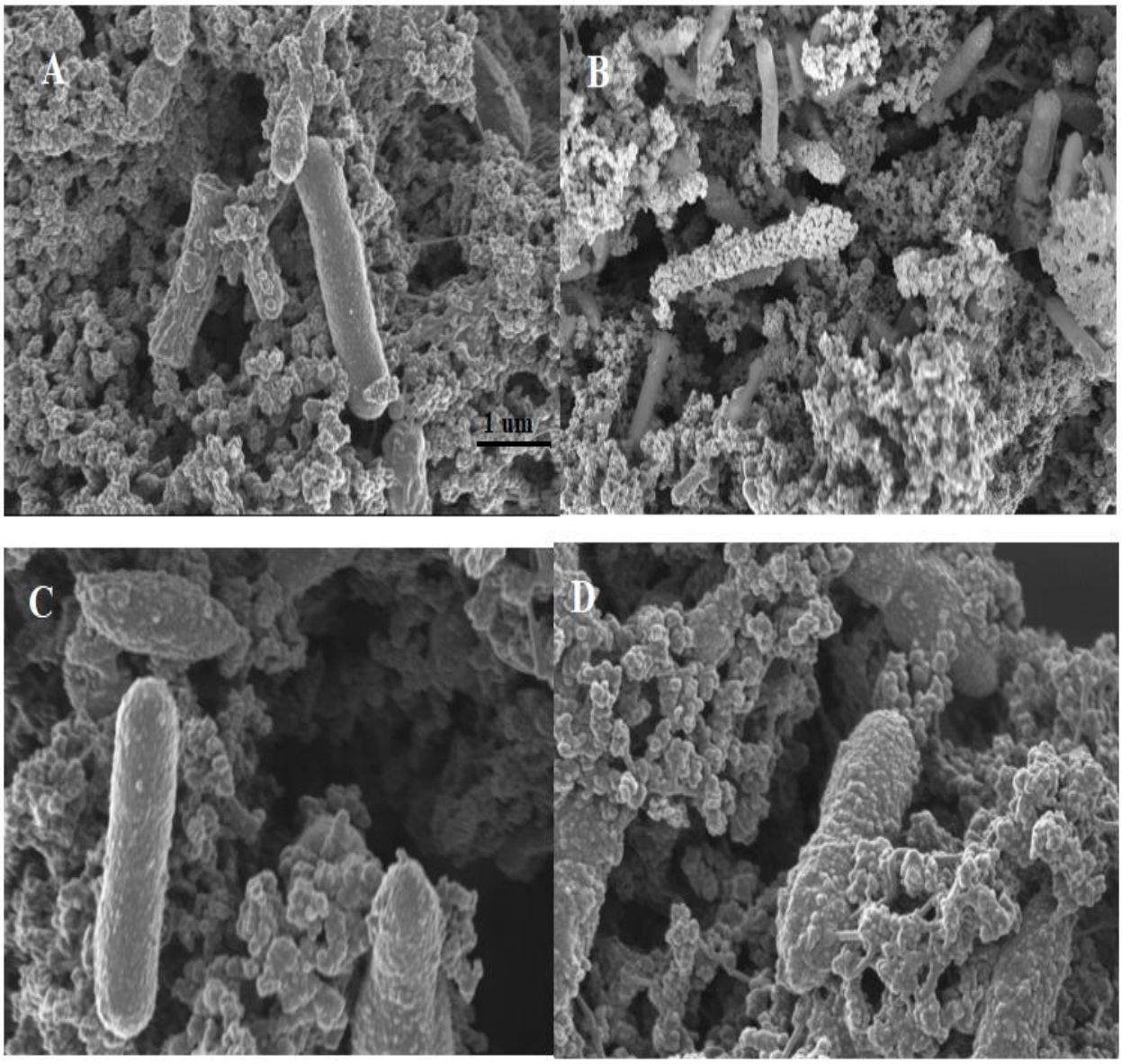

Figure 1.1 SEM analysis of bacterial cells before and after being challenged with Pd(II). A) unchallenged SRB; B) challenged SRB; C) unchallenged *Desulfovibrio desulfuricans*; D) challenged *Desulfovibrio desulfuricans*

Appendix D

SEM analysis for platinum

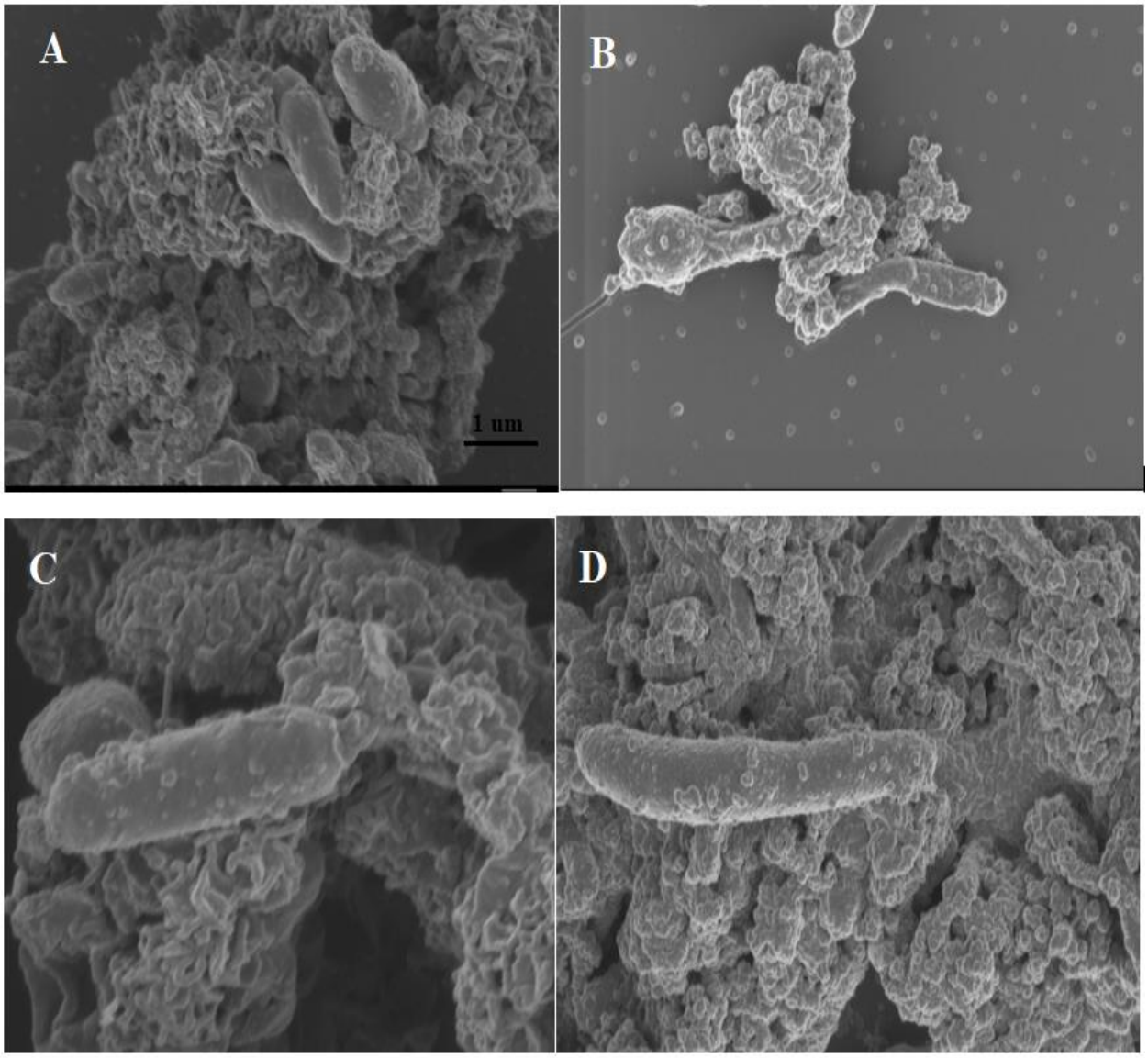

Figure 1.2 SEM analysis of bacterial cells before and after being challenged with Pt(II). A) unchallenged SRB; B) challenged SRB; C) unchallenged *Desulfovibrio desulfuricans*; D) challenged *Desulfovibrio desulfuricans*

Appendix E

```
**************************************************************************

AQUASIM Version 2.0 (win/mfc) - Listing of System Definition

**************************************************************************

Date and time of listing:  01/31/2021 14:26:24


**************************************************************************
Variables
**************************************************************************
C:              Description:          Concentration 356
                Type:                 Dyn. Volume State Var.
                Unit:                 mg/L
                Relative Accuracy:    1e-006
                Absolute Accuracy:    1e-006
--------------------------------------------------------------------------
C2:             Description:          Concentration 631
                Type:                 Dyn. Volume State Var.
                Unit:                 mg/L
                Relative Accuracy:    1e-006
                Absolute Accuracy:    1e-006
--------------------------------------------------------------------------
C3:             Description:          Concentration 964
                Type:                 Dyn. Volume State Var.
                Unit:                 mg/L
                Relative Accuracy:    1e-006
                Absolute Accuracy:    1e-006
--------------------------------------------------------------------------
C4:             Description:          Concentration 1094
                Type:                 Dyn. Volume State Var.
                Unit:                 mg/L
                Relative Accuracy:    1e-006
                Absolute Accuracy:    1e-006
--------------------------------------------------------------------------
C5:             Description:          Concentration 1607
                Type:                 Dyn. Volume State Var.
                Unit:                 mg/L
                Relative Accuracy:    1e-006
                Absolute Accuracy:    1e-006
--------------------------------------------------------------------------
C6:             Description:          Concentration 1929
                Type:                 Dyn. Volume State Var.
                Unit:                 mg/L
                Relative Accuracy:    1e-006
                Absolute Accuracy:    1e-006
--------------------------------------------------------------------------
Co:             Description:          Initial Concentration
                Type:                 Formula Variable
                Unit:                 mg/L
                Expression:           356
```

Co2:	Description:	Intial concentration
	Type:	Formula Variable
	Unit:	mg/L
	Expression:	631
Co3:	Description:	Intial concentration
	Type:	Formula Variable
	Unit:	mg/L
	Expression:	964
Co4:	Description:	Initial concentration
	Type:	Formula Variable
	Unit:	mg/L
	Expression:	1094
Co5:	Description:	Initial concentration
	Type:	Formula Variable
	Unit:	mg/L
	Expression:	1607
Co6:	Description:	Intial concentration
	Type:	Formula Variable
	Unit:	mg/L
	Expression:	1929
K:	Description:	Half velocity concentration for Pd(II)356
	Type:	Constant Variable
	Unit:	mg/L
	Value:	18.554318
	Standard Deviation:	1
	Minimum:	0
	Maximum:	1000
	Sensitivity Analysis:	active
	Parameter Estimation:	active
K2:	Description:	Half velocity concentration Pd(II)631
	Type:	Constant Variable
	Unit:	mg/L
	Value:	48.990721
	Standard Deviation:	1
	Minimum:	0
	Maximum:	1000
	Sensitivity Analysis:	active
	Parameter Estimation:	active
K3:	Description:	Half velocity concentration for 964
	Type:	Constant Variable
	Unit:	mg/L
	Value:	99.686942
	Standard Deviation:	1
	Minimum:	0
	Maximum:	1000
	Sensitivity Analysis:	active
	Parameter Estimation:	active

```
---------------------------------------------------------------------------
K4:             Description:          Half velocity concentration 1094
                Type:                 Constant Variable
                Unit:                 mg/L
                Value:                578.42271
                Standard Deviation:   1
                Minimum:              0
                Maximum:              1000
                Sensitivity Analysis: inactive
                Parameter Estimation: active
---------------------------------------------------------------------------
K5:             Description:          Rate coefficient Pd1607
                Type:                 Constant Variable
                Unit:                 mg/L
                Value:                988.74469
                Standard Deviation:   1
                Minimum:              0
                Maximum:              1000
                Sensitivity Analysis: inactive
                Parameter Estimation: active
---------------------------------------------------------------------------
K6:             Description:          Half velocity concentration 1929
                Type:                 Constant Variable
                Unit:                 mg/L
                Value:                104.34794
                Standard Deviation:   1
                Minimum:              0
                Maximum:              1000
                Sensitivity Analysis: inactive
                Parameter Estimation: active
---------------------------------------------------------------------------
Kc:             Description:          max Pd reducing capacity 356
                Type:                 Constant Variable
                Unit:                 mg/mg
                Value:                5.7710333
                Standard Deviation:   1
                Minimum:              0
                Maximum:              20
                Sensitivity Analysis: active
                Parameter Estimation: active
---------------------------------------------------------------------------
Kc2:            Description:          max reducing capacity 631
                Type:                 Constant Variable
                Unit:                 mg/mg
                Value:                9.872274
                Standard Deviation:   1
                Minimum:              0
                Maximum:              20
                Sensitivity Analysis: active
                Parameter Estimation: active
---------------------------------------------------------------------------
Kc3:            Description:          max reducing capacity 964
                Type:                 Constant Variable
                Unit:                 mg/mg
                Value:                14.838486
                Standard Deviation:   1
                Minimum:              0
```

```
              Maximum:              20
              Sensitivity Analysis: active
              Parameter Estimation: active
-------------------------------------------------------------------------
Kc4:          Description:          max reducing capacity 1094
              Type:                 Constant Variable
              Unit:                 mg/mg
              Value:                16.279566
              Standard Deviation:   1
              Minimum:              0
              Maximum:              50
              Sensitivity Analysis: inactive
              Parameter Estimation: active
-------------------------------------------------------------------------
Kc5:          Description:          max reducing capacity 1607
              Type:                 Constant Variable
              Unit:                 mg/mg
              Value:                47.867425
              Standard Deviation:   1
              Minimum:              0
              Maximum:              50
              Sensitivity Analysis: inactive
              Parameter Estimation: active
-------------------------------------------------------------------------
Kc6:          Description:          max redu cap 1929
              Type:                 Constant Variable
              Unit:                 mg/mg
              Value:                26.548725
              Standard Deviation:   1
              Minimum:              0
              Maximum:              50
              Sensitivity Analysis: inactive
              Parameter Estimation: active
-------------------------------------------------------------------------
meas_Pd1094:  Description:          Pd measured concentration
              Type:                 Real List Variable
              Unit:                 mg/L
              Argument:             t
              Standard Deviations:  global
              Rel. Stand. Deviat.:  0
              Abs. Stand. Deviat.:  1
              Minimum:              0
              Maximum:              1e+009
              Interpolation Method: cubic spline interpolation
              Sensitivity Analysis: inactive
              Real Data Pairs (7 pairs):
                 0                  1094.2
                 1                  149.1
                 2                  455.9
                 3                  186.7
                 4                  149.5
                 5                  72.9
                 6                  53.6
-------------------------------------------------------------------------
meas_Pd1607:  Description:          Pd measured conc
              Type:                 Real List Variable
              Unit:                 mg/L
```

```
                Argument:             t
                Standard Deviations:  global
                Rel. Stand. Deviat.:  0
                Abs. Stand. Deviat.:  1
                Minimum:              0
                Maximum:              1e+009
                Interpolation Method: cubic spline interpolation
                Sensitivity Analysis: inactive
                Real Data Pairs (7 pairs):
                   0                  1607.1
                   1                  1021.4
                   2                  1109.4
                   3                  483.8
                   4                  486.6
                   5                  329.5
                   6                  113.3
-------------------------------------------------------------------------
meas_Pd1929:    Description:          Pd measured concentration
                Type:                 Real List Variable
                Unit:                 mg/L
                Argument:             t
                Standard Deviations:  global
                Rel. Stand. Deviat.:  0
                Abs. Stand. Deviat.:  1
                Minimum:              0
                Maximum:              1e+009
                Interpolation Method: cubic spline interpolation
                Sensitivity Analysis: inactive
                Real Data Pairs (7 pairs):
                   0                  1928.5
                   1                  466
                   2                  637.6
                   3                  460.2
                   4                  463.1
                   5                  252.4
                   6                  109.3
-------------------------------------------------------------------------
meas_Pd356:     Description:          measured Pd 365
                Type:                 Real List Variable
                Unit:                 mg/L
                Argument:             t
                Standard Deviations:  global
                Rel. Stand. Deviat.:  0
                Abs. Stand. Deviat.:  1
                Minimum:              0
                Maximum:              1e+009
                Interpolation Method: cubic spline interpolation
                Sensitivity Analysis: inactive
                Real Data Pairs (7 pairs):
                   0                  356.3
                   1                  23
                   2                  36.9
                   3                  23.9
                   4                  27
                   5                  25.2
                   6                  14.2
-------------------------------------------------------------------------
```

```
meas_Pd631:    Description:          measured Pd reducton conc
               Type:                 Real List Variable
               Unit:                 mg/L
               Argument:             t
               Standard Deviations:  global
               Rel. Stand. Deviat.:  0
               Abs. Stand. Deviat.:  1
               Minimum:              0
               Maximum:              1e+009
               Interpolation Method: cubic spline interpolation
               Sensitivity Analysis: inactive
               Real Data Pairs (7 pairs):
                  0                  631.4
                  1                  51.8
                  2                  65.8
                  3                  54.5
                  4                  40.1
                  5                  36.2
                  6                  25.4
--------------------------------------------------------------------------
meas_Pd964:    Description:          Pd concentraton
               Type:                 Real List Variable
               Unit:                 mg/L
               Argument:             t
               Standard Deviations:  global
               Rel. Stand. Deviat.:  0
               Abs. Stand. Deviat.:  1
               Minimum:              0
               Maximum:              1e+009
               Interpolation Method: cubic spline interpolation
               Sensitivity Analysis: inactive
               Real Data Pairs (7 pairs):
                  0                  964.3
                  1                  49.7
                  2                  140.3
                  3                  72.3
                  4                  82.5
                  5                  59.1
                  6                  38.6
--------------------------------------------------------------------------
t:             Description:          Time
               Type:                 Program Variable
               Unit:                 h
               Reference to:         Time
--------------------------------------------------------------------------
u_max:         Description:          Pd356 reduction rate
               Type:                 Constant Variable
               Unit:                 mg/L/hr
               Value:                46.815505
               Standard Deviation:   1
               Minimum:              0
               Maximum:              50
               Sensitivity Analysis: active
               Parameter Estimation: active
--------------------------------------------------------------------------
u_max2:        Description:          concentration reduction rate Pd631
               Type:                 Constant Variable
```

```
              Unit:                 mg/L/hr
              Value:                49.939374
              Standard Deviation:   1
              Minimum:              0
              Maximum:              50
              Sensitivity Analysis: active
              Parameter Estimation: active
--------------------------------------------------------------------------
u_max3:       Description:          Pd reduction rate 964
              Type:                 Constant Variable
              Unit:                 mg/L/hr
              Value:                264.24326
              Standard Deviation:   1
              Minimum:              0
              Maximum:              1000
              Sensitivity Analysis: active
              Parameter Estimation: active
--------------------------------------------------------------------------
u_max4:       Description:          Pd Reduction rate 1094
              Type:                 Constant Variable
              Unit:                 mg/L/h
              Value:                49.459258
              Standard Deviation:   1
              Minimum:              0
              Maximum:              50
              Sensitivity Analysis: inactive
              Parameter Estimation: active
--------------------------------------------------------------------------
u_max5:       Description:          Pd reduction rate 1607
              Type:                 Constant Variable
              Unit:                 mg/L/h
              Value:                13.678536
              Standard Deviation:   1
              Minimum:              0
              Maximum:              50
              Sensitivity Analysis: inactive
              Parameter Estimation: active
--------------------------------------------------------------------------
u_max6:       Description:          conc reduction
              Type:                 Constant Variable
              Unit:                 mg/L/hr
              Value:                47.310165
              Standard Deviation:   1
              Minimum:              0
              Maximum:              50
              Sensitivity Analysis: inactive
              Parameter Estimation: active
--------------------------------------------------------------------------
X:            Description:          initial biomass concentration
              Type:                 Formula Variable
              Unit:                 mg/L
              Expression:           60
**************************************************************************
```

```
**************************************************************************
Processes
**************************************************************************
Red_Rate356:       Description:          palladium reduction
                Type:                 Dynamic Process
                Rate:                 (u_max*C*(X-((Co-C)/Kc)))/(K+C)
                Stoichiometry:
                  Variable : Stoichiometric Coefficient
                  C : -1
--------------------------------------------------------------------------
Red_Rate1094:  Description:          Reduction rate
                Type:                 Dynamic Process
                Rate:                 (u_max4*C4*(X-((Co4-C4)/Kc4)))/(K4+
                                      C4)
                Stoichiometry:
                  Variable : Stoichiometric Coefficient
                  C4 : -1
--------------------------------------------------------------------------
Red_Rate1607:  Description:          Reduction rate
                Type:                 Dynamic Process
                Rate:                 (u_max5*C5*(X-((Co5-C5)/Kc5)))/(K5+
                                      C5)
                Stoichiometry:
                  Variable : Stoichiometric Coefficient
                  C5 : -1
--------------------------------------------------------------------------
Red_Rate1929:  Description:          Reduction rate
                Type:                 Dynamic Process
                Rate:                 (u_max6*C6*(X-((Co6-C6)/Kc6)))/(C6+
                                      K6)
                Stoichiometry:
                  Variable : Stoichiometric Coefficient
                  C6 : -1
--------------------------------------------------------------------------
Red_rate631:   Description:          Reduction rate
                Type:                 Dynamic Process
                Rate:                 (u_max2*C2*(X-((Co2-C2)/Kc2)))/(C2+
                                      K2)
                Stoichiometry:
                  Variable : Stoichiometric Coefficient
                  C2 : -1
--------------------------------------------------------------------------
Red_Rate964:   Description:          Reduction rate
                Type:                 Dynamic Process
                Rate:                 (u_max3*C3*(X-((Co3-C3)/Kc3)))/(K3+
                                      C3)
                Stoichiometry:
                  Variable : Stoichiometric Coefficient
                  C3 : -1
**************************************************************************




**************************************************************************
```

```
Compartments
**************************************************************************
Batch1:         Description:          Reactor 356
                Type:                 Mixed Reactor Compartment
                Compartment Index:    0
                Active Variables:     C, Co, K, Kc, meas_Pd356, u_max, X,
                                       t
                Active Processes:     example
                Initial Conditions:
                  Variable(Zone) : Initial Condition
                  C(Bulk Volume) : Co
                Inflow:               0
                Loadings:
                Volume:               1
                Accuracies:
                  Rel. Acc. Q:        0.001
                  Abs. Acc. Q:        0.001
                  Rel. Acc. V:        0.001
                  Abs. Acc. V:        0.001
--------------------------------------------------------------------------
Batch2:         Description:          Pd batch reactor 631
                Type:                 Mixed Reactor Compartment
                Compartment Index:    0
                Active Variables:     C2, Co2, K2, Kc2, meas_Pd631, t, u_
                                      max2, X
                Active Processes:     Red_rate631
                Initial Conditions:
                  Variable(Zone) : Initial Condition
                  C2(Bulk Volume) : Co2
                Inflow:               0
                Loadings:
                Volume:               1
                Accuracies:
                  Rel. Acc. Q:        0.001
                  Abs. Acc. Q:        0.001
                  Rel. Acc. V:        0.001
                  Abs. Acc. V:        0.001
--------------------------------------------------------------------------
Batch3:         Description:          Reactor 964
                Type:                 Mixed Reactor Compartment
                Compartment Index:    0
                Active Variables:     C3, Co3, K3, Kc3, meas_Pd964, t, u_
                                      max3, X
                Active Processes:     Red_Rate964
                Initial Conditions:
                  Variable(Zone) : Initial Condition
                  C3(Bulk Volume) : Co3
                Inflow:               0
                Loadings:
                Volume:               1
                Accuracies:
                  Rel. Acc. Q:        0.001
                  Abs. Acc. Q:        0.001
                  Rel. Acc. V:        0.001
                  Abs. Acc. V:        0.001
--------------------------------------------------------------------------
Batch4:         Description:          Reactor4
```

```
                Type:                   Mixed Reactor Compartment
                Compartment Index:      0
                Active Variables:       C4, Co4, K4, Kc4, meas_Pd1094, t, u
                                        _max4, X
                Active Processes:       Red_Rate1094
                Initial Conditions:
                  Variable(Zone) : Initial Condition
                  C4(Bulk Volume) : Co4
                Inflow:                 0
                Loadings:
                Volume:                 1
                Accuracies:
                  Rel. Acc. Q:          0.001
                  Abs. Acc. Q:          0.001
                  Rel. Acc. V:          0.001
                  Abs. Acc. V:          0.001
--------------------------------------------------------------------------
Batch5:         Description:            Reactor 5
                Type:                   Mixed Reactor Compartment
                Compartment Index:      0
                Active Variables:       C5, Co5, K5, Kc5, meas_Pd1094, t, u
                                        _max5, X
                Active Processes:       Red_Rate1607
                Initial Conditions:
                  Variable(Zone) : Initial Condition
                  C5(Bulk Volume) : Co5
                Inflow:                 0
                Loadings:
                Volume:                 1
                Accuracies:
                  Rel. Acc. Q:          0.001
                  Abs. Acc. Q:          0.001
                  Rel. Acc. V:          0.001
                  Abs. Acc. V:          0.001
--------------------------------------------------------------------------
Batch6:         Description:            Reactor 6
                Type:                   Mixed Reactor Compartment
                Compartment Index:      0
                Active Variables:       C6, Co6, K6, Kc6, meas_Pd1929, t, u
                                        _max6, X
                Active Processes:       Red_Rate1929
                Initial Conditions:
                  Variable(Zone) : Initial Condition
                  C6(Bulk Volume) : Co6
                Inflow:                 0
                Loadings:
                Volume:                 1
                Accuracies:
                  Rel. Acc. Q:          0.001
                  Abs. Acc. Q:          0.001
                  Rel. Acc. V:          0.001
                  Abs. Acc. V:          0.001
**************************************************************************



**************************************************************************
```

```
Definitions of Calculations
**************************************************************************
cal:            Description:          Pd redutcion
                Calculation Number:   0
                Initial Time:         0
                Initial State:        given, made consistent
                Step Size:            0.1
                Num. Steps:           100
                Status:               active for simulation
                                      active for sensitivity analysis
**************************************************************************

**************************************************************************
Definitions of Parameter Estimation Calculations
**************************************************************************
fit:            Description:          Pd(II) Reduction
                Calculation Number:   0
                Initial Time:         0
                Initial State:        given, made consistent
                Status:               active
                Fit Targets:
                  Data : Variable (Compartment,Zone,Time/Space)
                  meas_Pd356 : C (Batch1,Bulk Volume,0)
                  meas_Pd631 : C2 (Batch2,Bulk Volume,0)
                  meas_Pd964 : C3 (Batch3,Bulk Volume,0)
                  meas_Pd1094 : C4 (Batch4,Bulk Volume,0)
                  meas_Pd1607 : C5 (Batch5,Bulk Volume,0)
                  meas_Pd1929 : C6 (Batch6,Bulk Volume,0)

**************************************************************************



**************************************************************************
Plot Definitions
**************************************************************************
Pd_reduction:  Description:          Palladium reduction by SRB
               Abscissa:             Time
               Title:                Palladium reduction
               Abscissa Label:       Hours (h)
               Ordinate Label:       concentration (mg/L)
               Curves:
                 Type : Variable [CalcNum,Comp.,Zone,Time/Space]
                 Value : C [0,Batch1,Bulk Volume,0]
                 Value : C2 [0,Batch2,Bulk Volume,0]
                 Value : C3 [0,Batch3,Bulk Volume,0]
                 Value : C4 [0,Batch4,Bulk Volume,0]
                 Value : C5 [0,Batch5,Bulk Volume,0]
                 Value : C6 [0,Batch6,Bulk Volume,0]
                 Value : meas_Pd356 [0,Batch1,Bulk Volume,0]
                 Value : meas_Pd631 [0,Batch2,Bulk Volume,0]
                 Value : meas_Pd964 [0,Batch3,Bulk Volume,0]
                 Value : meas_Pd1094 [0,Batch4,Bulk Volume,0]
                 Value : meas_Pd1607 [0,Batch5,Bulk Volume,0]
                 Value : meas_Pd1929 [0,Batch6,Bulk Volume,0]
**************************************************************************
```

```
**************************************************************************
Calculation Parameters
**************************************************************************
Numerical Parameters:    Maximum Int. Step Size:  1
                         Maximum Integrat. Order: 5
                         Number of Codiagonals:   1000
                         Maximum Number of Steps: 1000
--------------------------------------------------------------------------
                         Fit Method:              simplex
                         Max. Number of Iterat.:  1000
**************************************************************************

**************************************************************************
Calculated States
**************************************************************************
Calc. Num.  Num. States  Comments
0           7            Range of Times: 0 - 6
**************************************************************************
```